DEVELOPMENT OF POLY(ETHYLENE GLYCOL) - COATED VESICLES AS CARDIOVASCULAR IMAGING AGENTS FOR NUCLEAR MEDICINE

by

Deepank R. Utkhede

B.Sc., University of British Columbia, 1994

A THESIS SUBMITTED IN PARTIAL FULFILLMENT OF
THE REQUIREMENTS FOR THE DEGREE OF
MASTER OF SCIENCE

in

THE FACULTY OF GRADUATE STUDIES
(Department of Biochemistry)

We accept this thesis as conforming
to the required standard

THE UNIVERSITY OF BRITISH COLUMBIA
January 1998

In presenting this thesis in partial fulfillment of the requirements for an advanced degree at the University of British Columbia, I agree that the library shall make it freely available for reference and study. I further agree that permission for extensive copying of this thesis for scholarly purposes may be granted by the head of my department of by his or her representatives. It is understood that copying or publication of this thesis for financial gain shall not be allowed without my written permission.

Department of Biochemistry
The University of British Columbia
Vancouver, Canada

Date : January 10, 1998

Abstract

Development of Poly(ethylene glycol)-Coated Vesicles as Cardiovascular Imaging Agents for Nuclear Medicine

Deepank R. Utkhede
University of British Columbia

Supervisors:
Drs. Colin Tilcock/Dana Devine

The development and use of poly(ethylene glycol) (PEG)-coated vesicles as nuclear medicine blood pool imaging agents is described from the initial synthesis of chelator, through labeling of vesicles with technetium-99m (^{99m}Tc), to the final testing in a human subject. Using hexamethyl-propyleneamine oxime (HM-PAO) as the chelate molecule, a novel pH gradient method was developed for the rapid, robust and reproducible labeling of pre-formed vesicles with labeling efficiencies greater than 90%. *In vivo* (pyrogen and hemodynamic studies in rabbits) and *in vitro* (CH50 hemolytic assay) studies were conducted to determine the safety and tolerability of PEG-coated vesicles. Results showed that there was no significant alterations in hemodynamic parameters or activation of the complement system. Also, vesicles and the vesicle preparation procedure were found to be non-pyrogenic. *In vivo* studies in rabbits revealed that vesicles with 4.5 mol% PEG, exhibited both lipid dose-dependent and -independent circulation half-lives contrary to published data. A circulation half-life of ~ 15 hours was achieved at lipid dose greater than ~1.0 μmol of total lipid/kg of body weight.

Based on these *in vitro* studies and *in vivo* rabbit results, a vesicle based kit was developed and tested in a human subject. The left ventricular ejection fraction (LVEF) was calculated using labeled vesicles and was compared to the LVEF calculated with the current standard of radiolabeled autologous red blood cells (RBCs). The values were found to be similar (69% for RBCs and 73% for vesicles) indicating that PEG-coated vesicles labeled with ^{99m}Tc are a suitable alternative to RBCs for cardiovascular imaging.

Table of Contents

List of Tables

List of Figures

Acknowledgments

I would like to first and foremost express my sincerest and most heartfelt thanks to Dr. Colin Tilcock for all his patience, encouragement and guidance throughout this project. Colin has been both a great supervisor and friend. As a supervisor, he has allowed me the freedom to pursue various avenues of research while still keeping focus on the project at hand. As a friend, Colin has always been there for support and friendship which has made my experience both educational and enjoyable. Colin, thank you very much.

I would like to thank Dr. Dana Devine for giving me the opportunity to work on this thesis as a graduate project. I would also like to thank Katherine, Amanda, Derek, Sara and Raymond for putting up with my seemingly constant barrage of questions and requests to borrow equipment. Also, my apprieciation goes to Dr. Don Lyster and the staff of the Nuclear Medicine departments at VGH and University site for all their assistance for the *in vivo* rabbit studies and the human volunteer study.

I would like to dedicate this thesis to
my wife and family,
for their unconditional support and encouragement
throughout this Master's project.

Chapter 1 :

Introduction

1.1 Objective

The purpose of this project was to develop an alternative radiopharmaceutical to radiolabeled autologous red blood cells (RBCs) that obviates drug interferences and handling issues of RBCs. In order to minimize scheduling difficulties and improve coordination between the radiopharmaceutical lab and the imaging floor, this alternative should be an off-the-shelf radiopharmaceutical which can be prepared and radiolabeled *in vitro* either before or immediately upon arrival of the patients in the nuclear medicine department. To eliminate the possibility of transmission of blood borne diseases it should not contain or be based upon any blood products or derivatives. To maximize patient comfort and minimize distress, this alternative should require only one venipuncture. To place this research in perspective and to provide a rationale for both the project as a whole, as well as the specific experimental approaches that were used, it is important to provide some background in the following areas:

- what radionuclide should be used to label this alternative imaging agent
- the problems and limitations with existing blood pool imaging agents
- the use of polymer-coated lipid vesicles as a blood pool marker and
- how to efficiently and reproducibly label vesicles.

1.2 Choice of Radionuclide

Technetium-99m (^{99m}Tc) is by far the most commonly used radioisotope in nuclear medicine because it is a pure gamma (γ) emitter with a short decay half-life (~6.0 hours) and decays to a long lived β-emitting daughter isotope (2.15×10^5 years) - both of

these factors decrease the radiation burden to the patient [1,2]. Although, the biodistribution of either orally or intravenously administered ^{99m}Tc is useful in the diagnosis of only a few pathophysiological states, such as imaging of Meckel's diverticulum, thyroid function and first pass studies of cardiac function, ^{99m}Tc can be complexed to a variety of pharmaceuticals in order to alter the biodistribution to image other pathophysiological disease states [2-4]. In addition, ^{99m}Tc is readily commercially available using ^{99}Mo/^{99m}Tc generators and, by comparison to other radionuclides, is relatively inexpensive.

1.3 Blood Pool Imaging - Radiolabeled Red blood Cells (RBCs)

An imaging agent commonly used in nuclear medicine to visualize the blood pool are the patients' own red blood cells (RBCs) radiolabeled with ^{99m}Tc. Radiolabeled autologous RBCs are commonly used in a number of cardiac and vascular imaging procedures such as left ventricular ejection fraction determinations (LVEF), detection of left-right shunts, vascular malformation, regurgitant fractions in valvular disease and detection of gastrointestinal bleed sites [5]. LVEF represents the average amount of blood ejected from the left ventricle during each heart beat and is an important prognostic factor in the accurate global assessment of heart function. For this procedure, the patients RBCs are labeled and the camera is positioned in the left anterior oblique (LAO) position which provides the best separation between the right and left ventricles. The patient is connected to an electrocardiographic monitor (ECG) which is used to divide the cycle of cardiac contractions into a number of discreet divisions. To provide increased sensitivity and accuracy, a number of cardiac cycles are acquired and the counts in each division are added together to provide a composite image of the left ventricle during each stage of the heart beat. The LVEF is then calculated by comparing the counts associated with the left ventricle at end diastole (when left ventricle contains the greatest amount of blood) and end systole (when left ventricle contains the least amount of blood). The percentage of

counts ejected from the left ventricle represents the LVEF. The normal LVEF for a patient is typically 60 ± 10%; patients suffering from cardiac dysfunction have values typically <40% [6,7].

Another area in which radiolabeled RBCs have proved to be an invaluable imaging tool is in the detection of gastrointestinal (GI) bleed sites. Other procedures available for the localization of GI bleeds include endoscopy and arteriography, however, these procedures suffer from significant disadvantages [8]. First, they are only able to detect GI bleeds if they are actively bleeding at the time of the procedure, and it has been well documented that GI bleeding, even massive hemorrhaging, can be intermittent and can stop and start in a matter of minutes [9]. Thus, endoscopy and angiography can lead to false negative results. Endoscopy is also restricted to the lower and upper regions of the GI tract. Second, both procedures are invasive and cause a considerable amount of patient discomfort. Third, in some cases radiographic contrast media commonly used in arteriography exhibit significant toxicities ranging from flushing and nausea to anaphylactic shock and death [10,11]. Imaging using radiolabeled RBCs does not suffer from the limitations of endoscopy and arteriography and provides a safe, minimally-invasive procedure to locate bleed sites throughout the entire GI tract [12-18].

The three methods (*in vivo*, modified *in vivo* and *in vitro*) used to label RBCs vary in terms of labeling efficiency, time to perform and number of steps involved. However, the principle of labeling for all three methods is similar. They all require stannous ions to reduce ^{99m}Tc which then binds to RBC components. The first step is the addition of stannous ions. These are transported via a specific membrane cation transport system to the interior of the RBCs [19]. After a brief waiting period, sodium pertechnetate ($Na^{99m}TcO_4$) is added to the pre-tinned RBCs. The added pertechnetate is thought to be transported to the interior of the RBCs via the band-3 anion transport system which is normally involved in chloride-bicarbonate exchange [20]. Once inside, the pertechnetate

ions are reduced by entrapped stannous ions. The reduced form of ^{99m}Tc strongly binds to the β chain of hemoglobin, thereby labeling the RBCs [21,22].

The *in vivo* method is by far the easiest and most straightforward of the three. This labeling method was discovered from the observation that, after performing a bone scan using stannous pyrophosphate and pertechnetate, subsequent pertechnetate injections resulted in the labeling of RBCs [23]. This led to the *in vivo* method of labeling first described by Pavel et al. [24]. The patient is injected with a pre-determined quantity of stannous pyrophosphate. After a brief waiting period of 10-15 minutes to allow stannous ions to be transported to the interior of RBCs and excess ions excreted, the patient is injected with 20 mCi (740 MBq) of pertechnetate. The *in vivo* procedure typically results poorer tagging efficiencies than the modified *in vivo* and *in vitro* labeling methods [5]. *In vivo* labeling is sufficient for most cardiac imaging studies but is generally not used for GI bleed detection, because the free unbound pertechnetate accumulates in the stomach and the GI tract, producing false-positive results [25].

The modified *in vivo* method is essentially the same as the *in vivo* method with a minor modification [26]. After administration of stannous pyrophosphate and the brief waiting period, a sample of blood is removed from the patient into a tube containing a pre-measured amount of pertechnetate. The tube is mixed and incubated at room temperature for 5 minutes before re-injection into the patient. This method leads to higher tagging percentages compared to the *in vivo* procedure, because labeling occurs in the tube and so the pertechnetate cannot equilibrate into the extravascular space. Thus, producing images with lower background activity than the *in vivo* method.

The *in vitro* method is the most time consuming and requires the greatest number of manipulations, but results in the highest tagging percentages. This method is generally reserved for patients undergoing GI bleed detection because of the presence of very little

free pertechnetate. The first reliable labeling procedure which did not require extensive RBC washing was described by Smith and Richards [27]. Briefly, blood is withdrawn into a tube containing heparin, stannous citrate, sodium citrate and dextrose. The contents are mixed and incubated for 5 minutes after which sterile saline is added and spun for 5 minutes. Packed RBCs are removed and added to a tube containing a pre-measured amount of pertechnetate and mixed. After 5 minutes, the RBC are re-injected into the patient. There are commercial kits now available which omit the centrifugation step and use chemical means to remove extracellular stannous ions (UltraTag RBC™ by Mallinckrodt Medical).

1.4 Advantages of Radiolabeled RBCs

There are a number of advantages to the use of RBCs as a cardiac and vascular imaging agent. They have a long circulation half-life, typically approximately 60 days when undamaged [28]. There is no issue of compatibility because the patient's own RBCs are used. As described previously, RBCs can be labeled with ^{99m}Tc using a variety of methods which are relatively simple and straightforward. Although radiolabeled RBCs have been extensively used and validated, their use is not without limitations.

1.5 Disadvantages of Radiolabeled RBCs

There are number of factors which complicate the use of radiolabeled RBCs. The most prevalent issue is the interference of various drugs on labeling. Certain drugs are known to interfere with the *in vivo* labeling process causing low tagging efficiencies as well as high background, which decreases image quality and, in the case of GI bleed detection, may lead to false-positives. Drugs which interfere with labeling include digitalis glycosides (digoxin), nitroglycerin, isosorbide dinitrate, nitroprusside, propranolol, amrinone, methyldopa, quinidine, adriamycin (doxorubicin), heparin, hydralazine,

dextrose, radiographic contrast media, prazosin, and penicillin [29-34]. Other instances in which low labeling has been observed include patients who have auto-antibodies to RBCs and patients suffering from sickle cell anemia [35,36]. These interferences often result in unusable images and often necessitate the use of the lengthier *in vitro* labeling procedures, increasing inconvenience and stress to both patients and staff alike.

To further complicate the problem, the group of patients imaged using radiolabeled RBCs dovetails the same group of patients on medications that interfere with the labeling process. An example of this conflict is seen with the use of the anti-cancer chemotherapeutic doxorubicin. Doxorubicin is commonly used to treat a wide variety of cancers but has known cardiotoxicities. The cardiotoxic side effects are dose dependent and is often the limiting factor in treatment. Radionuclide angiography is used to follow the cardiotoxic effects of doxorubicin on cardiac function [37-39]. However, doxorubicin interferes with the *in vivo* labeling method producing unusable images [40]. The exact mechanism of this interaction is unknown but is thought to be caused by the decrease in hemocrit resulting from doxorubicin therapy. The *in vitro* or modified *in vivo* labeling procedures have to be used in order to overcome the labeling difficulties [40].

Another disadvantages of RBCs is the pragmatic issue of scheduling difficulties which may arise during the course of a normal working day. Unlike other imaging modalities where images are acquired by the simple push of a button, nuclear medicine requires careful coordination between the front desk, radiopharmaceutical preparation lab and the imaging floor. Due to the short decay half-life of ^{99m}Tc, radiopharmaceuticals are generally prepared just before, or after the arrival of the patient in the department. In some cases the radiopharmaceutical is prepared at the beginning of the day. After preparation and before administration, the radiopharmaceutical undergoes quality control testing to ensure absence of contaminants and formation of the proper complex. Complications can arise from the late arrival of the patient. Also, the RBC labeling

procedure cannot begin until after the patient arrives in the nuclear medicine department thus, the late arrival of patients not only causes delays in their imaging study, but also any study subsequently scheduled on the same camera. These delays can be compounded by unforeseen drug interferences.

Another issue regarding the use of radiolabeled RBCs is the handling of blood products - this is undesirable with the current concerns of blood borne diseases such as HIV and hepatitis. Finally, there are the concerns over patient discomfort due to multiple injections. The *in vivo* and *in vitro* labeling procedures generally require two separate injections.

1.6 Polymer Coated Vesicles as Blood Pool Imaging Agents

Prior to investigations into the effects of surface modifications with hydrophilic polymers such as poly(ethylene glycol), the clinical use of vesicles had been severely restricted due to their short circulation half-life and accumulation in the liver and spleen. Once injected into the circulation, vesicles behave like other foreign particulates and are quickly removed from the circulation by the reticuloendothelial system (RES). The major organs that comprise the RES are principally the liver and spleen and to a lesser extent lung and bone marrow. Early studies using vesicles as drug delivery system or imaging agents were restricted to delivery or imaging of RES organs [41-43]. The rate of clearance and biodistribution of vesicles in biological systems is a complex function of lipid dose, charge, size and composition [reviewed in 44,45]. In general, small unilamellar vesicles composed of neutral lipids have the longest circulation times when administered at high lipid doses. The circulation times can be further increased by the including gangliosides, such as GM1, or sphingomyelin into the vesicle composition [46,47].

Abuchowski and colleagues discovered that covalently coupling poly(ethylene glycol) to various proteins not only increased the circulating time of the modified proteins, but also decreased their toxicity and immunogenicity [48-53]. Similarly, Illum and Davis observed that PEG dramatically altered the biodistribution of polystyrene microspheres [54]. In the absence of the polymer, the microspheres were rapidly taken up into the liver and spleen. However, coating the microspheres with PEG resulted in greatly reduced activity in the liver and spleen and higher activity associated with the blood, heart, lung and carcass. Covalent modification of vesicles with PEG has produced similar results - increased circulation time and decreased RES uptake [55,56]. PEG is not unique in this regard and other polymers exhibit similar effects [57,58].

The circulation half-life of unmodified vesicles increases with increasing lipid dose - this is thought to occur as a result of RES blockade or saturation [44,45]. For PEG-modified vesicles, various studies have shown that the circulation half-life is: a) independent of lipid dose above ~3.0 μmol of total lipid/kg of body weight, and b) is > 15 hours [59-64]. Similar lipid dose-independent clearance has been observed in mice down to lipid doses of 0.5 μmol/kg [62]. However, these studies are not directly applicable to rats and rabbits, and ultimately humans, because recognition and removal of liposomes in mice is different from that of rats and rabbits [65]. The circulation half-life of unmodified vesicles is critically dependent on the lipid composition of the bilayer. PEG-modification abolishes or minimizes this dependence and the circulation half-life is independent of cholesterol content, degree of lipid saturation or the inclusion of charged lipids [64].

Another possible alternative of interest to radiolabeled RBCs, is radiolabeled albumin. Until recently, the use of radiolabeled albumin has been severely restricted because the weak binding of reduced ^{99m}Tc to albumin results in the rapid equilibration of activity with the extravascular space, leading to high background and short circulation half-lives [66,67]. A number of investigators have produced derivatized albumins in order

to increase the binding strength [68-70]. Although such derivatized albumins show reduced equilibration with the extravascular space and have improved circulation kinetics, it suffers from the principle disadvantage that it still uses human serum albumin. Also, there are problems with long term storage due to oxidation of the sulphydryl groups of albumin. Thus, PEG-coated vesicles were selected for further investigation as alternative blood pool imaging agent.

1.7 Labeling of Vesicles with ^{99m}Tc

Several labeling techniques have been developed which can be classified into two broad groups, passive and active labeling. Passive labeling describes techniques by which vesicles are non-specifically labeled during their formation. Active labeling involves the use of carrier molecules and chelators to label pre-formed vesicles.

With passive labeling there are three different techniques that have been developed. The first, and by far the easiest, involves the inclusion of the radioisotope in the rehydration buffer added to the lipid film [71-76]. The spontaneous formation of multilamellar vesicles (MLVs) and entrapment of the added aqueous milieu produces labeled vesicles. The second method is termed surface labeling and relies on the non-specific electrostatic attraction between reduced ^{99m}Tc and negatively charged moieties on the vesicle surface [76-81]. The third method involves the inclusion of radiolabeled lipids into the lipid compositions of vesicles. For example, lipids have been labeled by replacing hydrogens and carbons with their radioactive counterparts, ^{3}H or ^{14}C [82-85].

There are three principle methods of active labeling. The first is similar to surface labeling described above, but in this case, instead of non-specific electrostatic interactions, a suitable chelator is covalently coupled to a lipid anchor [86-89]. This results in pre-formed vesicles with the chelator at the surface, able to bind reduced ^{99m}Tc. The second

method employs a pH gradient and the differential permeability of the lipid bilayer to charged and neutral molecules. The hydrophobic lipid bilayer of a vesicle is relatively impermeable to charged molecules, while uncharged or neutral molecules can readily cross the bilayer. This property of the bilayer and the fact that the charged state of many molecules is dependent on the pH is exploited in this labeling method [75,90-93]. The required pH of the interior and exterior aqueous media is determined by the pKa of the molecule of interest. The exterior pH is equal to the pH in which the molecule is neutral, while the interior pH should equal the pH in which the molecule is charged. After the addition of the molecule to the vesicles, the neutral form of the molecule can cross the bilayer. After traversing the lipid bilayer, the molecule comes in contact with the acidic interior and becomes charged. The charged molecule can no longer readily cross the bilayer and is trapped inside. This method is termed 'remote loading' and labeling efficiencies as high as 90% have been reported [93].

Although all these methods can be used to produced ^{99m}Tc-labeled vesicles, the vesicles so produced are not ideally suited for nuclear medicine imaging. Encapsulation by inclusion of label in the initial hydration buffer produces low labeling efficiencies and requires the removal of untrapped label [75,76]. This would prove impractical in a clinical setting because ^{99m}Tc has a short decay half-life (~6 hours), and would necessitate the production of vesicles immediately before use. The surface labeling methods, both non-specific and chelator-based, result in relatively short circulation half-lives because the label is easily exchanged from the vesicle surface [81]. The use of β-emitting radiolabeled lipids is unworkable because it is not possible to produce high quality images on the basis of bremsstrahlung radiation. Also, β emitters would result in a high radiation burden to the patient. The use of radiolabeled vesicles using a γ-emitter such as Iodine-123-labeled lipids, remains an interesting alternative that has not been studied. The pH gradient method would not work due to complications with non-specific binding of ^{99m}Tc to vesicle surface.

The remaining method of labeling involves the use of a specific carrier molecules to transport the label across the vesicle bilayer to the interior. The use of carrier molecules to label vesicles are generally more technically complex and labor intensive, but have a number of key advantages. Firstly, these methods are robust and produce high labeling efficiencies, eliminating the need for subsequent chromatography to remove untrapped label. Secondly, because the label in trapped within the vesicles as opposed to bound at the surface, the label is not free to exchange with circulating serum components, resulting in a longer circulation half-life.

Different carrier molecules have been used with different radioisotopes with varying results [73,94,95]. The method used in this thesis is based on the carrier molecule HM-PAO (hexamethyl-propyleneamine oxime). HM-PAO was originally designed and synthesized for use as a regional cerebral blood flow imaging agent because it could transport ^{99m}Tc across the lipophilic blood brain barrier (BBB) [96-100]. Initially after rehydration with pertechnetate ($Na^{99m}TcO_4$) and stannous ions in saline, HM-PAO forms a lipophilic complex with reduced ^{99m}Tc. The lipophilic complex can cross the BBB where it interacts with cellular components and is converted to a hydrophilic form which can no longer cross the BBB, trapping ^{99m}Tc within the brain. Although the structure of the initial lipophilic complex has been elucidated, the isolation and identity of the secondary hydrophilic complex remains unknown [101]. It was originally thought that HM-PAO interacted with intracellular glutathione which reduced HM-PAO from the lipophilic form to the hydrophilic form [102,103]. This was also the basis for the labeling procedure described by Phillips et al. [104,105] (discussed later). However, studies have shown that other reducing agents, such as dithiothrietol, are also effective at converting HM-PAO [106].

HM-PAO is available commercially as a cerebral blood flow imaging agent known as Ceretec^{TM} (Amersham International) which contain 7.6 μg of $SnCl_2.2H_2O$, 4.5 mg of

NaCl, and 0.5 mg of d,l-HM-PAO [107]. Phillips et al. designed a method to label vesicles using the Ceretec^{TM} kits [104,105]. Vesicles were prepared by rehydration of the lipid film with 30 mM glutathione in saline followed by extrusion. The lipid dispersion was washed 2-3 times with saline by centrifugation to give a dispersion with only encapsulated glutathione. An HM-PAO kit was reconstituted with 5 ml of saline and 5 mCi of ^{99m}Tc. After a 5 minute incubation period, 0.83 ml of the solution was added to the vesicles and incubated for a further 15 minutes. The resulting labeling efficiencies were reported to be consistently greater than > 90% thus, developing a simple and effective means for the reproducible labeling of vesicles with ^{99m}Tc. A schematic diagram of the labeling of vesicles is given in Figure 1.1.

1.8 Synopsis of Experimental Approach

Based on the preceding considerations, pre-formed PEG-coated lipid vesicles labeled with ^{99m}Tc using HM-PAO were developed and examined as a possible alternative pharmaceutical to radiolabeled RBCs for blood pool imaging. This research project was divided into five stages:

- development of a method to internally label vesicles efficiently with ^{99m}Tc
- biodistribution and kinetic behavior of labeled vesicles *in vivo* in rabbits to establish appropriate lipid doses for eventual human testing
- subsequent optimization of the vesicle preparation and labeling procedure based on animal studies
- examination of *in vitro* and *in vivo* toxicity of vesicles and
- preliminary testing of radiolabeled vesicles in a human volunteer to compare radiolabeled RBCs to vesicles to determine LVEF.

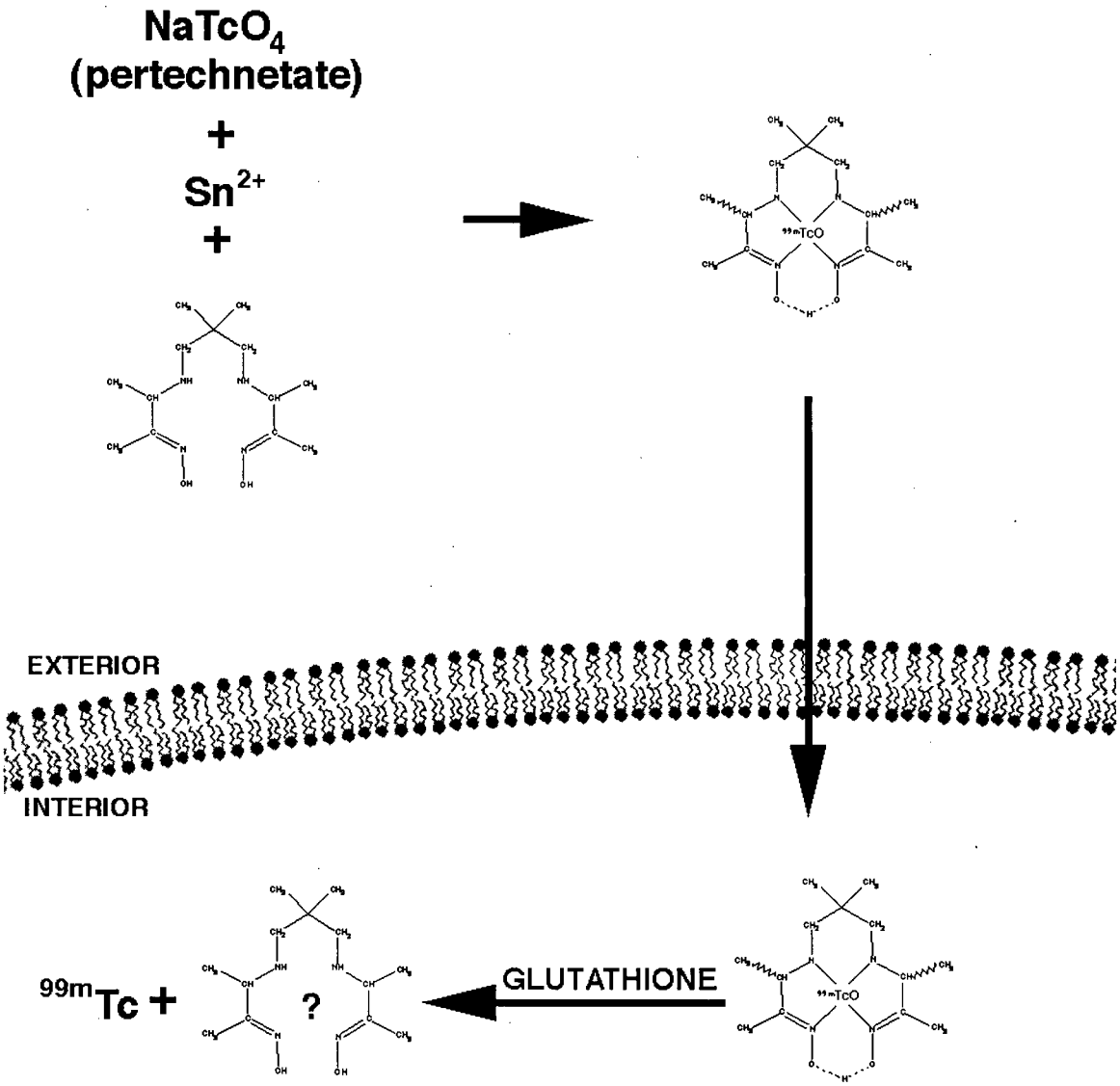

Figure 1.1. Diagram outlining the labeling of vesicles using HM-PAO to transport ^{99m}Tc across the lipid bilayer. Initially after rehydration, HM-PAO forms a lipophilic complex with reduced ^{99m}Tc which can cross the lipid bilayer. After crossing the bilayer, HM-PAO comes into contact with encapsulated glutathione which converts HM-PAO to a hydrophilic form. The hydrophilic form of HM-PAO can not cross the bilayer thus, trapping ^{99m}Tc within the vesicles. The question mark denotes the unknown structure of the converted hydrophilic form of HM-PAO.

Chapter 2 :

Labeling Vesicles Using Hexamethyl-propylene amine oxime (HM-PAO)

Introduction

This chapter examines various aspects of vesicle labeling using HM-PAO. The first step was the synthesis of HM-PAO because commercially available Ceretec™ kits contain pre-determined amounts of HM-PAO, $SnCl_2.2H_2O$ and NaCl. It was not possible to systematically examine the effect of variation of these components using the existing kits. Although the synthesis of HM-PAO is not novel, it is reported because the synthesis was found to be sensitive to the purity of the starting materials and that NMR may not always be the best method for assessing purity. Also described is a new method for the purification of the starting material 2,3-butanedione monoxime.

The synthesized HM-PAO was used to prepare kits similar to Ceretec™ kits to observe the effects of reducing the rehydration volume, lipid composition and the chromatography of vesicles on labeling. The volume of saline (5.0 ml) normally used to reconstitute the kits had to be reduced in order to label vesicles with a sufficient quantity of ^{99m}Tc for imaging, while minimizing the dilution of vesicles [107-111]. Although this may seem a relatively minor modification, there were a number of confounding issues which required the reformulation of the kit with a new preparation protocol. Also, an alternative method to the centrifugation of vesicles to remove external glutathione described by Phillips et al. was developed [104-105].

Materials

2,3-butanedione monoxime and 2,2-dimethyl-1,3-propanediamine were purchased from Aldrich Chemical Company (Milwaukee, WI). Dipalmitoylphosphatidylcholine (DPPC), palmitoyloleoylphosphatidylcholine (POPC), distearoylphosphatidylcholine (DSPC), dimyristoylphosphatidylglycerol (DMPG), and dipalmitoylphosphatidyl-ethanolamine-poly(ethylene glycol) 5000 (PE-PEG 5000) were obtained from Avanti Polar Lipids (Brimingham, AL). Acetic acid, benzene, acetonitrile, ethanol, sodium borohydride ($NaBH_4$), $SnCl_2.2H_20$ and ethyl acetate were purchased from Fisher Scientific (Nepean, ON). Cholesterol (Chol), α-tocopherol (Vit. E), glutathione and Sephadex G50 were purchased from Sigma Chemical Company (St. Louis, MO). [^{3}H]-labeled glutathione was obtained from Dupont NEN Inc. (Mississauga, ON). All solvents were HPLC grade and used without further purification.

Methods

Sublimation of 2,3-butanedione monoxime

The purification of 2,3-butanedione monoxime was performed using a sublimation apparatus. A sample of 2,3-butanedione monoxime was placed in the apparatus under vacuum using a water aspirator. The apparatus was placed in a water bath to the level of the 2,3-butanedione monoxime and heated to ~40°C and the sublimation finger was filled with ice water. Sublimed 2,3-butanedione monoxime was collected until ~5.8 g was isolated which was used immediately in an HM-PAO synthesis reaction. A sample was removed for NMR and melting point analysis.

Synthesis of HM-PAO

The synthesis of HM-PAO was based on the procedure outlined in Canadian patent 1 243 329 [112]. The general synthesis procedure is given in Figure 2.1. A noted alteration in the synthesis protocol occurred after the synthesis of the intermediate. According to the patent, after cooling the reaction to room temperature, the intermediate should precipitate out of solution. However, the precipitate that formed after cooling the reaction was not the intermediate. Drying the mother liquor under a stream of nitrogen left a dry white solid which was washed with cold acetonitrile (-10°C) and suction filtered. The resulting solid was determined to be the intermediate bisimine by NMR.

Separation and purification of meso-HM-PAO was performed by double recrystallization from acetonitrile. Briefly, 0.50 g (1.9 mmol) of the crude mixture of HM-PAO was slurried in 30 ml of acetonitrile and heated to reflux. The solution was filtered through a preheated filter apparatus and allowed to cool to room temperature. The resulting white solid was removed by suction filtration and washed with cold acetonitrile (-15°C), dried and the procedure repeated. The solid was analyzed by NMR.

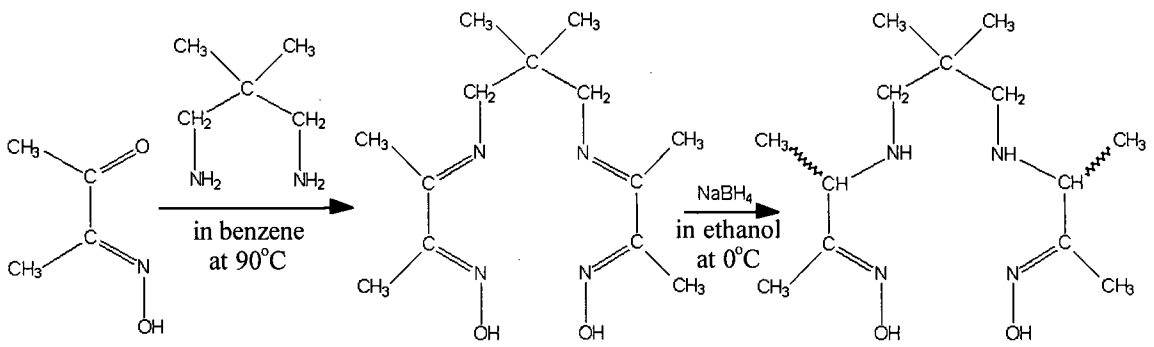

Figure 2.1. General reaction scheme for the synthesis of HM-PAO.

NMR analysis

All NMR analysis were acquired using a Bruker Model WP200, 200 Mhz instrument in either $CDCl_3$ or CD_3OD.

Preparation of Vesicles

Lipids were combined from known stock solutions in chloroform in the final molar composition of DSPC/Chol/DMPG/Vit.E/PE-PEG 5000 (45.5:40:9:1:4.5), DPPC:Chol: PE-PEG 5000 (47.75:47.75:4.5), POPC (100) and DPPC (100). Excess solvent was removed under a stream of nitrogen to form a thin lipid film. Residual solvent was removed by storage under vacuum (< 0.25 mm Hg). The lipid film was rehydrated with 30 mM glutathione in 0.9% (w/v) NaCl to a final lipid concentration of 200 mM. A batch of DPPC:Chol:PE-PEG 5000 vesicles were rehydrated with 30 mM glutathione spiked with [^{3}H]-labeled glutathione. Multilamellar vesicles were formed by mild heating and vortexing, followed by extrusion through polycarbonate filters using a thermobarrel extrusion device (Lipex Biomembranes, Vancouver, B.C.) to form unilamellar vesicles. The lipid dispersion was extruded 5x through one 0.400 μm, 5x through one 0.200 μm and then 10x through two stacked 0.200 μm filters to ensure uniformity. The vesicles were sized using a Nicomp Model 370 particle sizer (Goleta, CA) and stored at 4°C until needed.

Preparation of HM-PAO Kits

HM-PAO kits were prepared containing the same amount of each compound as the commercially available Ceretec™ kits (Amersham International). Studies on the chromatographic removal of external glutathione and the effect of vesicle composition, used kits prepared with the crude mixture of meso and d,l HM-PAO. Kits with the

purified meso HM-PAO isomer were used for all other studies. Stock solutions of HM-PAO (in 95% ethanol), $SnCl_2.2H_2O$ (in 0.04 N HCl) and NaCl (in distilled water) were prepared. Kits were prepared in 5 ml cryotubes and stock solutions added to give 0.5 mg of HM-PAO, 7.6 μg of $SnCl_2.2H_2O$ and 4.5 mg of NaCl per tube. The sample were frozen in liquid nitrogen and stored under reduced pressure for 4 hours. The tubes were then capped and stored at -10°C until needed.

Determination of tagging efficiency

The percentage of added ^{99m}Tc chelated by HM-PAO to form the lipophilic complex was determined using the partition assay described by Ballinger et al. [113]. The HM-PAO kits were hydrated with 0.5 ml of saline and mixed to dissolve contents for 10 seconds. Then ~10 mCi of pertechnetate was added to the kit and allowed to incubate at room temperature for 15 minutes. After incubation, 50 μl of the ^{99m}Tc/HM-PAO solution was added to a test tube containing 2.0 ml of ethyl acetate and 2.0 ml of saline. The tube was mixed vigorously for 1 minute, then allowed to stand for 1 minute to allow phases to separate. A 0.5 ml aliquot was sampled from the ethyl acetate phase (top) and the saline phase (bottom). The radioactivity in each phase was counted using a RadCal Model 4502 dose calibrator (Monrovia, CA). To calculate the percentage of ^{99m}Tc activity in the lipophilic form, the ethyl acetate phase activity was divided by the sum of activity in both phases.

Labeling Procedure

The prepared HM-PAO kits were reconstituted with 5.0 or 0.5 ml of 0.9 % NaCl followed by the addition of a premeasured amount of pertechnetate. The contents were mixed and incubated at room temperature for 10 minutes. After incubation, 0.8 ml of the

solution was added to vesicle dispersion, mixed and incubated for another 10 minutes. Labeling efficiency was determined by chromatography on Sephadex G50.

Results

Synthesis of HM-PAO

The NMR of the starting compounds, 2,3-butanedione monoxime and 2,2-dimethyl-1,3-propanediamine, are presented in Figure 2.2 (A and B, respectively). The NMR of the isolated intermediate in $CDCl_3$ is presented in Figure 2.2 C. The NMR shows the presence of peaks corresponding to that reported in the patent, indicating the formation of the intermediate. Compared to the NMR profiles of the starting materials, the most important peak in the NMR profile indicative of the formation of the intermediate corresponds to the peak at ~3.3 ppm representing the methyls at position 2. The NMR of both starting compounds show peaks very similar to those observed in the NMR profile of the intermediate. However, they do not have peak at 3.3 ppm, the corresponding peak in the 2,2-dimethyl-1,3-propanediamine profile is positioned at ~1.0 ppm. This large downfield shift is caused by the deshielding effects of the newly formed adjacent N=C bond.

The reduction of the intermediate with sodium borohydride results in the production of a mixture of both d,l- and meso-HM-PAO. The NMR profile of the resulting mixture in CD_3OD is presented in Figure 2.3. The presence of a mixture of the two isomers is evident from the multiplet centered at ~2.3 ppm [114]. Closer inspection of the multiplet reveals that it appears to be two overlapping quartets with different coupling constants (Figure 2.4 A). Inspection of the NMR profile of the purified meso-HM-PAO shows a clean quartet centered at ~2.3 ppm (Figure 2.4 B). From the

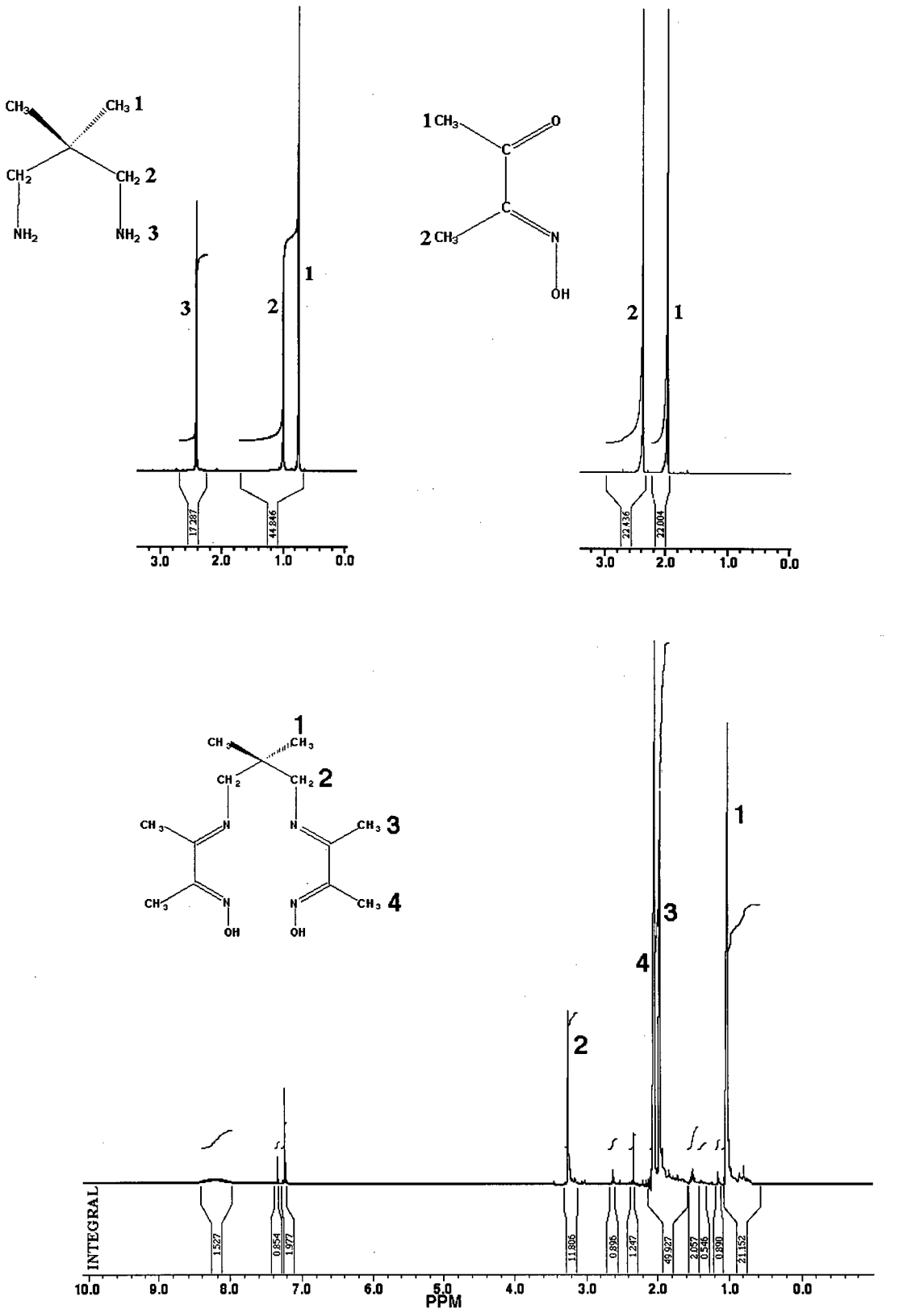

Figure 2.2. NMR of starting materials and intermediate bisimine.

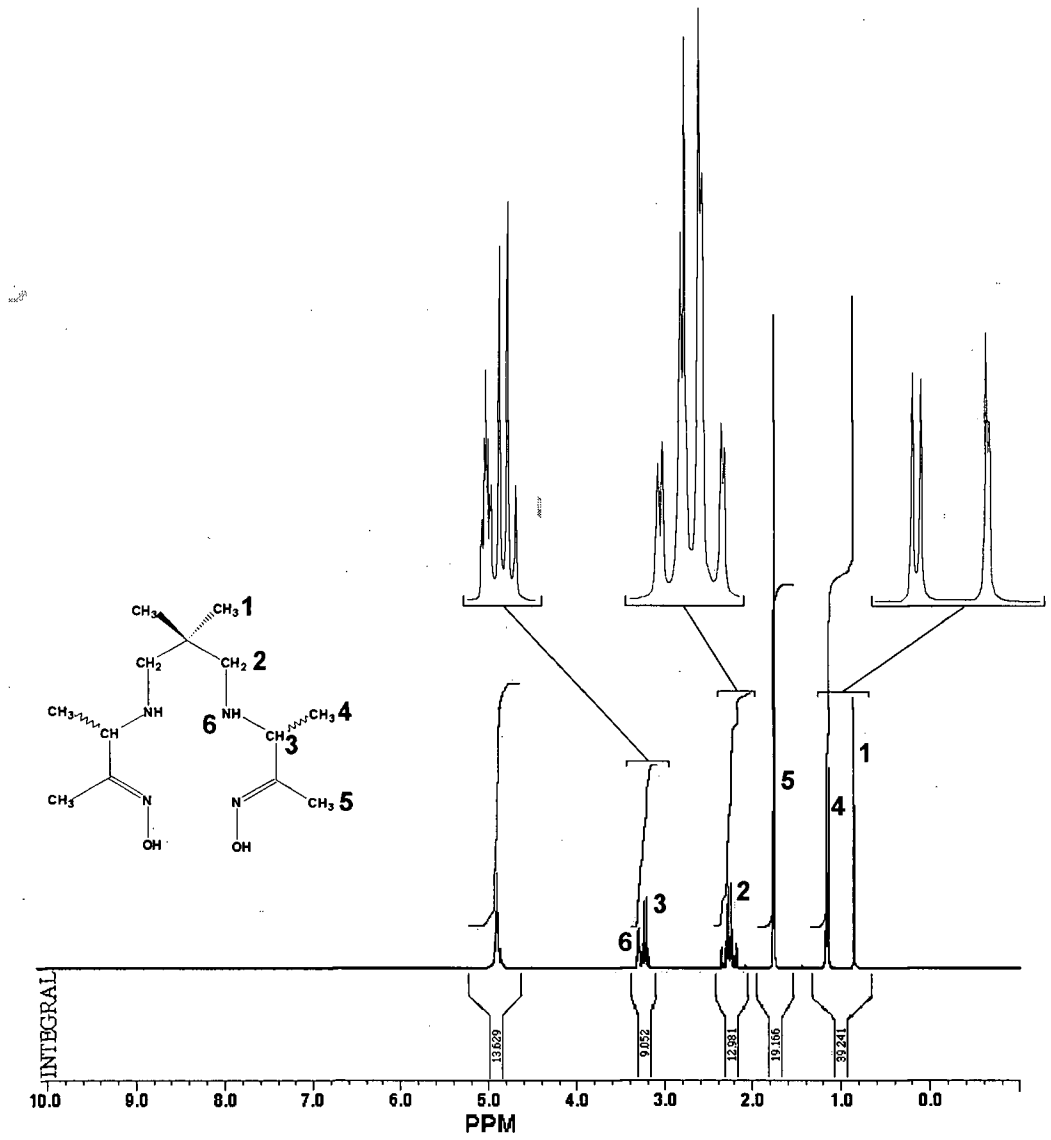

Figure 2.3. NMR of mixture of d,l- and meso-HM-PAO.

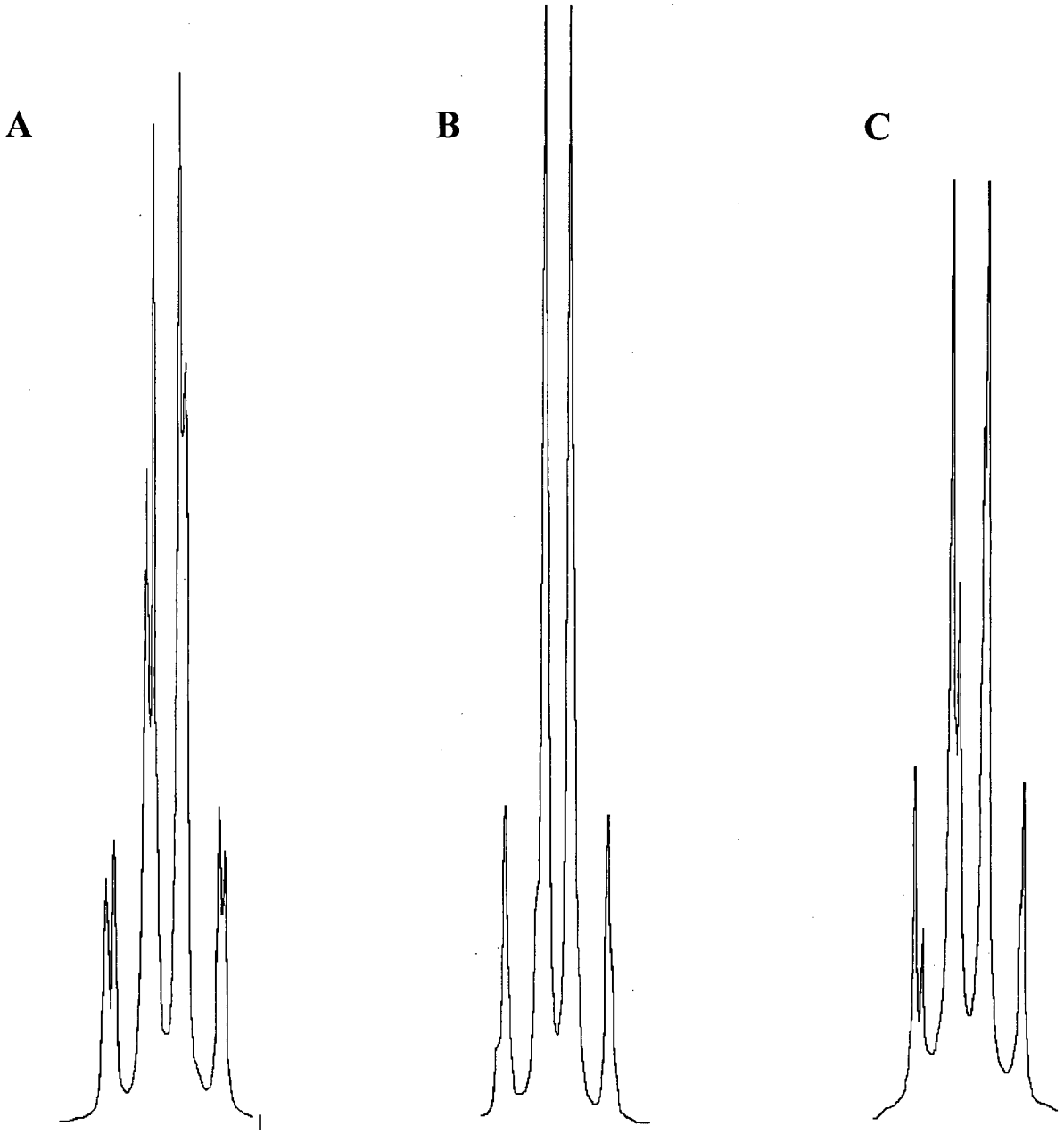

Figure 2.4. Isolated NMR profiles of quartets centered at ~2.3 ppm for unpurified (A), meso- enriched (B) and d,l- enriched (C) HM-PAO.

quartet of the unpurified (crude) mixture, there is an excess of the meso isomer compared to the d,l isomer present in the sample. After recrystallization and separation of meso-HM-PAO from acetonitrile, the resulting acetonitrile should contain a d,l-HM-PAO enriched mixture of HM-PAO. The NMR profile show that indeed there is a reversal in the intensity of the peaks of the overlapping quartets with a greater fraction of d,l present than was present in the crude unpurified mixture (Figure 2.4 C).

Removal of External Glutathione using Gel Exclusion Chromatography

Gel exclusion chromatography was examined as an alternative method for the removal of external glutathione. Vesicles (DPPC:Chol:PE-PEG 5000) were prepared using 30 mM glutathione spiked with [^{3}H]-labeled glutathione to follow the separation of internal and external glutathione. A load volume of 0.50 ml of vesicles was chromatographed on Sephadex G50 (1.5 x 18 cm column) using 0.9% NaCl as the eluant and collecting 25 drop fractions. The typical column profile is present in Figure 2.5. Vesicles eluted in the void volume of column represented by the first peak. These fractions contained vesicles with entrapped glutathione, where as free glutathione eluted in later fractions as evident from the large second peak. There was clear baseline separation between entrapped and free glutathione.

To ensure that chromatography efficiently removed external glutathione, vesicles were prepared and chromatographed. Early lipid fractions were pooled and labeled with ^{99m}Tc using the HM-PAO kits. The labeling percentages were consistently greater than 90% (93.4 ± 1.0, mean ± SD, n=8). Thus, gel exclusion chromatography is a valid alternative to centrifugation for the removal of external glutathione.

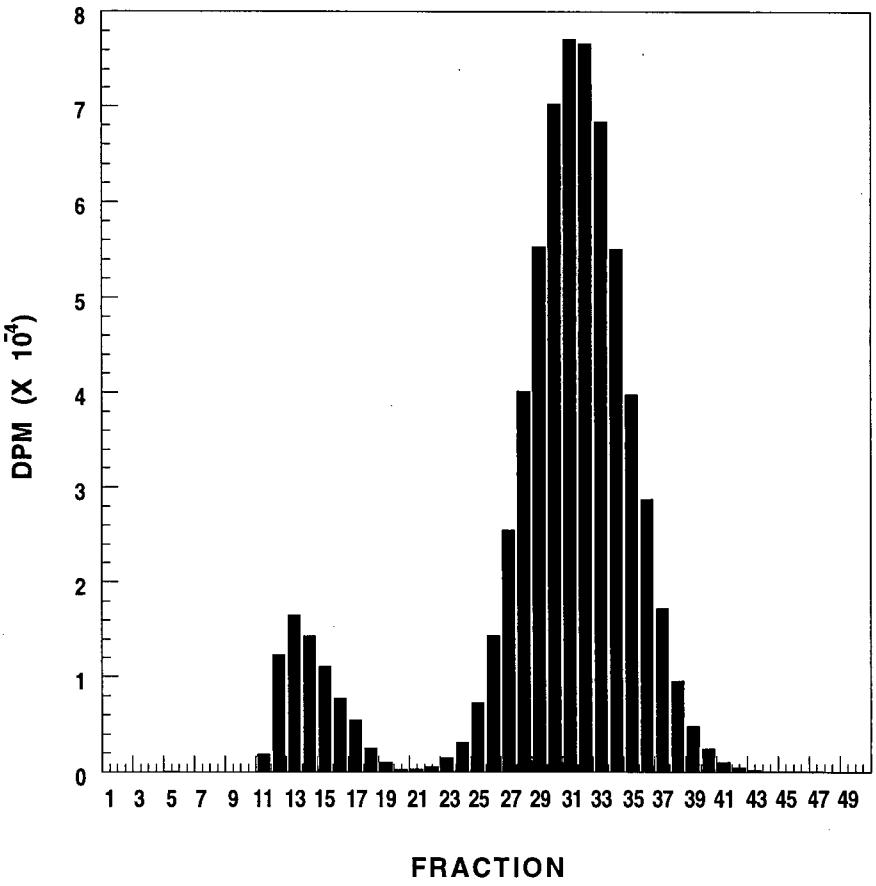

Figure 2.5. Gel exclusion separation of glutathione encapsulated within vesicles from free external glutathione. Sephadex G50 was used as the gel exclusion chromatography matrix with 0.9% NaCl as the eluant. The column was 1.5 x 18 cm with a load volume of 0.50 ml and a flow rate of 2.5-3.0 ml/min.

Effect of Lipid Composition on Labeling

Vesicles of varying lipid composition were labeled to determine the effect of lipid composition of the ability of HM-PAO to transport ^{99m}Tc across the bilayer. Also tested was the effect of temperature on labeling. The results are presented in Table 2.1. From these results, it was observed that efficient labeling of vesicles with ^{99m}Tc using HM-PAO is independent of lipid composition and, since DPPC is gel-state at 22°C but still gave excellent labeling, the physical state of the bilayer.

Table 2.1. Effect of lipid composition and temperature on labeling.

Lipid Composition (molar percentage)	**Temperature**	**Labeling % (mean ± SD)**
DSPC:PE-PEG:Chol:Vit. E (45.5:4.5:40:9:1)	22°C	96.6±1.3 (n=3)
DPPC:Chol:PE-PEG (47.65:47.65:4.5)	22°C	92.7±0.5 (n=3)
DPPC (100)	22°C	93.7, 87.8
DPPC (100)	50°C	92.5, 91.3
POPC (100)	22°C	91.2±0.8 (n=3)

Effect of Reducing the Rehydration Volume

Kits were prepared containing the same amount of each component as found in the commercially available Ceretec™ kits except that meso-HM-PAO was used instead of d,l-HM-PAO (0.5 mg meso-HM-PAO, 4.5 mg NaCl and 7.6 μg $SnCl_2.2H_2O$). The kits were rehydrated with either 5.0 ml or 0.5 ml of saline before the addition of 20 mCi of pertechnetate and followed for 30 minutes. The resulting tagging efficiencies are presented in Figure 2.6. For the kits rehydrated with 5.0 ml, there was a gradual increase in the tagging efficiency over time and reach a maximum at ~12-15 minutes after rehydration. For the kits rehydrated with only 0.5 ml of saline, the resulting tagging efficiency was much lower and reached a maximum value of ~60%.

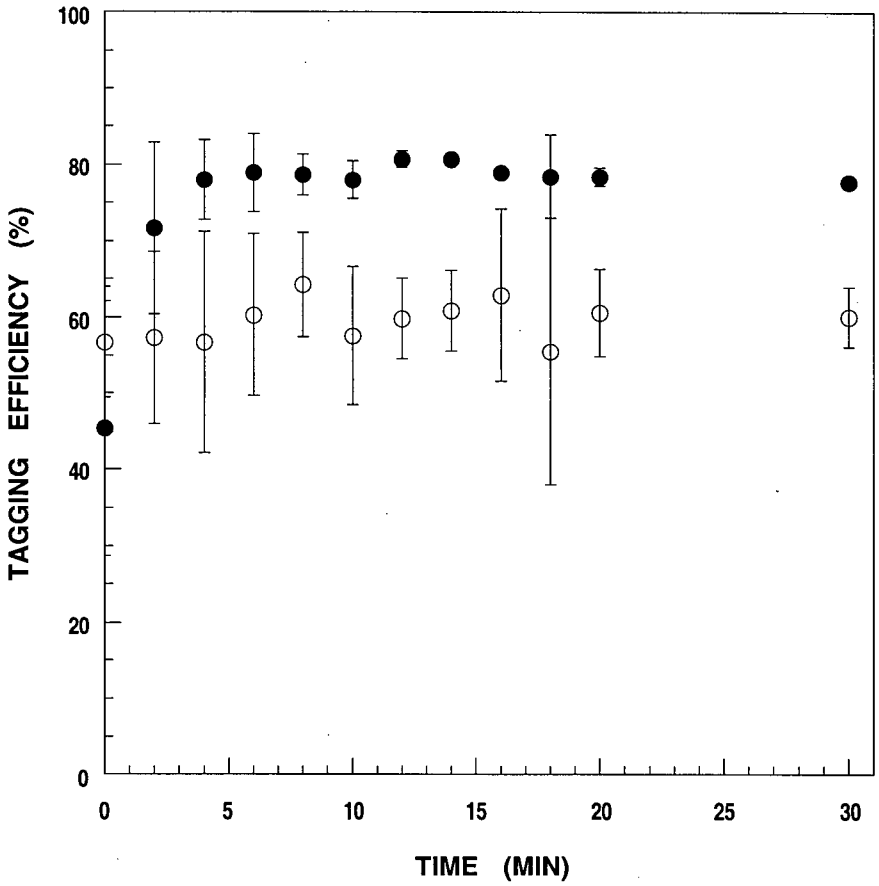

Figure 2.6. Effect of decreasing the rehydration volume from 5.0 ml (●) to 0.5 ml (○) of saline on the tagging efficiency of kits composed of meso-HM-PAO. Data represents mean ± SD (n=3).

Two Ceretec™ kits were also rehydrated with 0.5 ml of saline in order to eliminate the possibility that the decrease in tagging efficiency is due to use of meso-HM-PAO rather than d,l-HM-PAO. The Ceretec™ kits were rehydrated with 0.5 ml of saline followed by the addition of 20 mCi of pertechnetate. The kits were incubated at room temperature for 10 minutes. The resulting tagging efficiencies were 33.3 and 63.1%. Thus, the decreased tagging efficiency was not a isomer effect but was due to the decreased rehydration volume.

Effect of Varying Amount of $SnCl_2$ with 0.5 ml Rehydration Volume

Following the observed decrease in labeling efficiency due to the reduction of the rehydration volume, the amount of $SnCl_2.2H_2O$ in each kit was varied to try to increase the tagging efficiency. Kits were prepared with decreasing amount of $SnCl_2.2H_2O$ (2.85, 1.9 and 0.95 μg) and rehydrated with 0.5 ml of saline followed by the addition of 20 mCi of pertechnetate. The resulting tagging efficiencies are presented in Figure 2.7.

For kits containing 2.85 and 1.9 μg of $SnCl_2.2H_2O$, the observed tagging efficiency was similar to that observed for kits with 7.6 μg of $SnCl_2.2H_2O$ rehydrated with 5.0 ml of saline. However, the association and degradation kinetics were radically different. Tagging efficiency was maximal after 2 minutes of incubation at room temperature and did not change significantly over the time course of the experiment. Further decreasing the $SnCl_2.2H_2O$ amount to 0.95 μg resulted in a dramatic decrease in tagging efficiency indicating that there was not enough tin to reduce technetium. Kits composed of 1.9 μg of $SnCl_2.2H_2O$ were chosen as optimal over kits with 2.85 μg of $SnCl_2.2H_2O$ due to the slightly higher tagging efficiency.

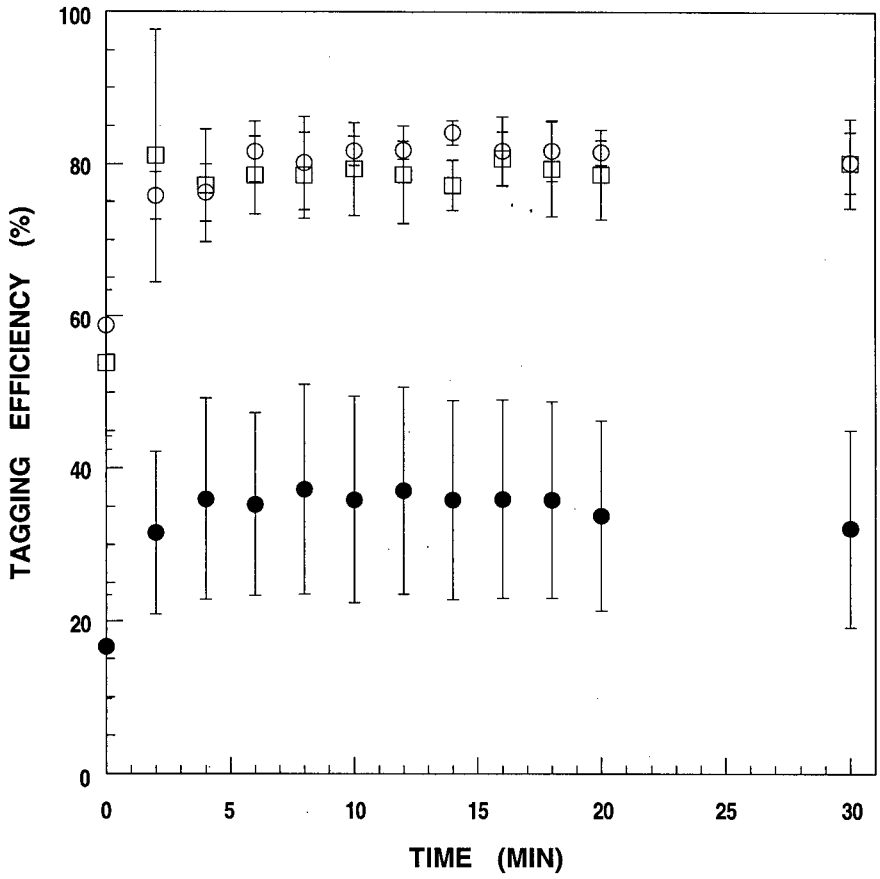

Figure 2.7. Effect of reducing the amount of $SnCl_2.2H_2O$ in each kit with a rehydration volume of 0.5 ml. Kits were prepared containing 0.95 (●), 1.9 (○) and 2.85 (□) μg of $SnCl_2.2H_2O$. Data represents mean ± SD (n=3).

Effect of Order of Rehydration

The package insert for Ceretec™ kits advise the rehydration of the kit with 5.0 ml of saline containing 20-30 mCi of pertechnetate, i.e. the simultaneous addition of saline and pertechnetate [107]. To determine if the order in which pertechnetate and 0.5 ml of saline is added to the newly formulated kits with 1.9 μg of $SnCl_2.2H_2O$ has any bearing on the tagging efficiency, kits were either rehydrated with 0.5 ml of saline containing pertechnetate (simultaneous) or first rehydrated with 0.5 ml of saline followed by the addition of pertechnetate (separate). The results are presented in Table 2.2. These results indicate that decreasing the rehydration volume to 0.5 ml requires the kits to be rehydrated with saline before the addition of pertechnetate.

Table 2.2. Effect of rehydration order on tagging efficiency

Order	Tagging Efficiency
Simultaneous	53.3, 60.7 %
Separate	90.9 ± 4.2 (mean±SD,n=5)

Effect of Generator Eluant Age

The new kits which contained 1.9 μg of $SnCl_2.2H_2O$ and a rehydration volume of 0.5 ml were used to test the effect of generator eluant age on tagging efficiency. Kits were reconstituted with 0.5 ml of saline and 20 mCi of pertechnetate that was eluted from the generator after 1 or 4 hours. The results are presented in Figure 2.8.

The new formulation showed a strong dependence on the age of generator eluant. Not only was the tagging efficiency higher for the eluant that was 1 hour old but the kinetics of degradation of the lipophilic complex were also different. For kits reconstituted with eluant that was 1 hour old, tagging efficiency achieved maximal values

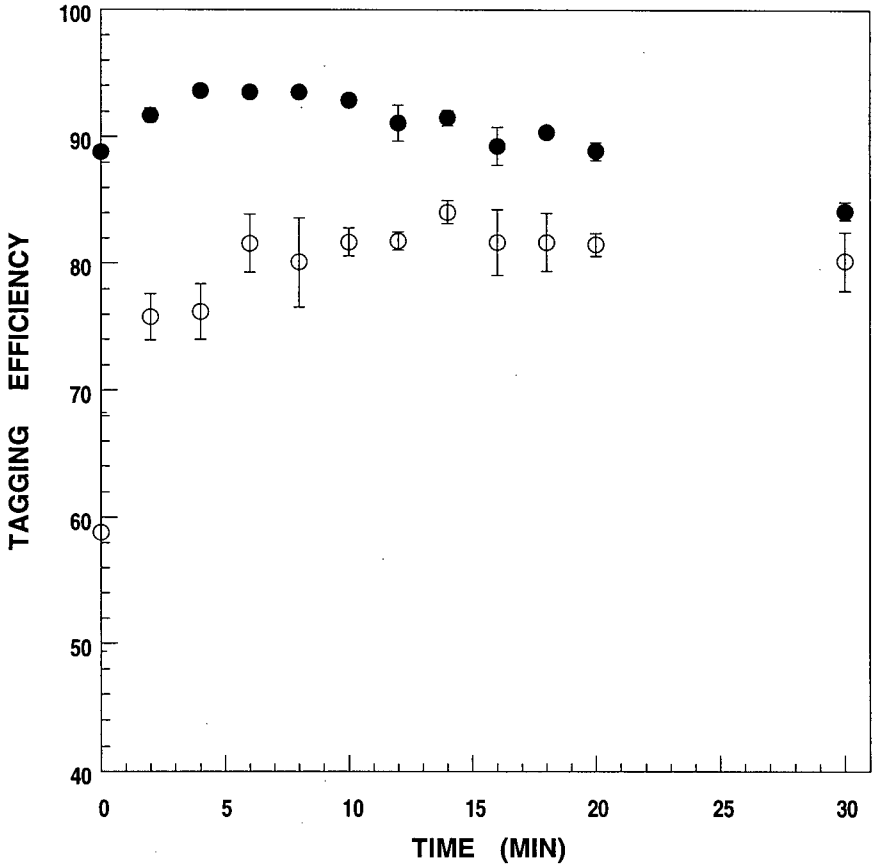

Figure 2.8. Effect on generator eluant age on the tagging efficiency. Kits containing 1.9 μg of $SnCl_2.2H_2O$, 4.5 mg NaCl and 0.5 mg of meso-HM-PAO were reconstituted with 0.5 ml of saline followed by the addition of eluant that was either 1 (●) or 4 (❍) hours old. Data represents mean ± SD, n=3.

approximately 4-8 minutes after reconstitution. For the kits reconstituted with 4 hour old eluant, the maximal value was achieved approximately 12 minutes after reconstitution. However, the kits reconstituted with 1 hour old eluant degraded much faster than kits reconstituted with the older eluant. The tagging efficiency began to decrease after 8 minutes for the 1 hour old eluant. For kits with 4 hour old eluant, the tagging efficiency remained essentially constant after reaching maximum tagging efficiency for the time course of the experiment. Although, using the 4 hour old eluant resulted in a more stable lipophilic complex, using 1 hour eluant resulted in higher tagging efficiencies.

Discussion

Although the synthesis procedure for HM-PAO appears simple and straightforward, initial attempts met with failure to produce the intermediate bisimine (Figure 2.1). The addition of the propanediamine to the keto oxime resulted in the formation of a brown benzene-insoluble oil instead of a white powder. The protocol was strictly followed according to weights to be used, solvent volumes and temperature. Further precautions were taken to weigh the propanediamine in a nitrogen filled glove bags to avoid absorption of atmospheric CO_2 without success. After repeated attempts, the purity of the starting materials was examined.

NMR profiles of both starting compounds were as expected with no obvious impurities (Figure 2.3 A and B). However, further analysis using melting point revealed that there were substantial impurities present in the 2,3-butanedione monoxime. The normal melting range of pure 2,3-butanedione monoxime is 75-78°C. The melting range of the Aldrich 2,3-butanedione monoxime started at 69°C and continued past 180°C at which point there was still some material which did not melt. These results not only indicated that there were impurities in the sample, but also that the impurities did not have any hydrogens because NMR shown no presence of contaminating substances. A literature

search found a paper describing the purification of 2,3-butanedione monoxime by recrystallization from dH_2O [115]. This method was employed to purify the 2,3-butanedione monoxime however, during the course of one recrystallization, too much water was added. In order to retrieve the keto oxime, the sample was frozen in liquid N_2 and placed on a lyophilizer. Upon retrieval of the sample the flask was empty, inspection of the cooling coil showed the formation of a coat of fine powder. This observation suggested that sublimation may be an alternative method for the purification of keto oxime.

There was no difference in the NMR profiles of the unpurified, water and sublimation purified keto oxime. However, melting point analysis showed that only the sublimed keto oxime was pure. The water purified keto oxime had a melting range similar to that of unpurified keto oxime (75-180°C). The sublimed oxime had a melting range of 74-76°C which is what was reported by the Merck index. Synthesis using the sublimed keto oxime resulted in the formation of the intermediate which was further reacted to form HM-PAO.

Using the synthesized HM-PAO, studies were undertaken to characterize and improve various aspects of labeling. Studies showed that labeling was independent of lipid composition and bilayer fluidity (Table 2.1). These observations eliminated the need for special labeling conditions, i.e. heating of dispersion, during the labeling process increasing the simplicity and ease of labeling.

Complications arose because the Ceretec™ kit rehydration protocol was modified by reducing the rehydration volume from 5.0 to 0.5 ml of saline. This modification resulted in a number of changes to the HM-PAO kit formulation and rehydration procedure. These changes may stem from the complex reaction between ^{99m}Tc and stannous ions. Technetium is eluted from the $^{99}Mo/^{99m}Tc$ generator in the VII oxidation

state and must reduced to V in order to chelate to HM-PAO [101]. The most common agent used for this reduction are stannous ions (Sn^{2+}). However, the reduction of technetium with tin is not as simple as adding Sn^{2+} to technetium in the presence of HM-PAO. The dissolution of stannous compounds in aqueous media results in the formation of stannous hydroxides which forms a colloid and precipitate out of solution as a white, cloudy gel-like substance [116]. The colloidal tin can not reduce technetium and significantly decreases the percentage of added ^{99m}Tc which is reduced and can form the ^{99m}Tc/HM-PAO lipophilic complex (i.e. tagging efficiency).

There is a fine line determining the amount of stannous ions required for the complete reduction of ^{99m}Tc and while minimizing colloid formation [117-119]. The addition of too much tin results in colloid which can trap ^{99m}Tc within the colloid matrix, dramatically lowering the tagging efficiency. Not enough tin results in the incomplete reduction of technetium which decreases the amount of ^{99m}Tc (V) available to bind to HM-PAO. The key factor in determining the optimal amount of stannous ions, oddly enough, is determined by the ratio of chelator-to-tin and not by technetium-to-tin. This ratio is unique and different for each chelating compound and subtle variations in this ratio, by as little as a factor 2, can result is poor tagging efficiencies [89].

The previous studies have focused only on the absolute molar chelate-to-tin ratio [89,117-119]. These studies demonstrate that the chelate-to-tin ratio is also dependent on the absolute concentration of ligand and tin in solution. Keeping the amount of HM-PAO constant in each kit, the results showed that reducing the rehydration volume to 0.5 ml reduced that amount of $SnCl_2.2H_2O$ required per kit from 7.6 μg to 1.9 μg. Another interesting observation was the effect of rehydration order on the tagging efficiency. Poor tagging efficiencies resulted if the pertechnetate was included in the initial 0.5 ml volume used to reconstitute the kits. High tagging efficiencies could only be achieved if the kit was first rehydrated with 0.5 ml of saline followed by the addition of pertechnetate. The

results also showed that freshly eluted pertechnetate must be used to reconstitute meso-HM-PAO kits, similar to the requirement for Ceretec^{TM} kits, to achieve high tagging efficiencies [107]. Although this requirement may seem trivial, it imposes some limitations to the potential use of PEG-vesicles as imaging agents in the clinical setting.

At major hospital sites the acquisitions of fresh pertechnetate is of little concern because the nuclear medicine department will have its own $^{99}Mo/^{99m}Tc$ generator and the acquisition of fresh pertechnetate simply requires the elution of the generator. However, difficulties arise at smaller hospitals, for example University Hospital at UBC. Due to funding cut back and staffing issues, University Hospital's nuclear medicine department no longer has it's own $^{99}Mo/^{99m}Tc$ generator. The department receives a daily allotment of pertechnetate shipped from Vancouver General Hospital (VGH) every morning. The pertechnetate arrives at University hospital approximately 1 hour after it has been eluted from the generator at VGH. Thus, vesicles must be labeled immediately after it arrives to achieve the greatest labeling percentages. This would normally not pose a problem in everyday running of the nuclear medicine department. It would require those imaging procedures using radiolabeled vesicles to be scheduled in the morning, so that the vesicles can be labeled and administered to the patient. Another way around this problem is that knowing the number of procedures for the day, a large batch of vesicles can be labeled in the morning. Then during the course of the day, labeled vesicles can be drawn from the initial batch to be administered to the patients. Problems arise when unscheduled emergency cases which arrive during the day or during non-scheduled hours when nuclear medicine technicians are on call. At VGH, this would not be a problem, because pertechnetate can be freshly eluted if needed. However, at University Hospital labeling could be a problem because of the lack of freshly eluted pertechnetate. Although this requirement will place restrictions on the use of vesicles in some locations, this should not however, detract from the general utility of vesicles as imaging agents.

Chapter 3:

Circulation Kinetics of PEG-Coated Vesicles Labeled with ^{99m}Tc

Introduction

The extended circulation half-life and decreased RES activity make PEG-coated vesicles ideal for blood pool imaging studies [see Chapter 1]. Recently, Goins et al. has demonstrated that radiolabled PEG-coated vesicles provide comparable results to radiolabeled RBCs in rabbits [120]. Thus, studies were undertaken to determine the ideal PEG concentration and lipid dose suited for the potential utility of PEG-vesicles as an imaging agent.

Materials

See Chapter 2 with the exception that PE-PEG 5000 was synthesized as described [87]. HM-PAO was used as the commercially available Ceretec^{TM} kit from Amersham (Mississauga, Ont.).

Methods

Preparation of lipid vesicles

Lipids were combined from stock solutions of known lipid concentration in chloroform to give a final mole ratio composition of DSPC/PE-PEG 5000/Chol/DMPG/ Vit. E (43:4.5:40:9:1). Preparation procedure as described in Chapter 2.

Labeling of vesicles

The labeling procedure used was a modification of Phillips et al. [104] as follows. Vesicles were chromatographed as described in Chapter 2. Early vesicles fractions were pooled to give 2 ml of lipid dispersion from which samples were removed for phosphorus assay. The lipid concentration was subsequently adjusted to 2 - 10 mM by addition of saline. A Certec^{TM} kit was reconstituted with 70 mCi of pertechnetate in 5 ml 0.9% NaCl and incubated for 10 minutes at room temperature. Then 0.8 ml of the ^{99m}Tc/Ceretec^{TM} solution was added to chromatographed vesicles. The mixture was incubated for 10 minutes at room temperature before use.

Biodistribution Studies

All animal studies were conducted in accordance with the principles contained in the Care of Experimental Animals - published by the Canadian Council on Animal Care (institutional animal care certificate #A93-1386). New Zealand white rabbits (2 - 3 kg) were injected via the ear vein with vesicles at a total lipid dose of ~ 0.2, 0.5, 1.3 and 2.1 μmol/kg. The vesicle dispersion was diluted with saline so that the injection volume at each lipid dose was the same. Planar radionuclide scans were obtained using Siemens mobile digital camera equipped with an appropriate collimator. Anterior images were acquired using a 128 x 128 matrix for a total of 350,000 counts at 1 minute, 1, 2, 4, 6, and 8 hours post injection. Regions of interest centered upon heart, liver, kidney, and bladder were identified and both counts and pixel number from those regions determined using commercial software. Counts in the region bounded by the heart were taken as a measure of counts in the circulation. Normalized counts were calculated by taking the counts associated with the heart immediately after administration to be 100%. The counts associated with the heart at subsequent time points were calculated as a percentage of original activity.

Results

Effect of PEG Concentration

Vesicles containing varying amount of PEG (0, 3.0 and 4.5 mol%) were prepared and injected into rabbits at a lipid dose of approximately 2.1 μmol/kg. The dependence of PEG content on the circulation clearance behavior of vesicles is presented in Figure 3.1. As expected, unmodified vesicles were quickly cleared from the circulation resulting in a circulation half-life of approximately 30 minutes. The inclusion of PEG dramatically altered the circulation behavior of vesicles. The resulting circulation half-life at PEG concentrations of 3.0 and 4.5 mol % was approximately 5 and 20 hours. To a good first approximation, the clearance of activity from the circulation was monoexponential. There were also significant changes in the biodistribution of activity (Figure 3.2). Immediately after injection of labeled vesicles with or without polymer, the heart and liver showed as area of primary activity (Figure 3.2 A). The vena cava and other principle structure of the vascular tree were also well visualized. After 8 hours, the biodistribution was radically different for the vesicles containing 4.5 mol % (Figure 3.2 C) compared to unmodified vesicles (Figure 3.2 B). For unmodified vesicles, the majority of the activity was associated with the liver and bladder, indicating RES uptake and removal of vesicles and activity from the circulation. In striking contrast, vesicles with 4.5 mol % PEG exhibited high activity still associated with the heart as well as the liver after 8 hours. The major structure of the vascular tree were also well visualized indicating that there is still a large amount of activity left in circulation.

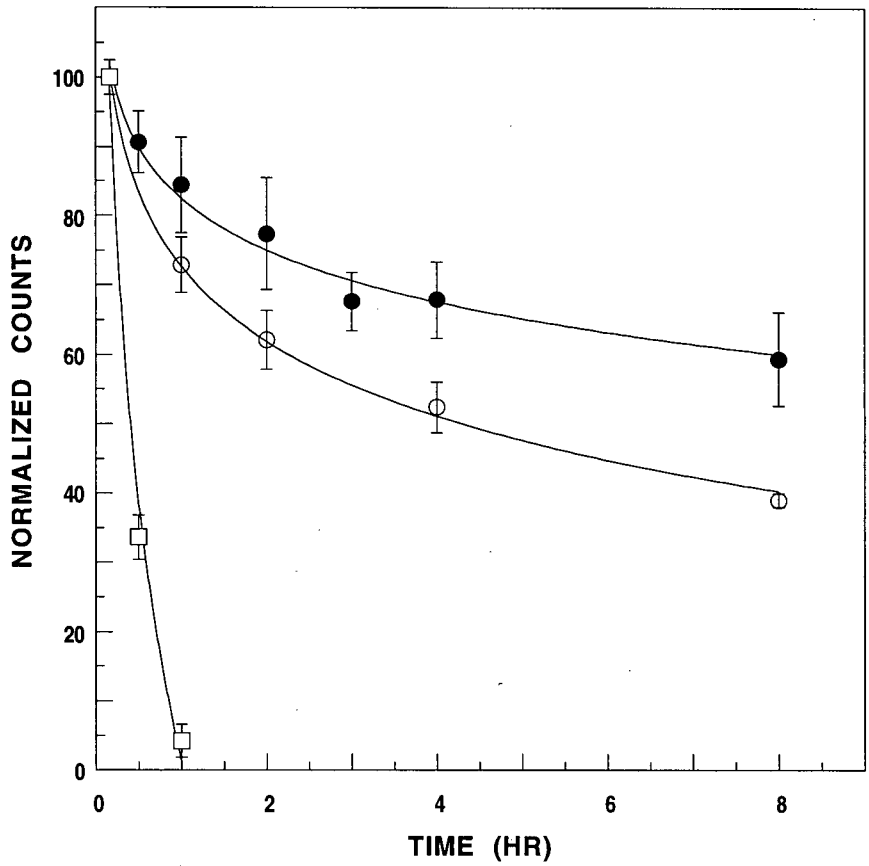

Figure 3.1. Effect of varying the amount of PEG in vesicle composition on circulation clearance kinetics. Vesicles were prepared with 0 (□), 3.0 (○) and 4.5 (●) mol% PEG and administered to rabbits at a lipid dose of ~2.1 μmol/kg. Data points represent mean ± SD, n=4.

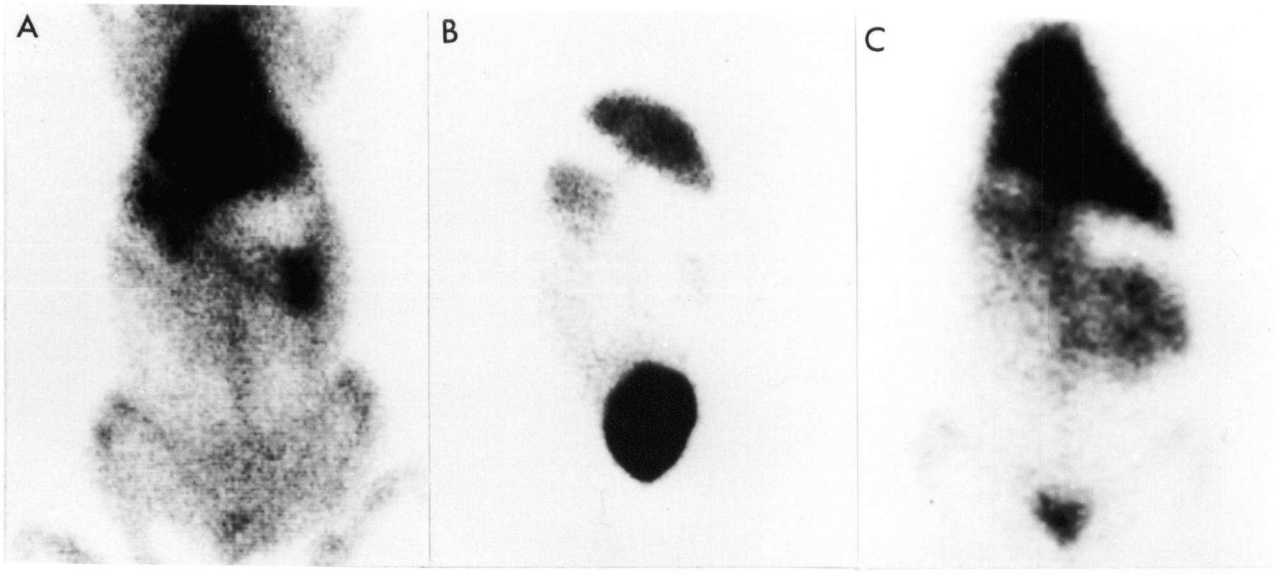

Figure 3.2. Typical gamma images of rabbits immediately (A) after injection of vesicles and 8 hours after injection for vesicles without (B) and with (C) 4.5 mol% PEG. The lipid dose was ~2.1 μmol/kg.

Effect of Lipid Dose

Figure 3.3 shows typical images for images for rabbits acquired immediately (A) and 8 hour post-injection at lipid doses of 0.2 (B), 0.5 (C), 1.3 (D), and 2.1 (E) μmol/kg. As before, immediately after injection the majority of the activity was associated with regions bounded by the heart and liver with the kidneys and major elements of the vascular tree also well visualized (Figure 3.3 A). For the highest lipid dose (2.1 μmol/kg) at 8 hour post administration the heart and liver still showed as areas of highest activity with the kidneys and vena cava still well visualized. At a lipid dose of 1.3 μmol/kg (Figure 3.3 D) there was a slight decrease in the activity associated with the heart and a slight increase in the activity associated with the liver and kidneys suggesting an increase in the rate of RES clearance. At a lipid dose of 0.5 μmol/kg (Figure 3.3 C), the majority of the activity was found in the liver; however, the region bounded by the heart remained well visualized . Finally at a lipid dose of 0.2 μmol/kg the corresponding 8 hour image shows effectively zero activity in the heart and the majority of activity in the liver, spleen and bladder.

Figure 3.4 graphs the biodistribution of PEG-modified lipid vesicles at the four lipid doses of 2.1 (A), 1.3 (B), 0.5 (C) and 0.2 (D) μmol/kg respectively. To a good first approximation (Pearson's $r > 0.98$), the clearance of liposomes from circulation was monoexponential for all lipid doses. As the lipid dose decreased there was a slight increase in the activity (counts/pixel) associated with the liver and greatly increased renal elimination with pooling in the bladder. The clearance of activity from the circulation at the four lipid doses, expressed as a percentage of the activity associated with the heart immediately after injection, is presented in Figure 3.5. The calculated circulation half-lives for lipid doses of 2.1, 1.3, 0.5, and 0.2 μmol/kg were 20.6 ± 4.5 (n=6), 16.5 ± 9.3 (n=5), 4.3 ± 1.8 (n=5), and 2.6 ± 1.6 (n=7) hours (mean ± SD), respectively.

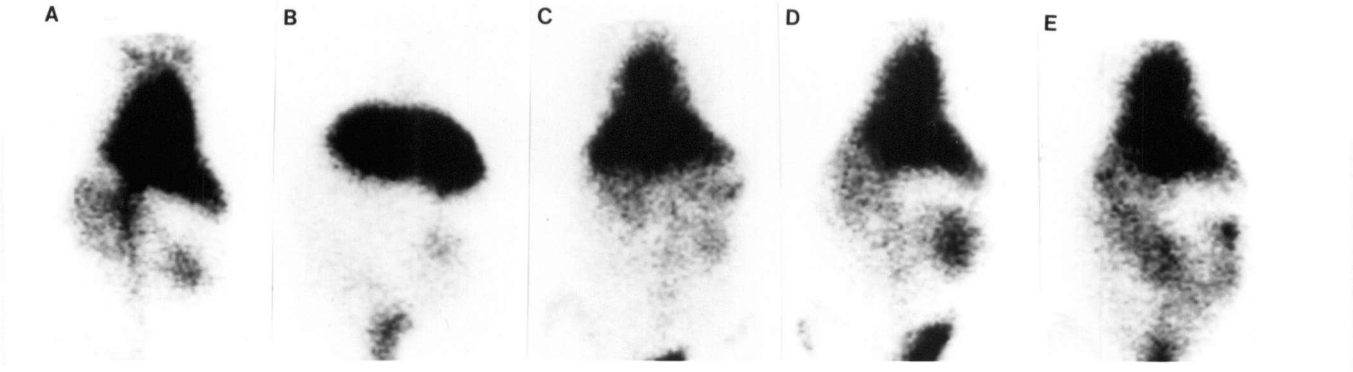

Figure 3.3. Typical gamma images of rabbits immediately (A) after injection of vesicles and 8 hours after injection at lipid doses of 0.2 (B), 0.5 (C), 1.3 (D) and 2.1 (E) μmol/kg.

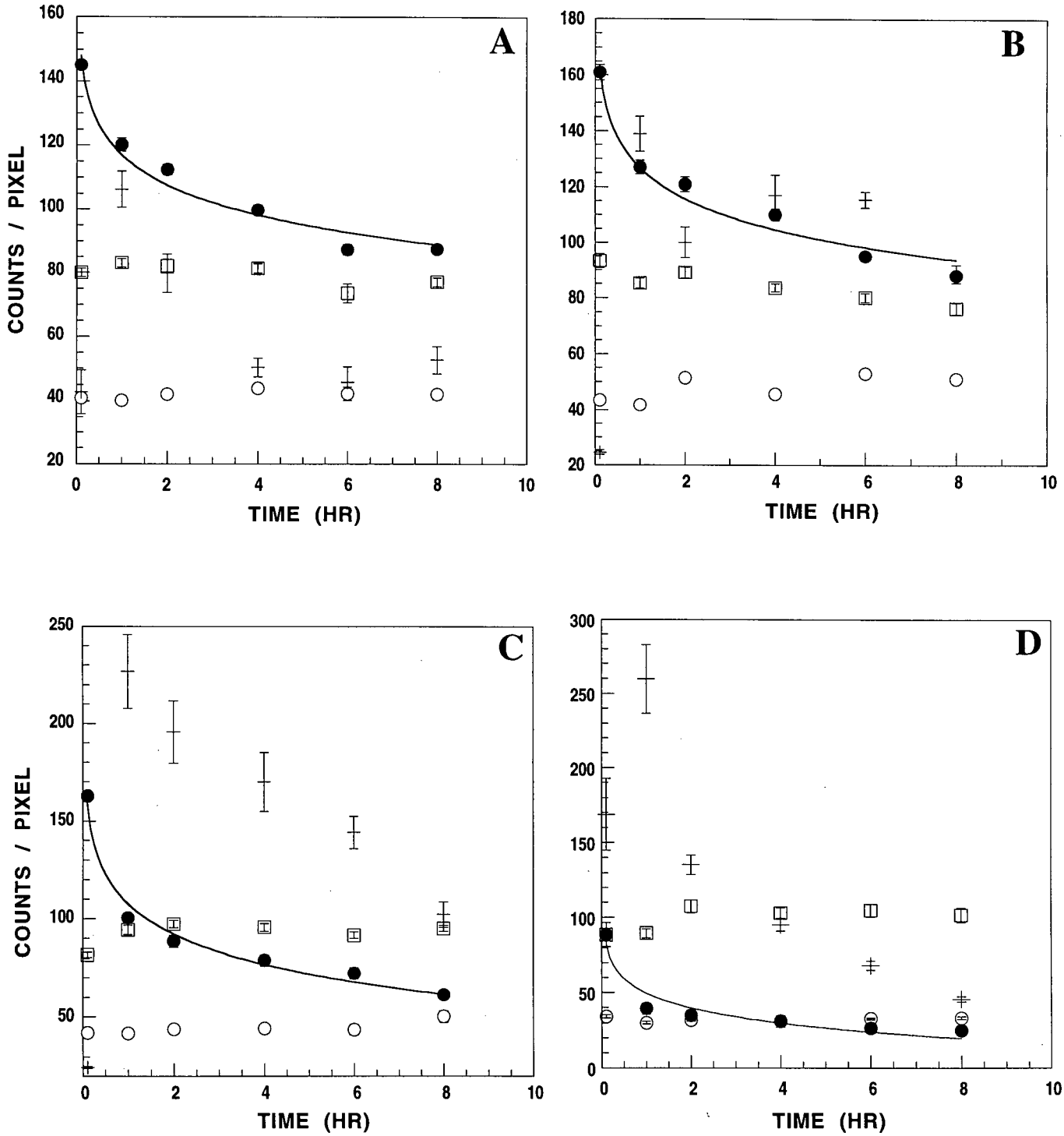

Figure 3.4. Effect of Lipid Dose on Biodistribution of PEG-Coated Vesicles. The distribution of radioactivity at lipid doses of 2.1 (A), 1.3 (B), 0.5 (C) and 0.2 (D) μmol/kg in the heart (●), liver (□), kidney (○) and bladder (+). Data points represent mean ± SD for 8 rabbits.

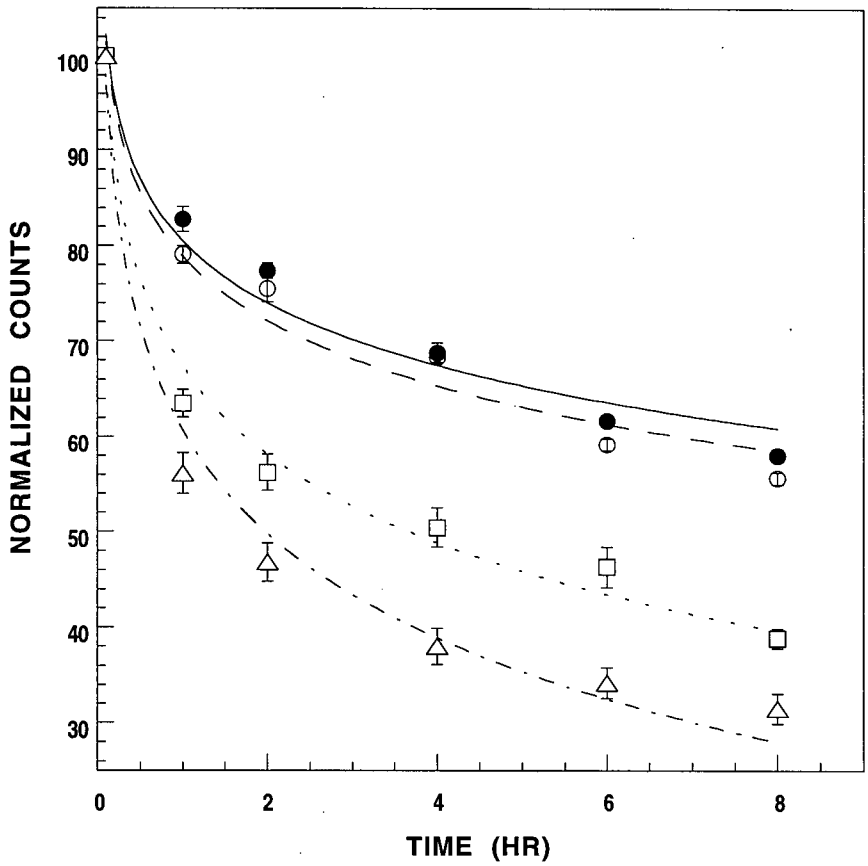

Figure 3.5. Clearance of PEG-coated vesicles from circulation at lipid doses of 2.1 (●), 1.3 (○), 0.5 (□) and 0.2 (△) μmol/kg. Counts in the area bounded by the heart were taken a measure of counts in the circulation. Normalized counts were calculated by assuming counts in the area bounded by the heart immediately after injection to be 100. Counts associated with the heart at later time points were compared to the initial value to get a percentage of activity remaining in the circulation. Data points represent mean ± SD for 8 rabbits.

Along with a long circulation half-life, a suitable substitute to radiolabeled RBCs must not accumulate in area which may obscure the organ of interest. In terms of cardiac imaging, excessive liver accumulation may interfere with cardiac images. The heart-to-liver ratios over time for the four lipid doses are given in Table 3.1. Immediately after injection, the heart to liver ratios for the three higher lipid doses were > 1.0, indicating a greater intensity of activity associated with heart compared to the liver. For the lowest lipid dose the ratio was < 1.0 immediately after injection indicating rapid uptake into the liver. At a lipid dose of 0.5 μmol/kg, the activity associated with the liver was greater than the heart after 1 hour. The two highest lipid doses, 1.3 and 2.1 μmol/kg, the ratios were similar and were > 1 through the entire time course of the experiment.

Table 3.1. Heart-to-Liver ratios at each lipid dose as a function of time.

Time Post-Injection (hr)	Lipid Dose (μmol/kg)*			
	0.2	**0.5**	**1.3**	**2.1**
0	0.9 ± 0.6	2.0 ± 0.2	1.8 ± 0.3	1.8 ± 0.1
1	0.4 ± 0.3	1.1 ± 0.3	1.5 ± 0.2	1.5 ± 0.3
2	0.4 ± 0.3	0.9 ± 0.3	1.4 ± 0.1	1.4 ± 0.2
4	0.2 ± 0.1	0.9 ± 0.3	1.3 ± 0.1	1.3 ± 0.3
6	0.3 ± 0.2	0.8 ± 0.3	1.2 ± 0.1	1.3 ± 0.2
8	0.3 ± 0.3	0.7 ± 0.2	1.1 ± 0.1	1.1 ± 0.2

* data represents mean ± SD for 8 animals

Discussion

The results presented herein describe the biodistribution and blood pool clearance kinetics of PEG-modified lipid vesicles with 4.5 mole percent PEG at lipid doses of 2.1, 1.3, 0.5 and 0.2 μmol of total lipid/kg of body weight. At these lipid dose, the observed circulation half-lives were ~20.6, 16.4, 4.3 and 2.6 hours, respectively.

The biodistribution of activity was similar for lipid doses of 2.1 and 1.3 μmol/kg (Figure 3.4 A and B). The activity associated with the heart remained greater than the activity associated with the liver during the time course of the experiment. This was also

reflected in the heart-to-liver ratio which were greater than 1 at all time points (Table 3.1). A change in the biodistribution was observed when the lipid dose was decreased to 0.5 μmol/kg (Figure 3.4 C). After 1 hour, the activity associated with the liver was greater than that of the heart. Also, the liver activity increased from 0 - 2 hours after which it remained constant. At 0.2 μmol/kg, the activity associated with the liver was greater than that of the heart at all time points (Table 3.1). The activity associated with the liver increased over the first 2 hours indicating active uptake and removal of vesicles from the circulation with a concomitant decrease in activity in the blood pool. There was a greater increase in liver activity at 2 hours for 0.2 μmol/kg (21.6%) than for 0.5 μmol/kg (18.8%). This increase in liver activity between 0 - 2 hours was not observed for the two higher lipid doses.

At first glance, these results appears to contradict the current body of literature, which reports that the circulation half-life of PEG-modified vesicles are essentially independent of lipid dose [59-64]. However, these studies were limited to the dose range of 3 - 400 μmol/kg. This work is the first to describe the circulation behavior of PEG-modified vesicles below a lipid dose of 3.0 μmol/kg. At doses of 2.1 and 1.3 μmol/kg, these results are consistent with the literature and, within experimental error, there was no significant difference in the resulting circulation half-life (Kruskal-Wallis ANOVA, $p>0.05$). Thus, the dose-independent range of PEG-modified vesicles can be extended from 3.0 to 1.3 μmol/kg. However, at lipid doses of 0.5 and 0.2 μmol/kg, there was an observed dose-dependent circulation half-life (Kruskal-Wallis ANOVA, $p<0.05$).

The exact mechanism of recognition and removal of vesicles and other particulates from the circulation by the RES is still poorly understood. Also, poorly understood is the mechanism by which polymers, such as PEG, extend the circulation half-life of particulates modified with these polymers [57,58]. It has been suggested that PEG creates a steric barrier on the surface of vesicles preventing either the activation and binding of

serum opsonins or preventing the recognition of bound opsonins [121-123]. Potential serum opsonins include IgG, complement component C3 and fibronectin. Much of the data on the identity and role of serum opsonins in RES uptake of vesicles has been acquired using the single pass liver perfusion system [65,124-127]. These studies showed that liver uptake is greatest when vesicles are preincubated with serum and that liver uptake could be abolished by addition of anti-C3 antibodies or heating the serum, both of which inactivate the complement system. The exact role of immunoglobins is still unclear, but may play a small role in recognition and opsonization [128]. These results are complicated by the observation that the extent of serum mediated liver uptake is species dependent [65,127]. Mice exhibit serum-independent uptake while rats show serum-dependent uptake.

It was believed that long circulation half-lives observed at high lipid doses resulted from saturation of the RES. However, recent studies have shown that there was no saturation of lipid uptake by the RES, but that the limiting factor was the pool of serum components involved in recognition and uptake [129,130]. At low lipid doses, there was a greater amount of protein bound per vesicles than at high lipid doses. Thus, increasing the lipid dose increases the number of vesicles that a fixed amount of blood protein must bind. Although decreasing the amount of bound protein per vesicle increases the circulation half-life, the lipid composition, most importantly the incorporation of charged lipids, also plays a role [126,128,131]. Different lipid compositions bind differing amounts of protein but even when the amount of protein for two different lipid compositions is the same, the circulation half-life may be radically different. Oja et.al. observed that PC/CHOL/DOPA (35:45:20) vesicles at 1000 mg/kg bound the same amount of protein as DSPC/CHOL (55:45) vesicles at 200 mg/kg but that the DOPA vesicles had a half-life of 75 min while the DSPC vesicles had a 450 min half-life [129]. These results indicate that specific proteins are responsible for binding to specific lipid

compositions which are involved in the removal of vesicles from circulation. However, the amount of protein per vesicles does not necessarily correlate to the circualtion half-life.

In all these studies, the most consistent finding is that small, unmodified vesicles composed of neutral lipids minimally activate the complement system and have the greatest *in vivo* longevity. However, the lipid doses required to achieve circulation time similar to those observed for PEG-modified vesicles are orders of magnitude greater. For example, the highest lipid doses tested in this paper, converting from μmol/kg, corresponds to ~3.0 mg/kg and the circulation half-life was calculated to be approximately 1200 min. Thus, based on the previous observation that there is a limited protein pool responsible for binding and recognizing specific lipid compositions, the long circulation half-lives of PEG-modified vesicles at very low lipid doses, compared to unmodifed vesicles, may be due to presence of an even smaller 'apparent' protein pool responsible for recognition compared to small, neutral liposomes. Apparent is used to describe this protein pool due to the possibility of three different mechanisms that may be at play; 1) the protein pool may be similar to that of neutral liposomes, but that PEG may interfere with the recognition of bound opsonins, 2) PEG may prevent the binding and activation of opsonins, or 3) a combination of the first two. Thus, a direct parallel between unmodified and modified vesicles can be extrapolated. In both cases a dose dependent circulation half-life is observed until a 'saturation' point is observed, after which further increases in lipid dose does not result in increased circulation half-life.

In terms of nuclear medicine blood pool imaging agent, the observed dose-dependent circulation half-life of PEG-modified vesicles would provide a means of determining the lipid dose required for a given procedure, assuming that the results observed in rabbits are directly transferable to humans. For example, for equilibrium gated radionuclide studies such as wall-motion analysis, ejection fractions, ventricle size and rate of contraction and relaxation, a circulation half-life of approximately 2-3 hours would

be sufficient. For procedures such as gastrointestinal bleeding detection, a long circulation half-life, i.e. >20 hours, is required due to the intermittent nature of some GI bleeding (see Chapter 1). Thus, a lipid dose of ~0.5 μmol/kg (0.70 mg/kg) would be required for most cardiac assessments, while a lipid dose of >1.3 μmol/kg (1.40 mg/kg) would be required for GI bleed detection.

In summary, the results presented better define the lipid doses required for future human testing of PEG-modified vesicles for nuclear medicine imaging procedures. A lipid dose of ~0.5 μmol/kg would be adequate for most cardiac studies, while higher lipid doses of the order of ~2.0 μmol/kg would be needed for GI bleed detection. These results may also help in the elucidation of the mechanism of PEG-modified vesicles longevity *in vivo* by drawing a parallel to the observed circulation kinetics of neutral unmodified vesicles and charged vesicles.

Chapter 4:

Methods to Increase the Lipid Concentration

Introduction

Based on the results presented in Chapter 3 and assuming that the circulation behavior observed in rabbits is directly applicable to humans, a lipid dose of ~1.0 μmol/kg would be adequate for most nuclear medicine imaging procedures [5]. Thus, an average volunteer weighing ~80 kg would require the administration of 80 μmol of total lipid. Chromatography to remove external glutathione invariably leads to the dilution of the lipid dispersion. Although the dilution factor is dependent on the flow rate, load volume and column dimensions, chromatography typically results in a 15 fold dilution in the lipid concentration. Thus, starting with an initial lipid concentration of ~160 mM, the lipid concentration after chromatography would be ~10-15 mM. At this lipid concentration, the average patient requiring ~80 μmol of lipid would require a volume of 5-8 ml plus the volume of the ^{99m}Tc/HM-PAO solution (~0.5 ml). For normal equilibrium blood pool studies this large a volume would not be an issue. However, this volume is too large for first pass studies of cardiac function which require that the radioactivity be injected in a total volume of ~1.0 ml [5]. Thus, a method to increase the lipid concentration or an alternative method for the production of vesicles was required. Two separate methods were developed and examined to increase the lipid concentration. The first method involves the use of centrifuge filters to remove excess untrapped saline from the vesicle dispersion after chromatography. The second method involved the use of a pH gradient to inactivate untrapped glutathione rather than removal by chromatography.

Ultrafiltration using commercially available centrifugal filter units provides a simple and rapid method for the separation of mixtures based on size. The molecule or aggregate of interest can be selected for by choosing the appropriate molecular weight

cutoff filter such that the molecule is either trapped by the filter or allowed to pass through the filter [132-134]. The ability to separate molecules and aggregates based on size was exploited as a possible means to increase the lipid concentration of vesicle dispersions. After chromatography, the resulting pooled lipid dispersion underwent centrifugation using either 10,000 or 30,000 molecular weight cutoff filters at low g forces to remove excess untrapped saline.

The use of a pH gradient was based on the hypothesis that glutathione may simply act as a reductant for HM-PAO and that the interfering effects of external glutathione could be decreased by altering the pH [107]. This would eliminate the need for chromatographic removal of external glutathione and the resulting dilution of the vesicle dispersion. However, the principle of using pH gradient in the following experiments differs from that described in remote loading [90,135-138]. In remote loading, the molecule of interest transverses the lipid bilayer without the assistance of a carrier molecule and is converted to an impermeable form. In ^{99m}Tc/HM-PAO labeling, the pH gradient is used to modulate the interaction between glutathione and HM-PAO.

Materials

See Chapter 2. 10,000 and 30,000 nominal molecular weight limits (NMWL) Ultrafree MC filter units equipped with low-protein-binding regenerated cellulose filters were obtained from Millipore Ltd. (Nepean, ON). Citric acid, N-[2-hydroxyethyl] piperazine-N'-[2-ethanesulfonic acid] (HEPES) and sodium hydroxide was obtained from BDH Inc. (Toronto, ON). Meso-HM-PAO was synthesized as described in Chapter 2.

Methods

Preparation of Vesicles

Lipids were combined from stock solutions of known lipid concentrations in chloroform to give final molar concentrations of DPPC/Chol/PE-PEG5000 (47.75:47.75:4.5) and DPPC/Chol/PE-PEG5000/POPE-flourescein (47.65:47.65:4.5:0.2). Preparation of vesicles same as described in Chapter 2 with the modification that a batch of vesicles was prepared using 30 mM glutathione in 0.9%(w/v) NaCl spiked with [^{3}H]-glutathione.

Centrifugation of Vesicles

Vesicles were chromatographed as described in Chapter 2. Initial studies to determine the appropriate molecular weight cutoff filter, recovery efficiency and centrifugation times were determined using 400 μl maximum sample volume 10,000 and 30,000 NMWL Millipore Ultrafree MC filter units. Before addition of vesicles, the filters were prewashed with 400 μl of saline. Vesicles were centrifuged using an Eppendorf benchtop centrifuge at 1,600 x g for 15 minute periods for a total of 2 - 2.5 hours. After each 15 minute interval, the content of the sample reservoir were mixed and the filtrate volume measured. After determination of various parameters, the procedure was scaled up using Millipore Ultrafree MC filter units with a maximum volume of 20 ml.

The ability of lipids to pass through the filters was qualitatively determined using vesicles labeled with fluorescein labeled lipid. After centrifugation, the filtrate and concentrated vesicles were analyzed under UV light for fluorescence activity. The stability of vesicles to the loss of internal glutathione during centrifugation was assayed using vesicles internally labeled with [^{3}H]-glutathione. Vesicles were chromatographed to

remove untrapped glutathione and [^{3}H]-glutathione. After centrifugation of vesicles, the resulting filtrate and concentrated vesicles were assayed for radioactivity using a Philips model PW4700 liquid scintillation counter (Holland).

Preparation of HM-PAO Kits

As described in Chapter 2.

Determination of Tagging Efficiency

As described in Chapter 2

Labeling Procedure

An HM-PAO kit was rehydrated with 0.50 ml of low oxygen saline (Technelite, Du Pont Radiopharmaceuticals, Billerica, MA). After complete dissolution of contents, ~10 mCi of sodium pertechnetate was added and incubated for 15 minutes with intermittent mixing. After incubation, 50 or 100 μl of the resulting solution was added to prepared vesicles. The vesicles were incubated for 5 minutes, with mixing, before chromatography on BioGel minicolumns.

BioGel Minicolumns

To calculate the labeling efficiency, i.e. the percentage of added activity trapped within the vesicles, and the amount free in solution, the labeled vesicles were chromatographed on BioGel minicolumn as follows. Minicolumns were prepared by plugging the end of a 1 ml tuberculin syringe with a small wad of glass wool. The syringe was filled to the 1 ml mark with Bio-Gel A15M 100-200 mesh (Bio-Rad, Missassauga,

ON) and washed with 5 ml of saline. After washing, the column was transferred to a new 13x100 mm glass test tube. Then 200 µl of labeled vesicles were loaded onto the column and allowed to stand for 5 minutes. The column was transferred to a second test tube and 200 µl of saline was added and the eluate collected for another 5 minute interval. This process was repeated until a total of 10 fractions were collected. The fractions and the column were then counted using a RadCal Model 4502 dose calibrator (Monrovia, CA). Activity associated with the vesicles eluted in the void volume of the column (fractions 2-4) while free activity eluted in later fractions (fraction 5-7).

Results

Centrifugal Filters

After chromatography, 400 µl of the resulting pooled vesicle dispersion was added to the sample reservoir of the centrifugal filter units and centrifuged at 1600 x g for 15 minute periods for a total of 2 - 2.5 hours. The small sample volumes of these filter units did not allowed for the removal of samples for phosphorus assays to determine the lipid concentration after each 15 minute centrifugation interval thus, only the final lipid concentration could be determined. The resulting filtrate volume for the 10,000 and 30,000 NMWL filter units are presented in Figure 4.1. From this figure, the flow rate through the 30,000 NMWL filters is greater than through the 10,000 NMWL filters. The increased flow rate resulted in decreased centrifugation times to achieve the same final lipid concentrations. The average starting lipid concentration was 9.7 ± 1.3 mM (mean ± SD, n=5). Using the 30,000 NMWL filters, after 2 hours of centrifugation the resulting lipid concentration was 61.3 ± 14.2 (mean ± SD, n=10). For the 10,000 NMWL filters, the lipid concentration after 2.5 hours of centrifugation was 53.7 ± 18.3 mM (mean ± SD, n=13). The lipid recovery for the 30,000 and 10,000 NMWL filters was 75.0 ± 8.2 % (mean ± SD, n=10) and 82.0 ± 8.1 % (mean ± SD, n=13), respectively.

Although the 30,000 NMWL filters resulted in shorter centrifugation times, the 10,000 NMWL filters were preferred due to the higher lipid recovery. To produce an clinically useful volume of concentrated vesicles, the procedure was scaled up using a Millipore Ultrafree MC filter unit with a maximum capacity of 20 ml. The filter unit was loaded with 15.4 ml of a vesicle dispersion at an initial lipid concentration of 12.6 mM. The filter unit was spun at 1600 x g for 15 minute intervals for a total spin time of 2.25 hours. After each 15 interval, 100 μl of concentrated vesicles was removed and assayed to follow the increase in lipid concentration over time. The results are presented in Figure 4.2. The final volume and lipid concentration was 2.8 ml and 55.6 mM, respectively.

To test whether lipids were able to pass through the filters, vesicles prepared with POPE-fluorescein were centrifuged using the 10,000 NMWL filters for 2.5 hours. After centrifugation the filtrate and the concentrated vesicles were examined under UV light for fluorescence activity. The concentrated vesicles fluoresced brightly while the filtrate showed no evidence of fluorescent activity. To determine if centrifugation affected the vesicles size and size distribution, two separate batches of vesicles were sized before and after 2.5 hours of centrifugation in 10,000 NMWL filters. The diameter of the vesicles before centrifugation was 173.6 ± 46 nm and 155.6 ± 39 nm. After centrifugation, the diameter of the vesicles was 168.8 ± 42 nm and 150.0 ± 40 nm. Thus, centrifugation had no significant effect on the size and size distribution of vesicles.

The stability of vesicles to the loss of internal glutathione during centrifugation was determined using vesicles with entrapped [^{3}H]-glutathione. After 2 hours of centrifugation, 95.5 ± 1.5 % (mean ± SD, n=4) of the recovered activity was associated with the vesicles. To determine if the minimal loss of internal glutathione would affect the subsequent labeling procedure, vesicles were centrifuged for 3 hours and labeled. The resulting labeling percentage was 92.2 ± 0.5 % (mean ± SD, n=3) indicating the loss of internal glutathione during centrifugation had no effect on the labeling procedure.

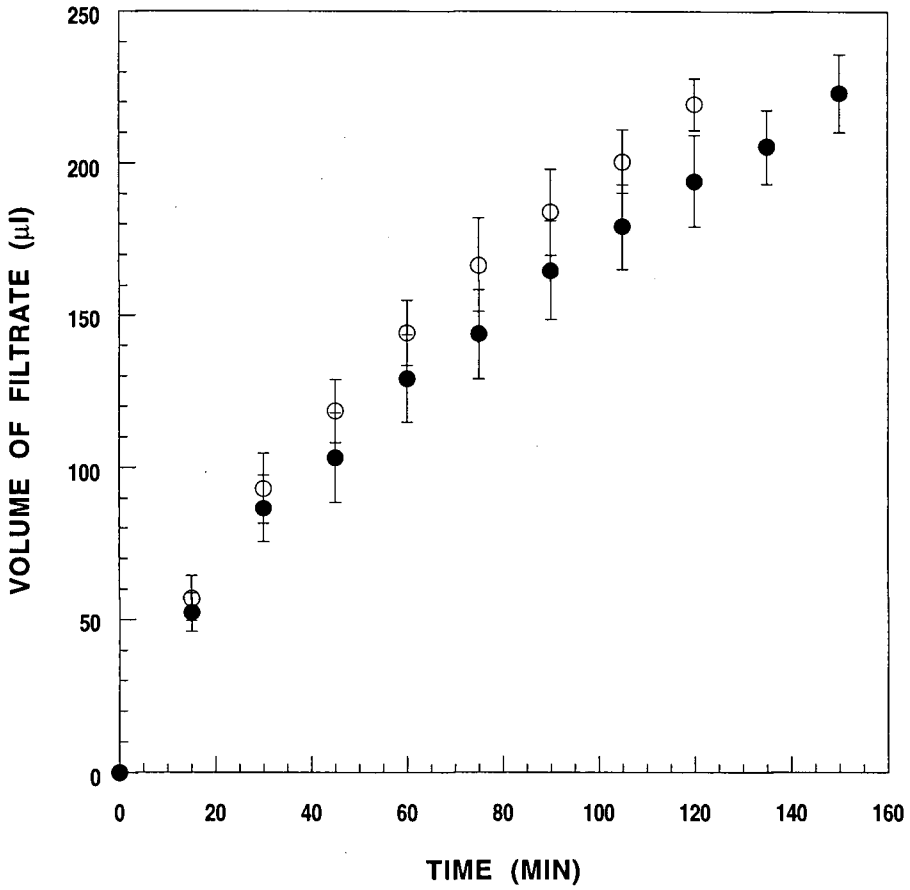

Figure 4.1. Comparison of flow rate through Millipore Ultrafree MC filter units.Total volume of filtrate filtered through 10,000 (●) (mean ± SD, n=14) and 30,000 (○) (mean ± SD, n=9) NMWL filter units over time.

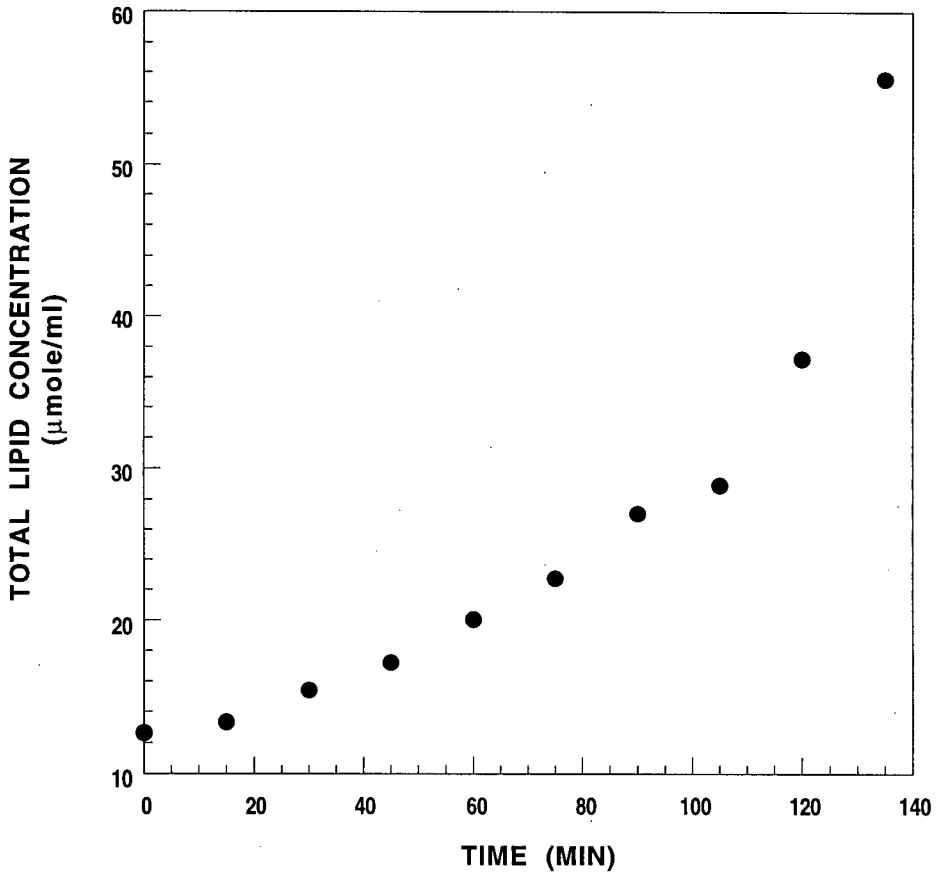

Figure 4.2. Increase in lipid concentration as a function of time. Millipore Ultrafree 10,000 NMWL filter unit with a maximum capacity of 20 ml was used. The starting lipid concentration was 12.6 mM. The final lipid concentration was 55.6 mM after 2.25 hours of centrifugation.

pH Gradient

Effect of buffers on Stability of HM-PAO

The stability of the lipophilic HM-PAO/^{99m}Tc complex in the presence of HEPES and citric acid buffers was determined. HEPES and citric acid buffers were selected because of their buffering ability in the desired pH ranges and their stability compared to a carbonate buffering system. A buffered solution of 100 mM HEPES, 100 mM citric acid in 0.9% (w/v) NaCl was prepared and adjusted to different pHs using sodium hydroxide. The tagging efficiency was determined using the partition assay described in Chapter 2 with the modification that 2 ml of buffered saline at different pHs was used instead of saline. The results are shown in Figure 4.3.

There was a slight decrease in the tagging efficiency for the buffered saline solutions compared to the control, saline/ethyl acetate. However, statistical analysis showed that there was no significant difference in the tagging efficiency between the control and the buffered saline solutions (Kruskal-Wallis one way analysis of variance on ranks, $p>0.05$), indicating that citric acid and HEPES buffers did not affect: 1) the stability of the lipophilic ^{99m}Tc/HM-PAO complex or 2) the rate of conversion from the lipophilic complex to the hydrophilic complex.

Effect of pH on the Ability of Glutathione to Convert HM-PAO

The effect of pH on the ability of glutathione to convert the lipophilic ^{99m}Tc/HM-PAO complex to the hydrophilic form was investigated. Glutathione solutions were prepared at various pHs and were buffered with either citric acid, for the pH range of 2.5 - 6.15 or HEPES, for the pH range of 6.0 - 8.5. The ability of glutathione to convert HM-PAO was assayed by using the partition assay with 2 ml aliquots of each buffered

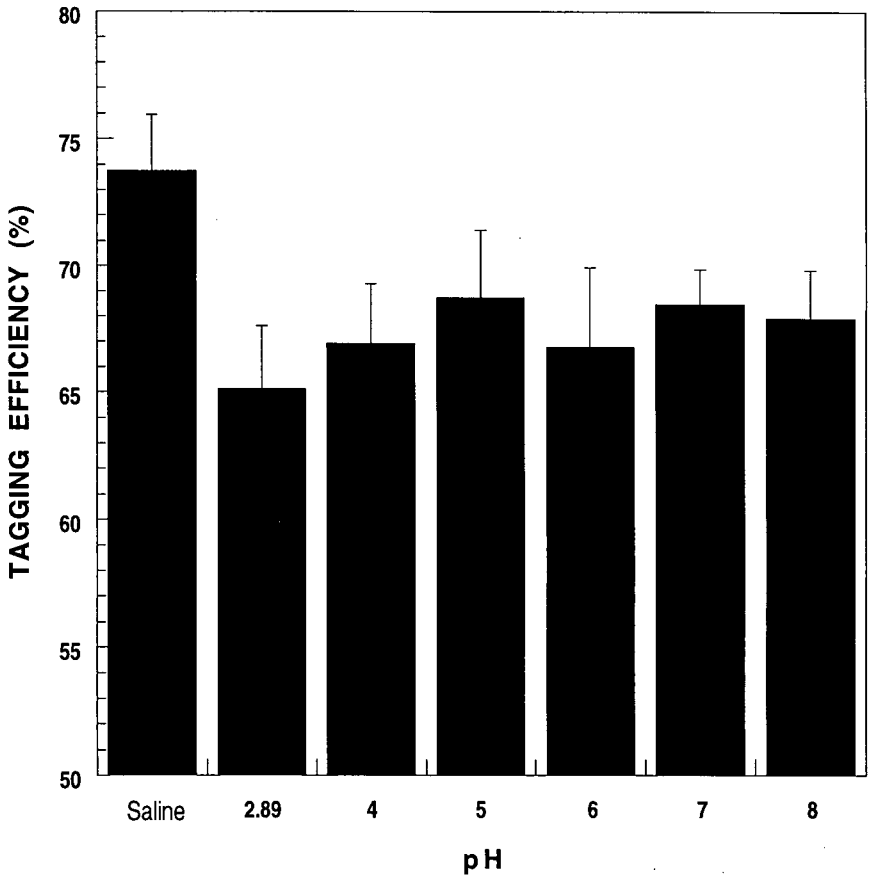

Figure 4.3. Effect of citric acid and HEPES buffers on the stability of HM-PAO. The stability of HM-PAO in the presence of citric acid and HEPES buffers showed no significant decrease in the tagging efficiency at different pHs. Bar represent mean ± SD, n=6.

glutathione solution into test tubes along with 2 ml of ethyl acetate. A HM-PAO kit was prepared with the modification that the initial rehydration volume of saline was 5.0 ml instead of 0.5 ml. After incubating at room temperature for 15 minutes, the tagging efficiency for each HM-PAO kit was determined by partition assay with unbuffered saline, and was determined to be 87.3 ± 4.4 % (mean ± SD, n=28). Then 200 µl of the HM-PAO/^{99m}Tc solution was added to test tubes containing buffered glutathione solutions at different pHs and ethyl acetate. The tubes were mixed by vortexing for 1 minute then allowed to stand for 1 minute to allow the phases to separate. Each phase was sampled, counted and the tagging efficiency was calculated (Figure 4.4).

From figure 4.4, the ability of glutathione to convert HM-PAO was maximal at pH 2.5 with only 2.6 ± 1.4 % (mean ± SD, n=3) of activity in the ethyl acetate phase, indicating that the majority of the lipophilic ^{99m}Tc/HM-PAO complex had been converted to the hydrophilic form. As the pH of the glutathione solutions increased from 2.5 to 7.5, there was also a steady increase in the tagging efficiency, i.e. increase in the percentage of activity in the lipophilic ^{99m}Tc/HM-PAO complex. At pH 7.5, the percentage of activity in the ethyl acetate phase was 88.5 ± 1.3 (mean ± SD, n=3). The tagging efficiency in glutathione solution at pH 7.5 was similar to the tagging efficiency observed in saline, indicating that glutathione was completely ineffective at converting the lipophilic ^{99m}Tc/HM-PAO complex to the hydrophilic form. As the pH was increased further to 8.5, the activity in the ethyl acetate phase decreased slightly.

These results indicate that the ability of glutathione to convert HM-PAO between the two forms is strongly dependent on pH. The conversion of the lipophilic complex to the hydrophilic form was maximal at low pHs, i.e. pH<3.0. At pH 7.5, ability of glutathione to convert HM-PAO was virtually eliminated and incubation of the lipophilic ^{99m}Tc/HM-PAO complex with glutathione at pH 7.5 did not result in its conversion to the hydrophilic form.

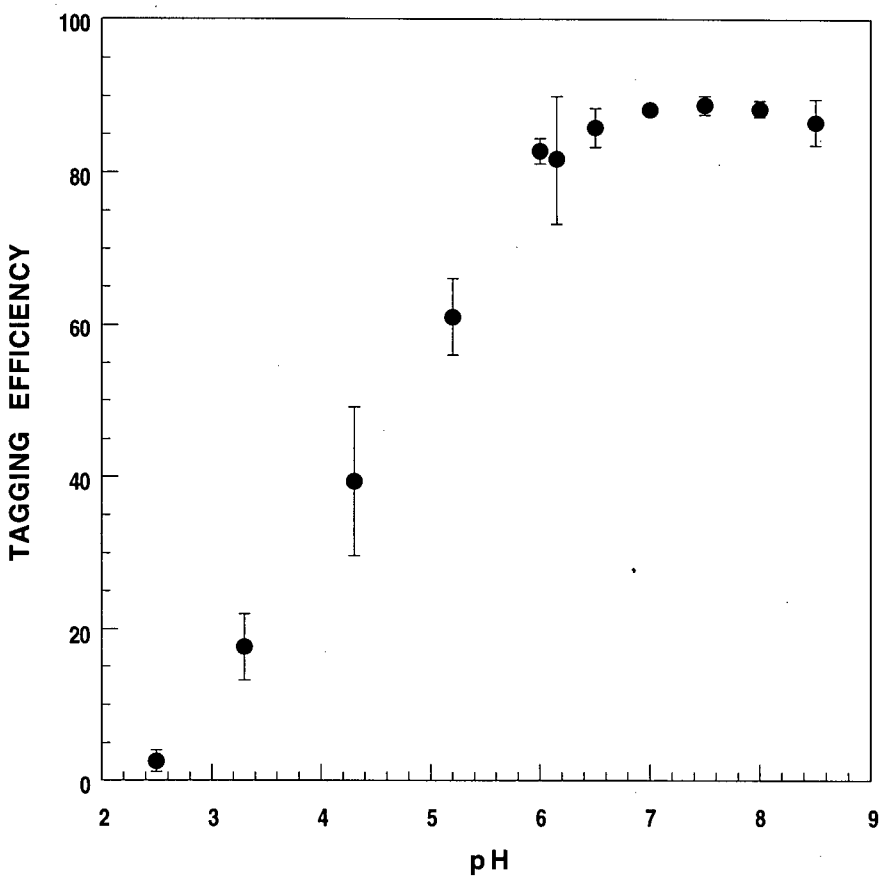

Figure 4.4. Effect of pH on glutathione. The effect of pH on glutathione ability to convert the lipophilic ^{99m}Tc/HM-PAO complex to the hydrophilic form was examined using buffered 30 mM glutathione solutions at various pHs. Tagging efficiency represents the percentage of added activity in the lipophilic ^{99m}Tc/HM-PAO complex. Each data point represents the mean ± SD, n=3.

Importance of Ethyl Acetate Phase

The importance of the ethyl acetate phase in the stability of the lipophilic ^{99m}Tc/HM-PAO complex to conversion by glutathione was examined by allowing the lipophilic ^{99m}Tc/HM-PAO complex to incubate for 10 seconds in the glutathione solutions at various pHs before the addition of ethyl acetate. The control consisted of 2.0 ml of unbuffered saline without glutathione, while the standard consisted of both ethyl acetate and pH 7.5 buffered glutathione. The results are presented in Figure 4.5.

From Figure 4.5, when the lipophilic ^{99m}Tc/HM-PAO complex is added to either saline and allowed to incubate for 10 seconds before addition of ethyl acetate or a tube containing glutathione (pH 7.5) with ethyl acetate, the tagging efficiency is greater than ~80%. Indicating that there is very little conversion of the lipophilic complex to the hydrophilic form. Dramatically different results were observed when the lipophilic complex is allowed to incubate with the buffered glutathione solutions before the addition ethyl acetate. In the pH range of 2.89 - 5.0, virtually all the lipophilic complex was converted to the hydrophilic complex resulting in low tagging efficiencies. The tagging efficiency increased over the pH range of 6.0 - 8.0, but never reaches the maximum observed when the buffered glutathione solutions were coincubated with ethyl acetate. These results indicate that the presence of the ethyl acetate phase, i.e. lipophilic phase, plays a key role in the stability of HM-PAO to glutathione at various pHs. In Figure 4.4, the tagging efficiency at pH 7.0 and 8.0 was > 80%, however, in Figure 4.5 the tagging efficiency dropped to ~50%.

Time course studies were conducted to characterize the reaction of glutathione with HM-PAO at pH 7.5 in the presence and absence of the ethyl acetate phase. The stability of the lipophilic complex to glutathione at pH 7.5 was examined under two different conditions. First, the lipophilic complex was added to a tube containing both

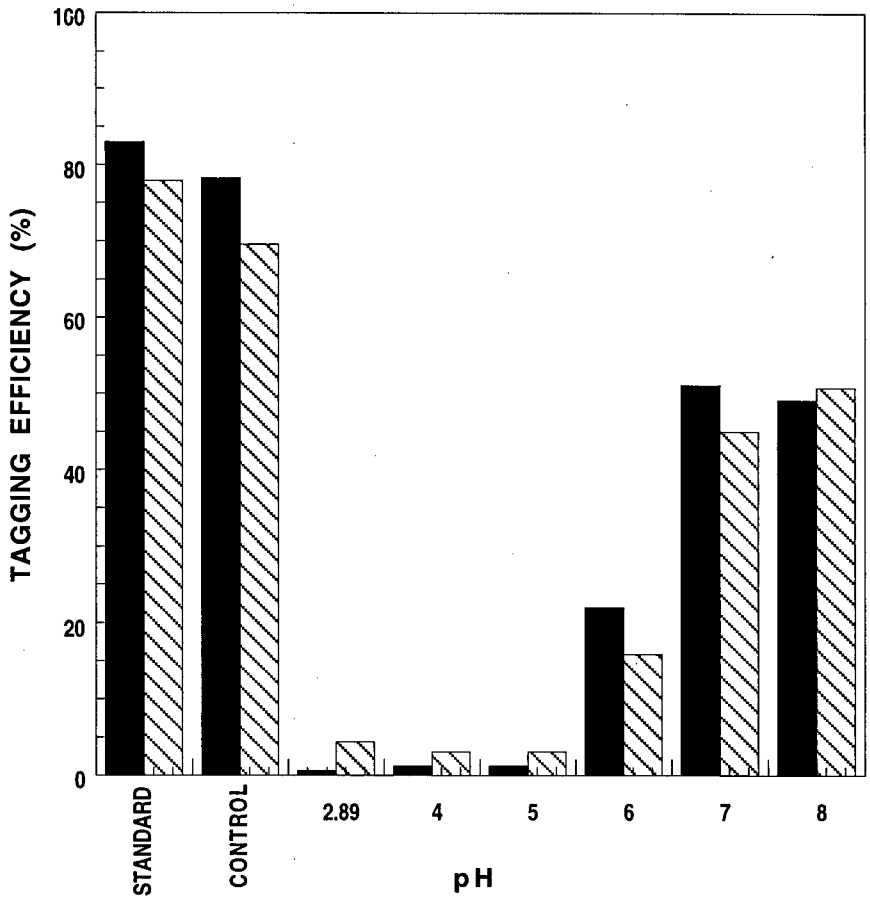

Figure 4.5. Effect of preincubation in the absence of ethyl acetate for 10 seconds. The lipophilic ^{99m}Tc/HM-PAO complex was incubated with glutathione solutions for 10 seconds before the addition of the ethyl acetate phase. Standard represents coincubation with ethyl acetate and glutathione at pH 7.5. Control represents incubation with saline for 10 seconds before addition of ethyl acetate. Bars represents duplicate trails.

glutathione (pH 7.5) and ethyl acetate phases, mixed and samples removed and counted at various time points to determine the tagging efficiency. Second, the lipophilic complex was added the glutathione (pH 7.5) and allowed to incubate for various times before the addition of ethyl acetate. The results are presented in Figure 4.6.

In the presence of the ethyl acetate phase, the lipophilic complex is stable to conversion by glutathione to the hydrophilic complex. After 10 minutes of incubation at room temperature, there was only a small decrease in the tagging efficiency. In the absence of the ethyl acetate phase, there was a time dependent decrease in the tagging efficiency indicating that at pH 7.5 the rate of reaction between glutathione and HM-PAO had not been eliminated but simply slowed.

Labeling of Buffered Vesicles

Based on the previous results, a vesicle dispersion was prepared using a rehydration buffer of 100 mM HEPES, 100 mM citric acid and 30 mM glutathione in 0.9% (w/v) NaCl to assess whether the pH dependent inactivation of the exterior glutathione could be used to prepare vesicles for labeling with ^{99m}Tc using HM-PAO. The dry lipid film was rehydrated with the buffered glutathione solution at pH 2.71. After extrusion, the final pH of the vesicles was adjusted to 7.5 using NaOH producing vesicles with a pH gradient. As a standard, another batch of vesicles were prepared in unbuffered glutathione and chromatographed on Sephadex G50. Each vesicle dispersion was labeled and chromatographed on BioGel minicolumn to determine the labeling efficiency. The results are presented in Table 4.1.

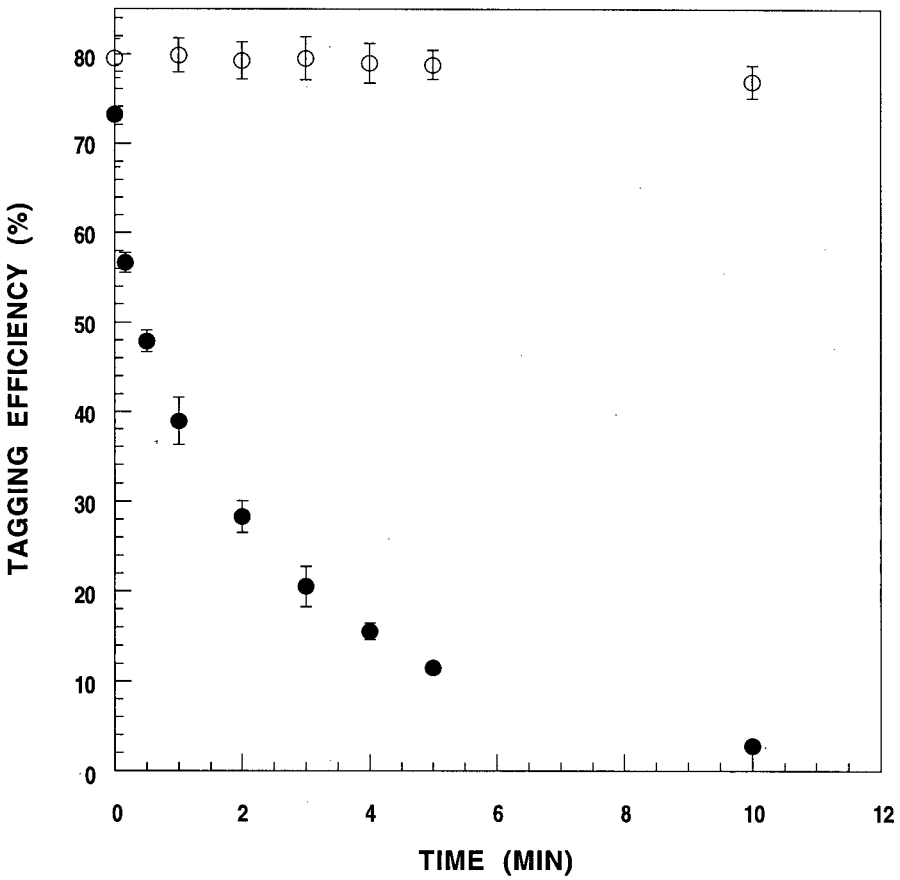

Figure 4.6. Time dependent interaction of glutathione with HM-PAO at pH 7.5. The effect of coincubating glutathione pH 7.5 with ethyl acetate on tagging efficiency (○) and the effect of incubating HM-PAO for various times with glutathione pH 7.5 before the addition of ethyl acetate on tagging efficiency (●). Data points represent mean ± SD, n=3.

Table 4.1. Labeling efficiency of vesicles with and without a pH gradient compared to the standard method of removing external glutathione by chromatography.

Vesicle Dispersion	Labeling Efficiency (%)
Control - no pH gradient	3.5, 5.2
Standard - post G50	89.0, 86.8
pH gradient vesicles	84.8 ± 3.7 (mean ± SD, n=8)

The labeling efficiency of the pH gradient vesicles was similar to the labeling efficiency of chromatographed vesicles. Thus, increasing the external pH to 7.5 to inactivate unentrapped glutathione is a viable alternative to the chromatographic removal of external glutathione. The principle advantage of this procedure is that the dilution which results from chromatography is avoided.

Titration of Glutathione

The titration curve of glutathione was determined in order to calculate the amount of NaOH required in raise the pH to 7.5 of an unbuffered solution of glutathione. The titration curve is presented in Figure 4.7. The figure was generated by titrating 150 μmol of glutathione with 100 mM solution of NaOH. Using this data, to achieve a pH of 7.5 approximately 170 μmol of NaOH must be added. This results in a NaOH-to-glutathione ratio of 1.13 (170/150=1.13). This ratio was then used to increase the external pH of an unbuffered vesicle dispersion to 7.5.

A vesicle dispersion was prepared of molar composition DPPC/Chol/PE-PEG (47.75:47.75:4.5) in 30 mM glutathione at a total lipid concentration of 83.7 mM. Aliquots of 200 μl were removed and 27.1 μl of a 250 mM solution of NaOH was added, which corresponds to a final NaOH:glutathione ratio of 1.13. The vesicles were labeled and chromatographed on BioGel minicolumns to determine the labeling efficiency. The labeling efficiencies before and after the addition of NaOH are reported in Table 4.2.

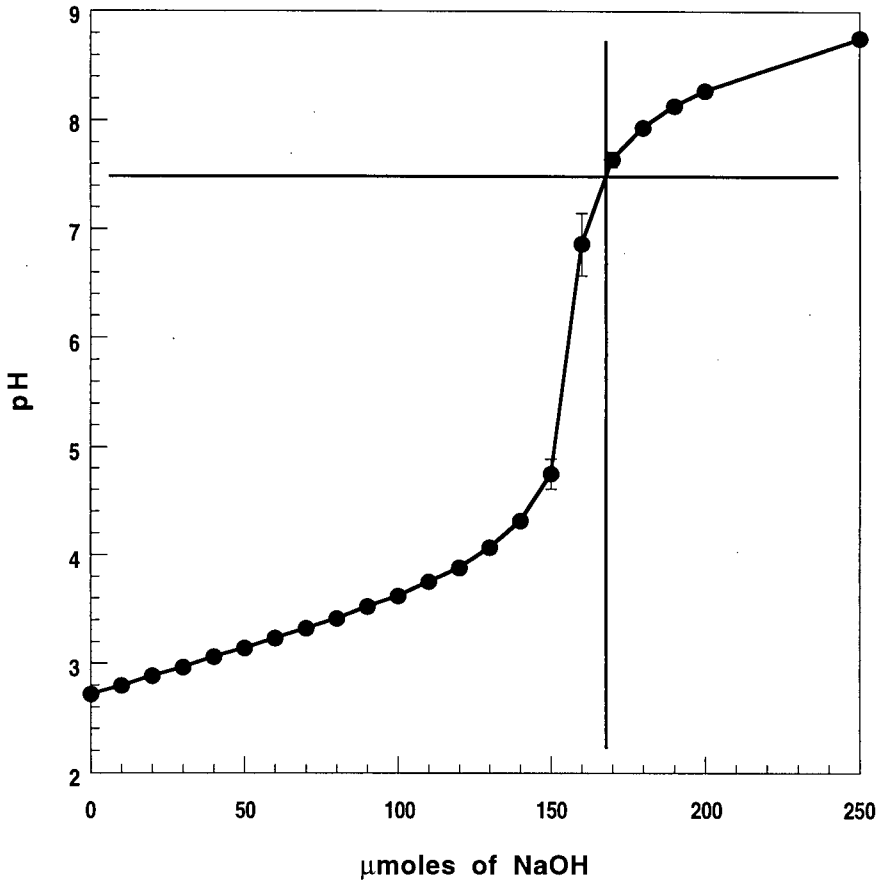

Figure 4.7. Titration curve of 150 μmoles of glutathione with 10 mM NaOH solution. 170 μmoles of NaOH was required to titrate 150 μmoles of glutathione to pH 7.5. Data points represent mean ± SD, n=3.

Table 4.2. Labeling efficiency of unbuffered vesicles

Vesicle Dispersion	Labeling efficiency (%)
no NaOH added	13.13, 16.55
added NaOH	84.62 ± 0.24 (mean ± SD, n=4)

The labeling of vesicles in the absence of the pH gradient resulted in poor labeling. In contrast, the labeling of pH gradient vesicles in the absence of buffers resulted in labeling efficiencies similar to those observed for buffered vesicles (see Table 4.1). Thus, these results suggest that vesicles can be prepared without buffers and the pH can be adjusted with the addition of a defined amount of NaOH immediately prior to labeling. This would eliminate the need for testing of various buffers while providing a convenient method for producing vesicles which exhibit high labeling efficiencies.

Stability of Labeled Vesicles

To determine whether the pH gradient affected the stability of vesicles to the loss of trapped ^{99m}Tc, labeled vesicles were incubated with normal human serum. Unbuffered vesicles were pH adjusted and labeled. After labeling, the vesicles were chromatographed on Sephadex G50 to remove free, untrapped ^{99m}Tc. The lipid fractions were pooled to give a vesicle dispersion with only entrapped ^{99m}Tc. 300 µl of the labeled vesicles was incubated with an equal volume of human serum and 200 µl samples were removed at 5 and 60 minutes and chromatographed on BioGel minicolumns (Figure 4.8). The labeling efficiency at 5 and 60 minutes were calcuated to be 97.5 ± 2.0 % (mean ± SD, n=8) and 96.3 ± 2.2 % (mean ± SD, n=8) , respectively. Thus, the use of a pH gradient had no effect of the stability of vesicles to the loss of ^{99m}Tc. If the pH gradient had affected the stability of the vesicles, incubation with human serum would have resulted in the association of large fraction of the radioactivity with the protein fractions (fraction 5-7) and a dramatic decrease in the activity associated with the lipid fractions (fraction 2-4).

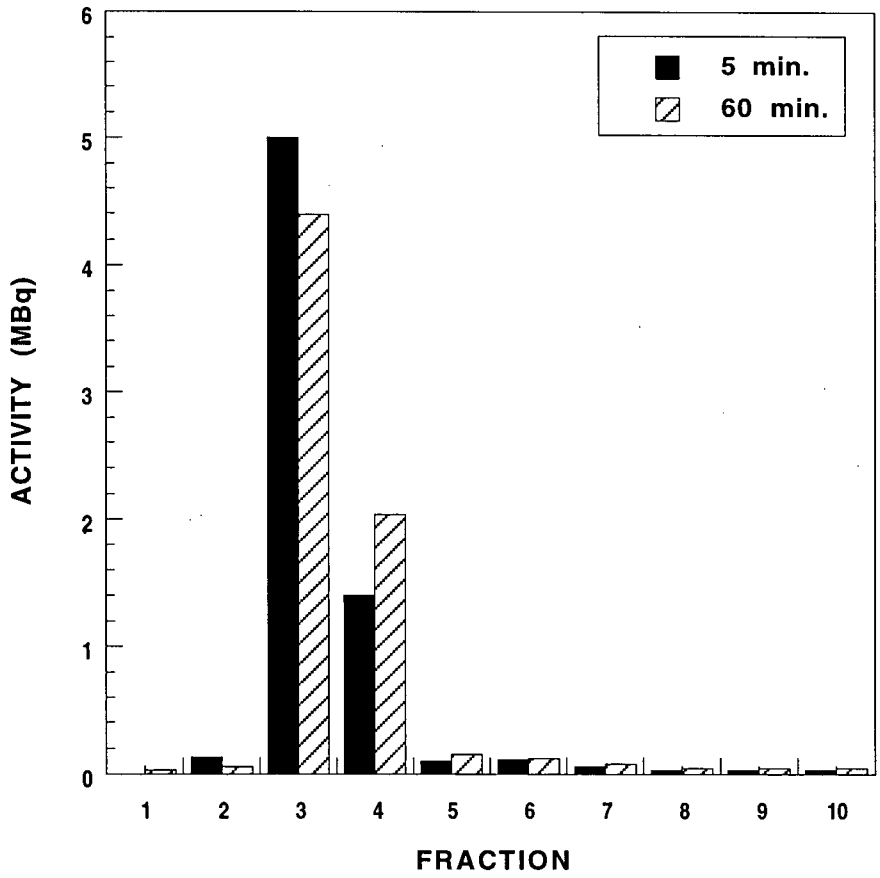

Figure 4.8. Stability of pH gradient vesicles. pH gradient vesicles were labeled and chromatographed on Sephadex G50. The lipid fractions were pooled and sample incubated with normal human serum for 5 and 60 minutes and then chromatographed on BioGel minicolumns. Overall stability measurements for 5 and 60 minutes were calculated to be 97.5 ± 2.0 % (mean ± SD, n=8) and 96.3 ± 2.2 % (mean ± SD, n=8), respectively.

Discussion

Chromatography on Sephadex G50 to remove external glutahione results in the dilution of the vesicle dispersion and a method was required to increase the lipid concentration. For this reason, Millipore Ultrafree MC units with 10,000 or 30,000 NMWL filters and the use of a pH gradient were tested as methods to increase the lipid concentration after chromatography. For the filter units, the assumption was that vesicles would be retained in the sample cup while centrifugation would force excess saline through the filter into the receiver tube thus, increasing the lipid concentration. After testing, both 10,000 and 30,000 NMWL filters were found to be effective in increasing the lipid concentration. Although the flow rate through the 30,000 NMWL filter was greater than 10,000 NMWL filter, which resulted in lower centrifugation times, the 10,000 NMWL were preferred due to the higher lipid recovery.

Increasing the lipid concentration by centrifugation filtration appears to cause no significant change in the vesicle properties. Centrifugation caused no significant change in the size or size distribution of the vesicle dispersion as determined by light scattering. Using fluorescently labeled lipids, there was no observable lipid in the filtrate and there was only minimal leakage of internally trapped glutathione after centrifugation. Finally, centrifugal concentration of vesicles dispersion has no significant effect on the subsequent labeling efficiencies with HM-PAO and ^{99m}Tc. Labeling efficiencies of the concentrated vesicle dispersion were greater than ~90%. Thus, using Millipore Ultrafree MC 10,000 NMWL filter was an effective means to increase the lipid concentration of a vesicle dispersion.

However, the use of centrifugal filtration as a means of increasing the lipid concentration does have significant disadvantages. The greatest disadvantage is the long centrifugation times, typically 2.5 hours, required to increase the lipid concentration by a

factor of ~6. The long centrifugation times are complicated by the requirement for constant mixing of vesicle dispersion in sample cup to prevent clogging of the pores which decreases the flow rate. Also, centrifugation provides variable results as revealed by the relatively high standard deviations. In the clinical setting, this would necessitate the constant monitoring of lipid concentration throughout the centrifugation process. Another disadvantage is that centrifugation adds an additional step to the production of vesicles. This not only increases the preparation time but also increases the chances for the introduction of contaminants. Although centrifugal filtration was effective, another method had to be developed to increase the lipid concentration which preferably resulted in a fewer preparation steps and more reproducible results. In this light, a pH gradient was examined as a means of inactivating external glutathione rather than removal by chromatography.

Before examining the results of pH on glutathione, the difference between tagging efficiency and labeling efficiency must be discussed in order to better understand the results. As discussed, HM-PAO is thought to exist in two forms: a lipophilic form and a hydrophilic form. Both forms are critical to labeling of vesicles. Initially after rehydration with ^{99m}Tc and saline, it forms the lipophilic ^{99m}Tc/HM-PAO complex. The percentage of added ^{99m}Tc activity which is in the lipophilic ^{99m}Tc/HM-PAO form is termed the tagging efficiency. The tagging efficiency is assessed using a partition assay comprised of equal volumes of saline and ethyl acetate [113]. The lipophilic ^{99m}Tc/HM-PAO complex partitions into the ethyl acetate phase, while free ^{99m}Tc and the hydrophilic ^{99m}Tc/HM-PAO complex partition into the saline phase. The percentage of the total activity in the ethyl acetate phase represents the percentage of activity in the lipophilic ^{99m}Tc/HM-PAO form which can cross the lipid bilayer. Thus, this percentage represent the maximum labeling efficiency that can be achieved. The labeling efficiency refers to the percentage of activity added to vesicles that is associated with the vesicles. The labeling efficiency is

determined using chromatography on BioGel minicolumns. Vesicles elute in the void volume of the column while free untrapped ^{99m}Tc elutes in later fractions [88].

The labeling efficiency is directly related to the tagging efficiency but the tagging efficiency is not dependent on the labeling efficiency. The labeling efficiency cannot exceed the tagging efficiency because the tagging efficiency represents the amount of activity in the lipophilic ^{99m}Tc/HM-PAO form which can potentially cross the lipid bilayer. Low labeling efficiencies do not necessarily correspond to low tagging efficiencies but a mandatory requirement for high labeling efficiencies are high tagging efficiencies.

The first step in the assessment of pH on glutathione was the selection of appropriate buffers. Previous studies have shown that presence of phosphate containing buffers significantly increase the rate of conversion of the lipophilic complex to the hydrophilic form while carbonate buffers had little effect [139]. Citric acid and HEPES were chosen as buffers for their ability to buffer solutions between 2.0- 8.5. These buffers had no effect on the either the stability of the lipophilic ^{99m}Tc/HM-PAO complex or the conversion to the hydrophilic form (Figure 4.3). The observed low tagging efficiencies are related to the time delay between the elution of the generator and the time of the experiment (see Chapter 2). This series of experiments was conducted ~4 hours after the elution of the generator which resulted in the low tagging efficiencies.

Using these buffers, 30 mM glutathione buffered solutions were prepared and tested to determine the ability of glutathione to converted the lipophilic complex to the hydrophilic form at various pHs. At low pH, i.e. pH < 3.0, glutathione rapidly and completely converted the lipophilic complex to the hydrophilic form as is evident from the very low tagging efficiency after incubation (Figure 4.4). As the pH was increased to pH 7.5, the tagging efficiency increased indicating that the ability of glutathione to convert HM-PAO decreased. Above pH 7.5, the tagging efficiency begins to decrease which may

be due HM-PAO instability at high pH [139]. At pH 7.5, glutathione was ineffective at converting HM-PAO which was evident from comparing the tagging efficiency after incubation with saline and glutathione at pH 7.5. With saline, the tagging efficiency was ~87% while incubation with glutathione at pH 7.5 it was ~88%. These results were then applied to a buffered vesicle system.

Based on the partition assay results, vesicles were prepared in a buffered glutathione solution at pH 2.71. After extrusion of vesicles the pH of the dispersion was raised to pH 7.5 producing vesicles with a pH gradient. The vesicles were labeled and the results showed that the labeling efficiencies for the pH gradient vesicles were similar to the labeling efficiencies of the Sephadex G50 vesicles (Table 4.1). It was also calculated that a molar ratio of NaOH:glutathione of 1.13 increases the pH of an unbuffered glutathione solution to 7.5. This would not only eliminate the need for buffers but also increase the simplicity of the preparation of vesicles. Unbuffered vesicles can be prepared and a volume of NaOH solution equal to 1.13 times the moles of glutathione can simply be added prior to labeling (Table 4.2). The pH gradient also does not affect the stability of the labeled vesicles to the loss of label (Figure 4.8).

An interesting effect was observed in absence of the ethyl acetate phase on tagging efficiency. In the presence of ethyl acetate, the tagging efficiency does not decrease over time when coincubated with glutathione at pH 7.5 (Figure 4.6, open circles). However, the tagging efficiency decreases exponentially when HM-PAO is allowed to incubate with glutathione at pH 7.5 before the addition of ethyl acetate (Figure 4.6 closed circles). The ethyl acetate phase seems to help stabilize HM-PAO, and in the absence of ethyl acetate, the ability of glutathione to convert HM-PAO is slowed but not completely inactivated.

The pH dependence of the reaction may also shed light on the interaction between HM-PAO and glutathione. Glutathione has four protonatable groups: 2 carboxylic acid

moieties (pKa's 2.12 and 3.53), 1 amine (pKa 9.12) and 1 sulphydryl (pKa 8.66) [140]. The carboxylate and amine groups have been shown not to interact with HM-PAO from the stability studies using citric acid and HEPES at various pH and also by other investigators [Figure 4.3, 139]. Thus, the sulphydryl group of cysteine must be the principle group involved in the interaction of glutathione with HM-PAO. At pH ≤ 3.0, the sulphydryl group is the protonated state. As the pH increases, protonation state changes and can be determined by using the Henderson-Hasselbach equation (Equation 1).

$$pH = pKa + \log \frac{[A^-]}{[HA]} \qquad \text{Equation 1}$$

Where A^- represents the unprotonated form (S^-) and AH represents the protonated form (SH). The degree of protontation as a function of pH is given in Table 4.2 along with the percentage of glutathione ability to convert HM-PAO. Based on these calculation the sulphydryl group must be in the full protonated state to be effective in converting HM-PAO. A decrease of only 0.3% in the concentration of SH results in decrease of 7.3% in the ability of glutathione to convert HM-PAO. Glutathione's ability to convert HM-PAO is completely suspended in the pH range of 7.0 - 8.0. This range can be expected to extend to include all pHs above 7.0 rather than stopping at pH 8.0 however, the instability of HM-PAO to strongly basic conditions becomes the limiting factor [139]. Thus, based on these results the protonation state of the SH of cysteine is the critical factor in regulating the interaction between glutathione and HM-PAO.

Table 4.3. Correlation between the protonation state of cysteine's sulphydryl group on the reactivity of glutathione to HM-PAO.

pH	Percentage of Sulphydryl group in the SH form	Ability to Convert HM-PAO (%)*
2.5	99.8	87.1
3.3	99.5	79.8
4.3	98.7	54.9
5.2	97.0	35.1
6	93.5	5.2
6.5	89.7	1.7
7.0	84.0	0
7.5	76.1	0
8.0	66.0	0
8.5	54.0	0.9

* - ability to convert HM-PAO represents the reactivity of glutathione to convert HM-PAO from the lipophilic complex to the hydrophilic form. Data represent the percentage of the initial lipophilic complex that is converted to the hydrophilic form.

Chapter 5:

Toxicity studies on PEG-Coated Vesicles

Introduction

Before testing of PEG-coated vesicles as nuclear medicine blood pool imaging agents in human volunteers, the possibility of potential toxicities associated with vesicle administration must be assessed. Vesicles have been tested extensively over the years both *in vitro* and *in vivo* using various lipid compositions and lipid doses [126,128,129, 131,141-159]. Toxicities observed *in vitro* using cultured cells range from decreased cell growth and viability to hemolysis of cells and cell death [141-146]. Other *in vitro* studies have examined the ability of vesicles to activate the complement cascade [126,128,129, 131]. *In vivo* studies can be grouped into toxicities associated with acute and chronic administration of vesicles [146-149]. Acute toxicity refers to effects observed immediately following the administration of a single dose of vesicles while chronic toxicity generally refers to the administration of multiple doses of vesicles over a period of time. Reported toxicities due to acute administration of vesicles range from no observable effects, to impaired phagocytic function and seizures, depending the route of administration [146]. Chronic administration generally resulted in reversible splenomegaly and hepatomegaly and also the formation of granulomas [147].

The toxicites observed in the these studies were critically dependent on the lipid composition of the vesicles - specifically the inclusion of charged lipids [126,128,129,131,141-146]. Charged lipids which exhibited the greatest toxicities were stearylamine and cardiolipin followed by dicetylphosphate, phosphatidylserine and phosphatidylglycerol. Neutral vesicles composed of DPPC and Chol (1:1) were found to be the least toxic even at high lipid concentrations *in vitro*. Exposure of cultured cells to DPPC:Chol resulted in no alteration in cell growth or viability [141-146]. *In vitro*

complement activation testing also found that there was no activation of the cascade for DPPC:Chol vesicles over the concentration range of 0.001 to 100 mM [128,131]. Although neutral vesicles composed of DPPC:Chol were nontoxic, overall neutral vesicles composed of cardiolipin:phophatidylcholine:cholesterol:stearylamine were found to be just as toxic as charged stearylamine:phosphatidylcholine:cholesterol vesicles [143]. Thus, the toxicity of vesicles is determined by the individual lipids components, i.e. stearylamine, and not the overall net charge of the vesicles.

In vitro toxicity testing using cell cultures does not accurately reflect effects *in vivo*. Unlike cultured cells which consist of a single cell types of related function, animal and human systems contain a variety of cell types and circulation systems which deliver vesicles to specific areas and organs which may result in localized toxicities. A number of investigations into the *in vivo* toxicities have been conducted using different lipid compositions, animal models and dosage regimes [146-149]. Organs which are generally affected to the greatest degree are those that comprise the reticuloendothelial system (RES), namely the liver and spleen. The most prominent systemic feature after a single administration of vesicles was the transient impairment of phagocytic activity. The phagocytic activity measure the ability of RES to remove foreign particulates from the circulation. Chronic administration of vesicles generally resulted in splenomegaly and in some cases hepatomegaly [146]. There was also the formation of granulomas in the liver during the course of injections, which disappeared shortly after the last vesicle administration [147].

No specific reports exist which solely examine the toxicities associated with administration of PEG-coated vesicles. However, there are a number of reports on the biodistribution and circulation kinetics of PEG-coated vesicles in various animal models and, based on these studies, one can draw some conclusions about the toxicities which may be associated with PEG [see Chapter 3]. Increased RES uptake of vesicles results in

short circulation half-lives. The increased uptake or localization of vesicles within the RES is also believed to cause the observed hepato- and splenomegaly as well as the formation of granulomas in the liver [147]. The activation of the complement system and deposition of activated complements on the surface of vesicles would increase RES clearance and result in short circulation half-lives. Thus, the observation that PEG-modification not only increase the circulation half-life of vesicles, but also results in vesicles with circulation half-lives which are independent of lipid composition, suggests that modification with PEG is relatively non-toxic. PEG-coated vesicles, loaded with various drugs, have been tested in humans clinical trials and the reported toxicities were related to the encapsulated drug and not the PEG-coated vesicles themselves [150-159].

A remaining issue concerning potential toxicity associated with PEG-coated vesicles is the pyrogenicity of PEG and the vesicle preparation procedure. Pyrogens are materials or compounds which initiate the fever response when injected parenterally in humans or animals. The most common pyrogens are endotoxins from bacterial cell walls [160]. The presence of bacterial endotoxins are generally the result of contamination during the production process. Other materials initiate the pyrogenic response by direct release of cytokines, rather than bacterial contamination. The two principle testing procedures are *in vivo*, where the material is injected into rabbits, and *in vitro* (limulus amebocyte lysate (LAL) assay), where the gelation of lysate from blood cell isolated from the American horseshoe crab is followed in the presence of the material [160,161]. The *in vivo* rabbit testing has the advantage of identifying materials which are contaminated and also directly release cytokines. The *in vitro* test is only able to detect bacterial contamination.

This chapter deals with the toxicity testing of PEG-coated vesicles. It was hypothesized that there would minimal toxicities associated with the intravenous administration of these vesicles based on a number of observations. First, the vesicles are

neutral and composed mainly of DPPC:Chol which has been shown to be the least toxic lipid composition [126,128,129,131,141-159]. Second, the aqueous solution used to prepare the vesicles was composed of normal physiological saline (0.9% NaCl) with 30 mM glutathione. Glutathione is a naturally occurring cellular component involved in amino acid transport, activator of certain enzyme, electron donor, detoxification, and protection of lipids against autoxidation and thus, is readily used for metabolism by cellular pathways in the body [162]. Finally, there were minimal issues of toxicities for HM-PAO and ^{99m}Tc because both are approved for medical use and used on a routine basis in nuclear medicine.

Materials

As decribed in Chapter 2. Normal human serum (NHS) was isolated from a pool of ~30 healthy volunteers and stored at -70°C.

Methods

Preparations of Vesicles

Lipids were combined from known stock solutions in chloroform in the final molar composition of DSPC/Chol/DMPG/Vit.E/PE-PEG (45.5:40:9:1:4.5) and DPPC:Chol:PE-PEG (47.75:47.75:4.5). Vesicle preparation was the same as described in Chapter 2.

Pyrogen Testing

After chromatography on Sephadex G50, the lipid dispersion was filtered into a vacutainer through a Satorius Minisart NML 0.200 μm filter unit (Toronto, ON). A sample were removed for phosphorus assay to determine the lipid concentration.

Pyrogen testing was conducted at Vancouver General Hospital using standard USP guidelines [161]. Rabbits were allowed access to water but not food for the duration of the test. The temperature was recorded using an approved remote rectal-temperature sensing probe. Temperature reading were recorded every 30 minutes. Before injection of vesicles, three rabbits were initially tested using sterile pyrogen free water to establish normal variation in body temperature of rabbits. The rabbits were followed for 1.5 hours, then injected with water and followed for a further 2.5 hours. The next day, the rabbits were followed for 1.5 hours to establish basal temperature and then injected with 1 ml of 11.52 mM DSPC/Chol/DMPG/Vit.E/ PE-PEG 5000 (45.5:40:9:1:4.5) and monitored for another 2.5 hours. The injected lipid dose per rabbit was 3.9 - 4.2 μmoles of lipid/kg of body weight.

CH50 Hemolytic Assay

The procedure used was that described by Devine et al. [131]. All dilutions, washings and incubations were performed in GVB^{2+} buffer (1.8 mM sodium barbitol, 3.1 mM barbitol, 145.4 mM NaCl, 0.15 mM $CaCl_2$, 1.0 mM $MgCl_2$, and 1 gram of gelatin in 1 liter of distilled H_2O), unless otherwise specified. Antibody-sensitized sheep red blood cells were prepared by centrifuging 10 ml of sheep blood anticoagulated in Alsiera's solution at 500 x g for 10 min. The supernatant was removed and the resulting red cells washed 3 times in GVB^{2+} buffer spinning at 500 x g for 10 min. After washing, the red cell concentration was adjusted to 0.5×10^{12} cells/L. Rabbit anti-sheep RBC antibodies (haemolysin) was then added to the diluted red cells to give a final dilution of 1:1000 and incubated at 37°C for 45 min. After incubating, the cells were pelleted and washed 3 times in GVB^{2+} and adjusted to 0.5×10^{12} cells/L.

Serial dilution of each lipid dispersion (DPPC/Chol/PE-PEG and DSPC/Chol/ DMPG/Vit.E/PE-PEG 5000) were prepared, in duplicate, using GVB^{2+} buffer and placed

on ice. To 100 µl of each dilution was added 100 µl of a 4 x dilution of NHS. Absorbance blanks, to account for light scattering due to vesicles, consisted of vesicles incubated without normal human serum and were analyzed in parallel with the test samples. The blank control contained no lipid or normal human serum and the 100% control contained only normal human serum and GVB^{2+} buffer. The samples were then incubated for 30 minutes at 37°C. After incubation, 300 µl of GVB^{2+} was added to each tube and mixed.

During the incubation of vesicles with NHS, tubes were set up in duplicate containing 50 µl of the antibody-sensitized sheep red blood cells. After incubating vesicles with NHS, 50 µl of each dilution was added to the corresponding tubes containing antibody sensitized sheep red blood cells and incubated for 1 hour at 37°C. The reactions was stopped by addition of 1 ml of EDTA/GVB buffer (GVB^{2+} buffer containing 20 mM EDTA and no $CaCl_2$ or $MgCl_2$). The tubes were spun at 500 x g for 5 minutes to pellet intact red cells. The samples were then loaded onto ELISA plates and read at 414 nm using an ELISA plate reader.

To calculate the percentage of complement activity remaining at each lipid concentration, the following equation was used (Equation 2) [128]:

$$\frac{\text{Sample } A_{414nm} - \text{Absorbance Blank } A_{414nm}}{100\% \ A_{414nm} - \text{Absorbance Blank } A_{414nm}} \times 100\% = \ \% \text{ Complement Activity Remaining}$$

Hemodynamic Studies

Rabbits were initially anesthetized with a Ketamine/Rompun mixture (35 mg/kg of Ketamine and 7 mg/kg of Rompun). After initial anesthesia with Ketamine/Rompun, the rabbits were intubated and maintained under anesthesia with Halothane administered using a North American DR'A'GER anesthesia ventilator. Rabbits were catheterized via

the carotid artery to measure blood pressure and heart rate using a Honeywell PM-28 and a Hewlett-Packard 78905A monitors. Temperature was followed using a rectal temperature probe (Electronics for Medicine DC1-9). Blood sample were collected via the ear artery using a HepLoc and analyzed for O_2 and CO_2 partial pressure, pH, and bicarbonate concentration ($[HCO_3]$) using a Corning 168 pH/Blood Gas Analyzer. The rabbits were kept under anesthesia for 1 hour before any injections to allow for equilibration of various parameters in the anesthetized state. After this period the animals were injected with a volume of saline equal to the volume of vesicles to be injected. The rabbits were monitored for 1 or 2 hours while recording systolic, diastolic, heart rate, temperature, pO_2, pCO_2, pH, and $[HCO_3]$ every 15 minutes. After 1 or 2 hours, the rabbits were injected with unlabeled vesicles at a lipid dose of either ~1.4 or ~4.0 μmol/kg of body weight and followed for another 1 or 2 hours. Controls rabbits were injected with saline followed for 2 hours and injected again with saline and monitored for another 2 hours. A total of 6 rabbits were followed for 1 hour after injection of saline or vesicles and a total of 4 rabbits were followed for 2 hours after the injection of saline or vesicles. There were two control rabbits.

Statistical Analysis of Hemodynamic Data

In order to minimize the high degree of inter- and intra-rabbit variation in the measured hemodynamic parameters, the data was analyzed in the following manner based on a modification of the method described by Rabinovici et al. [163]. Data values at 0, 15, 30, 45 and 60 minutes (for rabbits followed for 1 hour - 6 rabbits) and at 75, 90, 105, 120 minutes (for rabbits followed for 2 hours - 4 rabbits) after first injection of saline were compared to the corresponding time points after the injection of vesicles. In the case of the control rabbits, comparisons of equivalent data time points after the first and second injections of saline. The absolute difference was taken of the data points for both experimental and control rabbits. A Mann-Whitney Rank Sum test was used to test the

null hypothesis that there was no significant difference in the absolute values of the experimental rabbits compared to the control rabbits. A significant difference in the values between the two groups for each measured parameter was taken as a $p < 0.05$.

Results

Pyrogen Test

The temperature increases for each rabbit before and after the administration of water, for the controls, and vesicles are presented in Table 5.1. The total temperature increase after the injection of water was 0.1°C. For the vesicles, the total temperature increase for all three rabbits was 0.3°C.

Table 5.1. Rabbit temperatures during pyrogen testing

Rabbit	Water (Control)			Vesicle		
	Before*	After†	Increase	Before*	After†	Increase
1	39.0	39.1	0.1	39.0	39.2	0.2
2	38.8	38.8	0.0	39.0	38.9	0
3	39.4	39.4	0.0	39.3	39.4	0.1

* average for 4 measurements
† average for 6 measurements

CH50 Hemolytic Assay

The effect of DSPC and DPPC vesicles, over a range of lipid concentrations, on the complement system was measured using a hemolytic assay where serum was reacted with antibody-sensitized sheep red blood cells. The maximal level of lysis of sheep red cells occurs when normal human serum is incubated with buffer which is determined to be 100% of complement activity. Using equation 2, which also corrects for light scattering and absorbance due to vesicles, the percentage of hemolytic activity remaining of normal human serum after incubation of vesicles at various lipid concentrations was determined.

The blank control, which accounted for absorbance due to buffer components, was similar to absorbance of empty wells.

The percentage of complement activity remaining of normal human serum after incubation with either DSPC or DPPC vesicles are presented in Figure 5.1. From this figure it can be observed that there was minimal or no activation of the complement system by PEG-coated vesicles under the conditions of this experiment. There was greater than 96% complement activity remaining over the entire range of lipid concentrations tested. However, there were two data points, at the lowest lipid concentrations, in one of the DPPC trials, showed that the remaining complement activity dropped to 90%. Previous work has shown that neutral vesicles, without PEG, do not activate the complement system *in vitro* at lipid concentration up to 100 mM [131]. Therefore, since we did not observe any complement activation at high lipid concentrations, we may assume that these two low data points are anomalies.

Hemodynamic Studies

After plotting the data for the 10 experimental rabbits (6 at 1.4 μmol/kg and 4 at 4.0 μmol/kg) and 2 control rabbits, it was observed that some parameters demonstrated a high degree of inter- and intra-rabbit variation while others remained relatively constant (Figure 5.2 - 5.13). Parameters such as temperature and pH were constant not only during the time course of the experiment for each rabbit, but the values were similar between different rabbits. Blood pO_2, on the other hand, exhibited highly fluctuating values during the course of the experiment and varied greatly amoung different rabbits. Other parameters such as diastolic and systolic blood pressure, pCO_2, pulse and $[HCO_3]$ also varied but to a lesser degree.

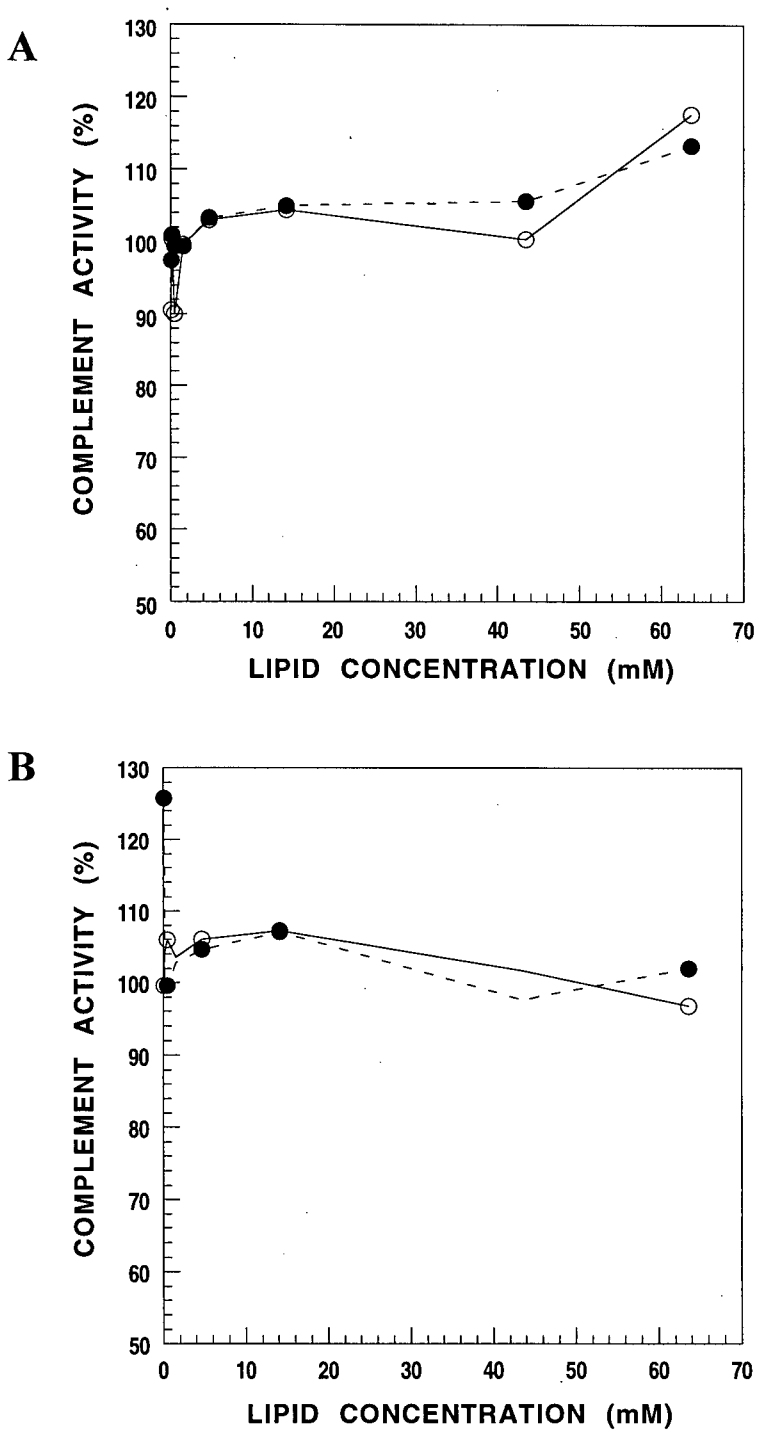

Figure 5.1. Percentage of complement acitivity remaining after incubation with DPPC (A) and DSPC (B) vesicles. Data represent duplicates trials.

The high degree of inter- and intra-rabbit variations in the hemodynamic parameters observed in the control rabbits suggests that large fluctuations are normal. Statistical analysis of the absolute difference in values after the injection of saline and the injection of vesicles for the experimental rabbits at both lipid doses, compared to the absolute difference after both injection of saline in the control rabbits exhibited no significant difference in most parameters (Table 5.2). However, this is not to say that there was no change, merely that any variation observed was not statistically significantly different than the controls using saline. There was a significant difference in pulse, $[HCO_3]$ and blood pH parameters for the lipid dose of 1.4 μmol/kg. However, there was no significant difference for the same parameters at the higher lipid dose. Thus, based on these results there was no significant alteration in the various hemodynamic parameters at lipid dose of 1.4 and 4.0 μmol/kg.

Table 5.2. Results of Statistical analysis of hemodynamic data.

Parameter Group	**p Value**	
	1.4 μmol/kg	**4.0 μmol/kg**
Heart rate (BPM)	0.017	0.473
Systolic blood pressure	0.762	0.130
Diastolic blood pressure	0.638	0.064
Temperature	0.437	0.952
$[HCO_3]$	0.041	0.972
pO_2	0.178	0.425
pCO_2	0.500	0.347
pH	0.028	0.671

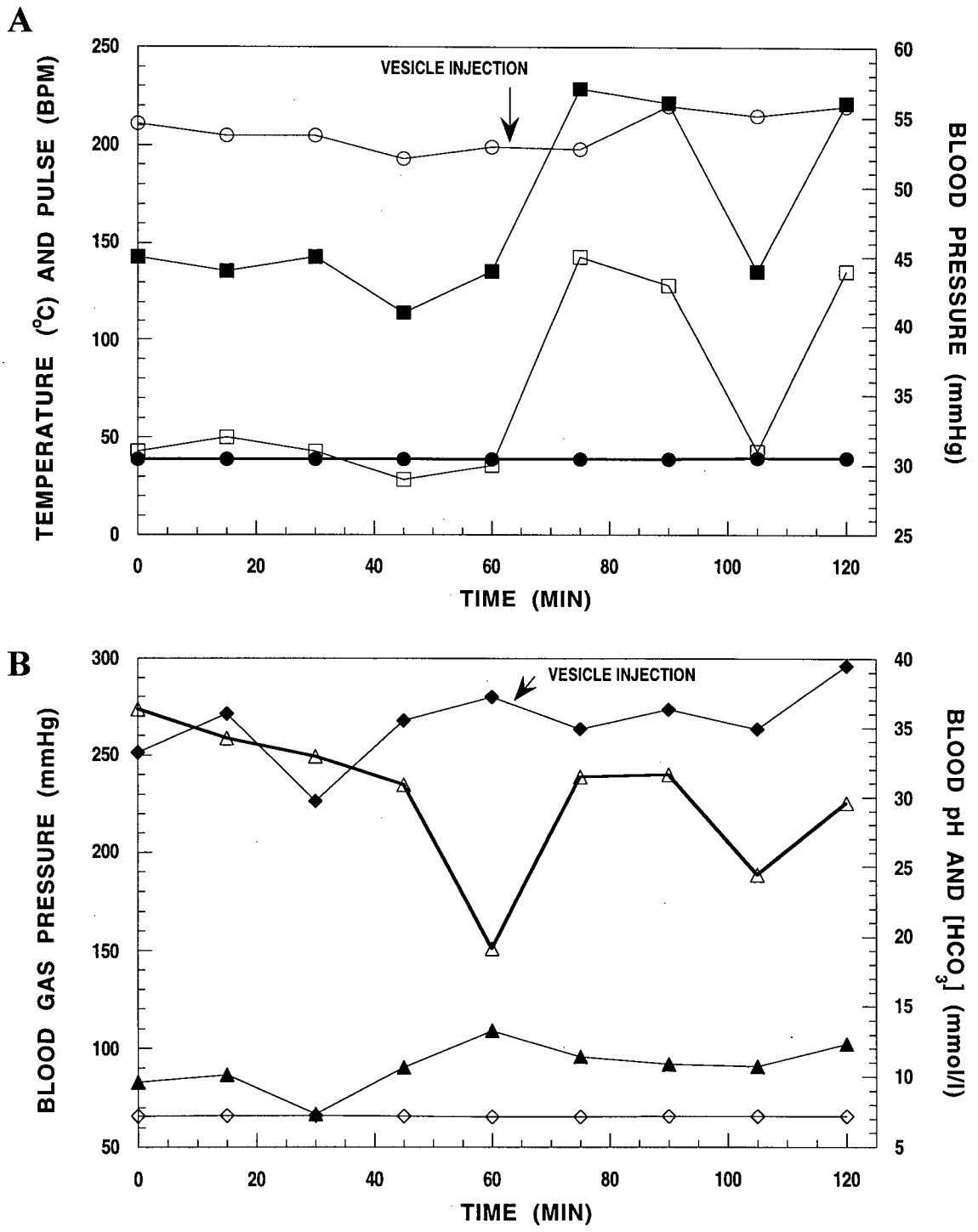

Figure 5.2. Hemodynamic data for experimental rabbit 1. Plot A displays variations in temperature (●), pulse (○), systolic (■) and diastolic (□) blood pressure. Plot B displays variations in pO_2 (Δ), pCO_2 (▲), blood pH (◊) and $[HCO_3]$ (◆). The rabbit was injected with 0.50 ml of saline at t = 0 and followed for 1 hour. After 1 hour the rabbit was injected with vesicles at a lipid dose of 1.4 μmol/kg and followed for another 1 hour.

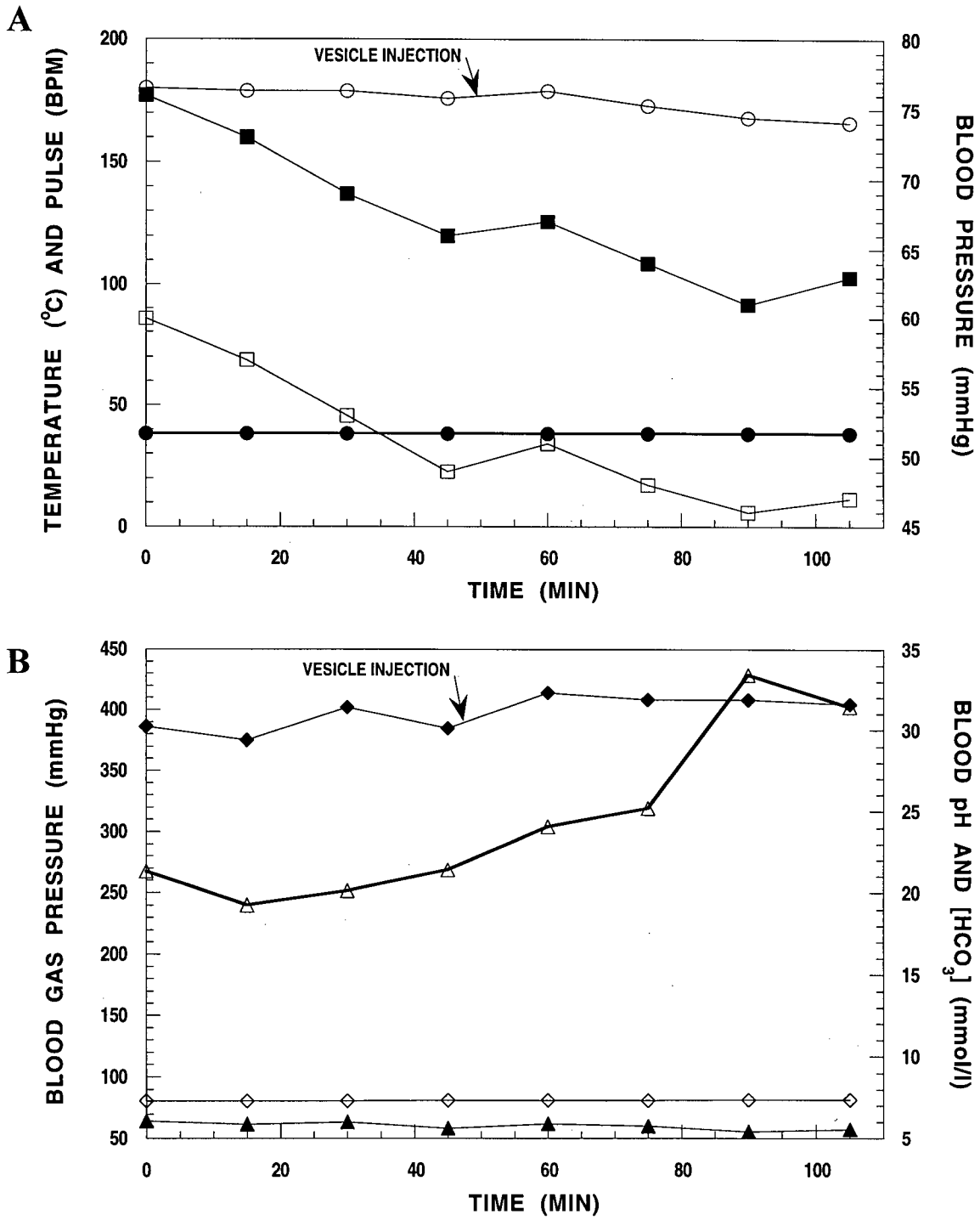

Figure 5.3. Hemodynamic data for experimental rabbit 2. Plot A displays variations in temperature (●), pulse (○), systolic (■) and diastolic (□) blood pressure. Plot B displays variations in pO_2 (Δ), pCO_2 (▲), blood pH (◊) and $[HCO_3]$ (◆). The rabbit was injected with 0.50 ml of saline at t = 0 and followed for 1 hour. After 1 hour the rabbit was injected with vesicles at a lipid dose of 1.4 μmol/kg and followed for another 1 hour.

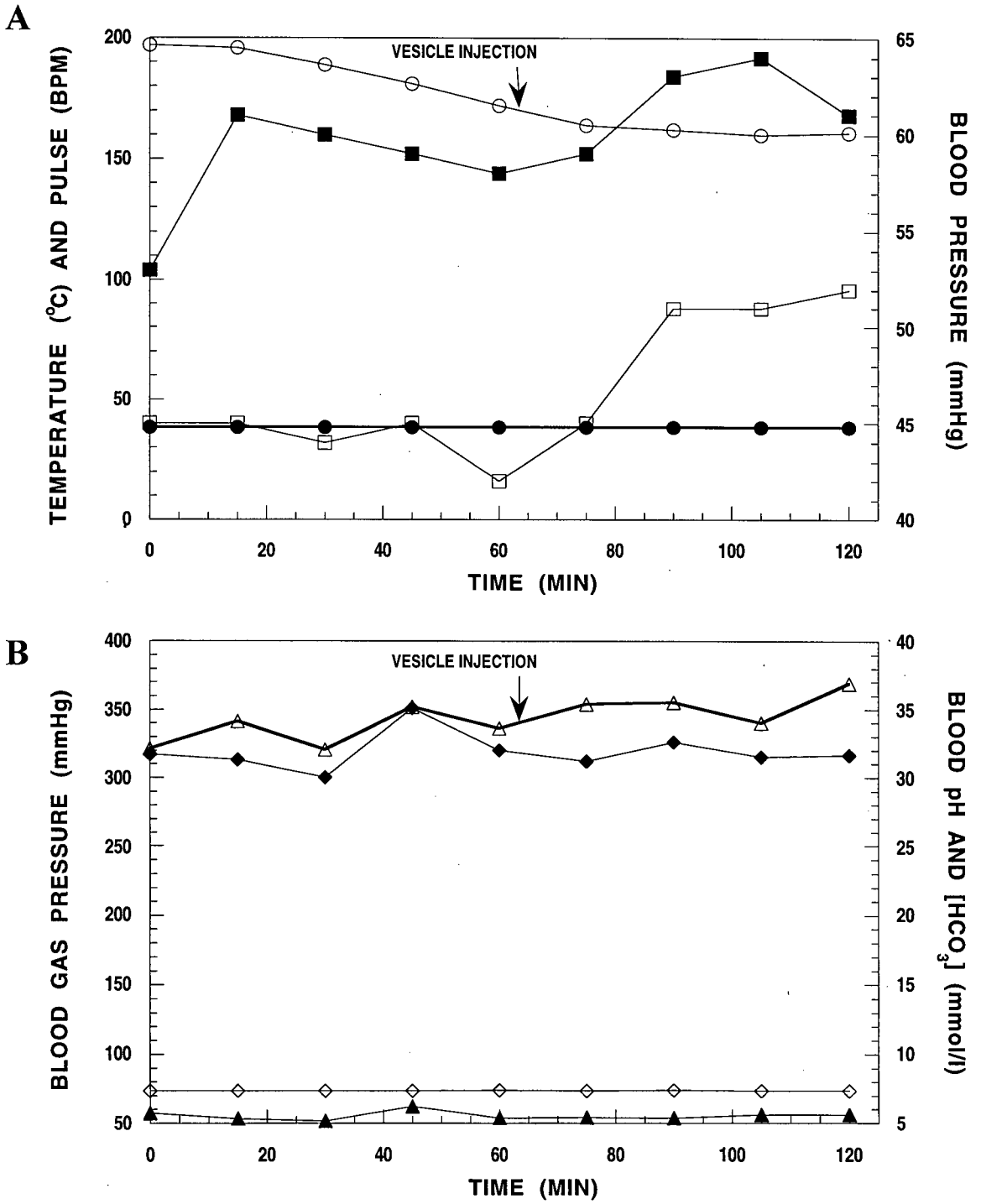

Figure 5.4. Hemodynamic data for experimental rabbit 3. Plot A displays variations in temperature (●), pulse (○), systolic (■) and diastolic (□) blood pressure. Plot B displays variations in pO_2 (Δ), pCO_2 (▲), blood pH (◊) and $[HCO_3]$ (◆). The rabbit was injected with 0.50 ml of saline at t = 0 and followed for 1 hour. After 1 hour the rabbit was injected with vesicles at a lipid dose of 1.3 μmol/kg and followed for another 1 hour.

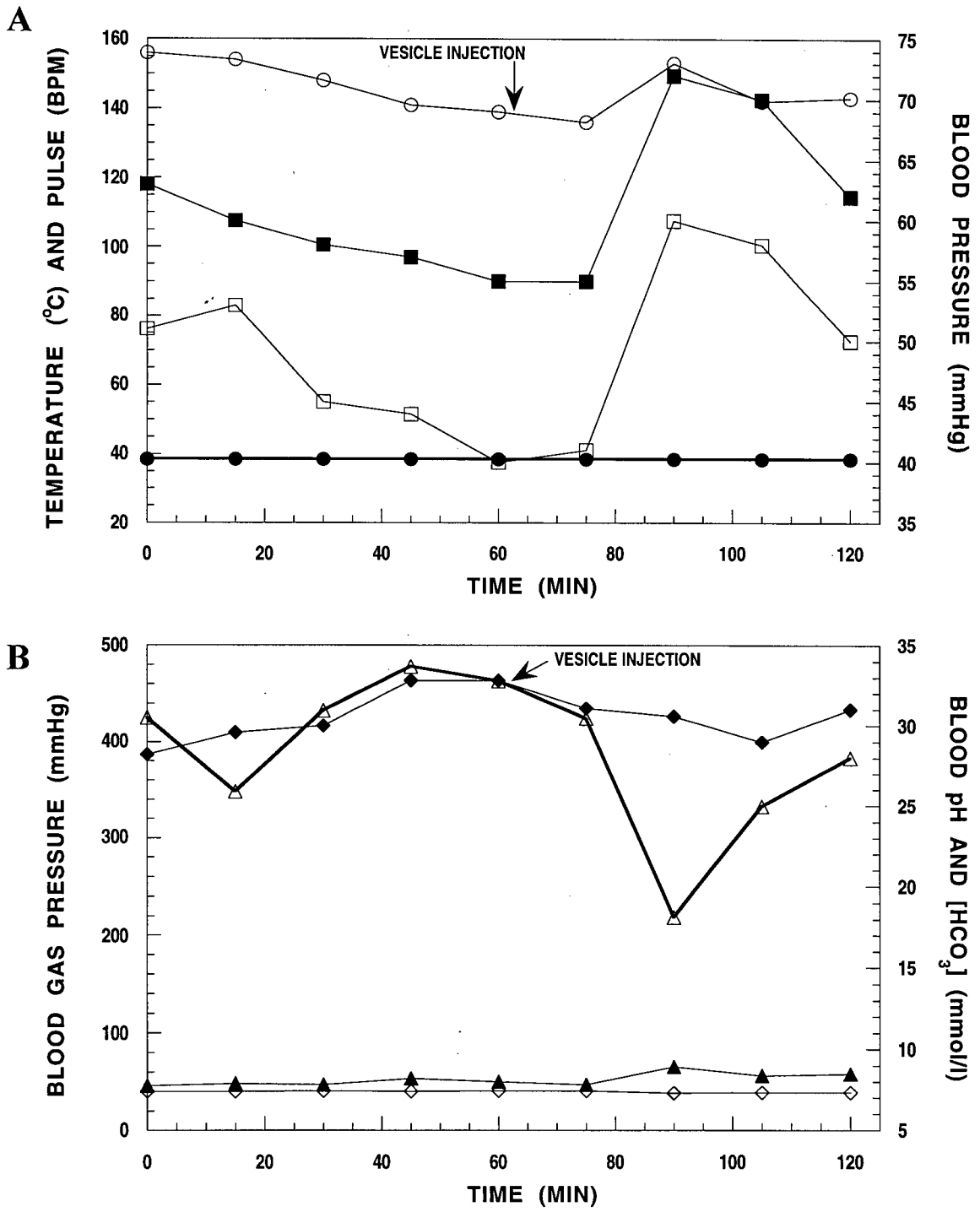

Figure 5.5. Hemodynamic data for experimental rabbit 4. Plot A displays variations in temperature (●), pulse (○), systolic (■) and diastolic (□) blood pressure. Plot B displays variations in pO_2 (Δ), pCO_2 (▲), blood pH (◊) and $[HCO_3]$ (◆). The rabbit was injected with 0.50 ml of saline at t = 0 and followed for 1 hour. After 1 hour the rabbit was injected with vesicles at a lipid dose of 1.4 μmol/kg and followed for another 1 hour.

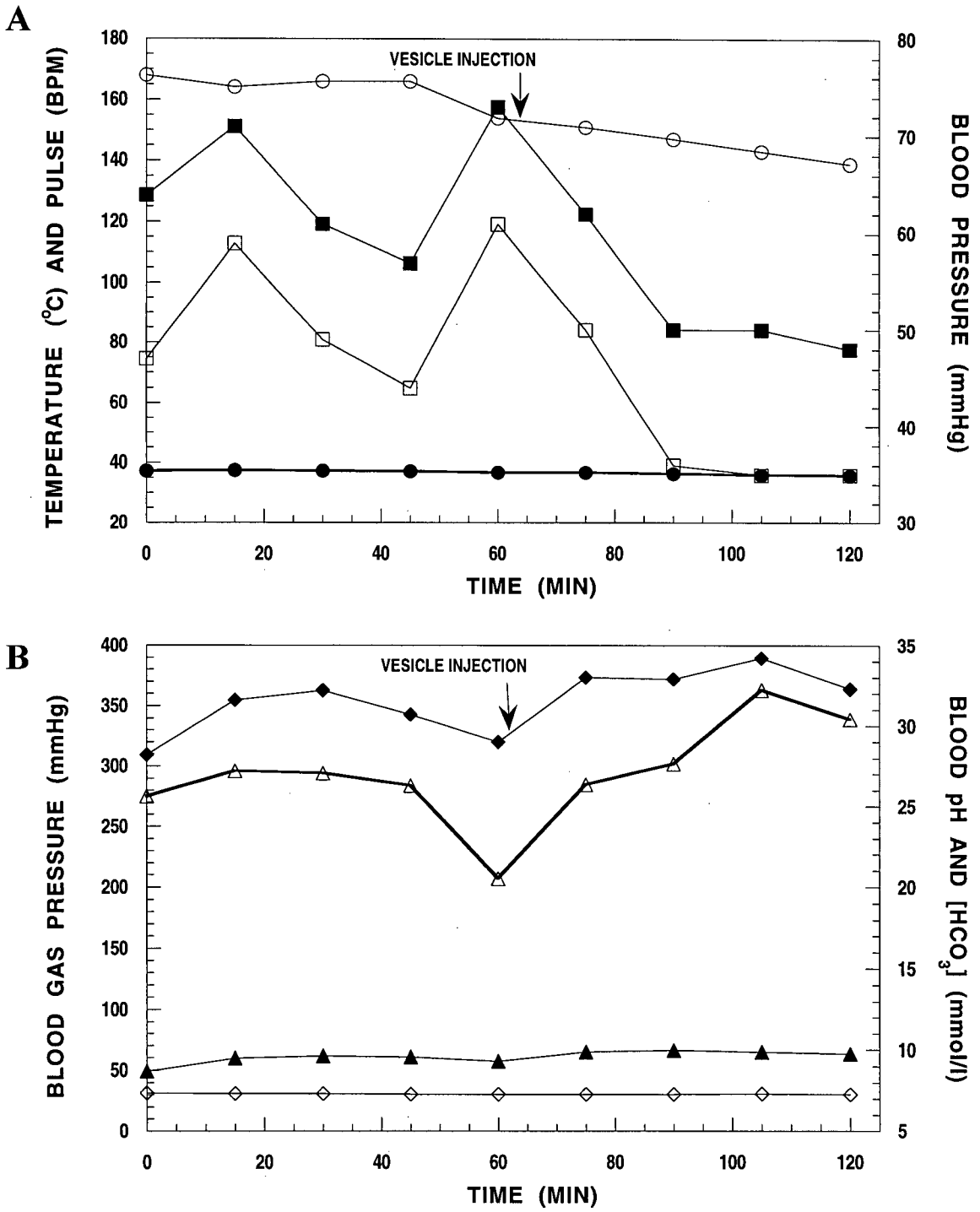

Figure 5.6. Hemodynamic data for experimental rabbit 5. Plot A displays variations in temperature (●), pulse (○), systolic (■) and diastolic (□) blood pressure. Plot B displays variations in pO_2 (Δ), pCO_2 (▲), blood pH (◊) and $[HCO_3]$ (◆). The rabbit was injected with 0.50 ml of saline at t = 0 and followed for 1 hour. After 1 hour the rabbit was injected with vesicles at a lipid dose of 1.4 μmol/kg and followed for another 1 hour.

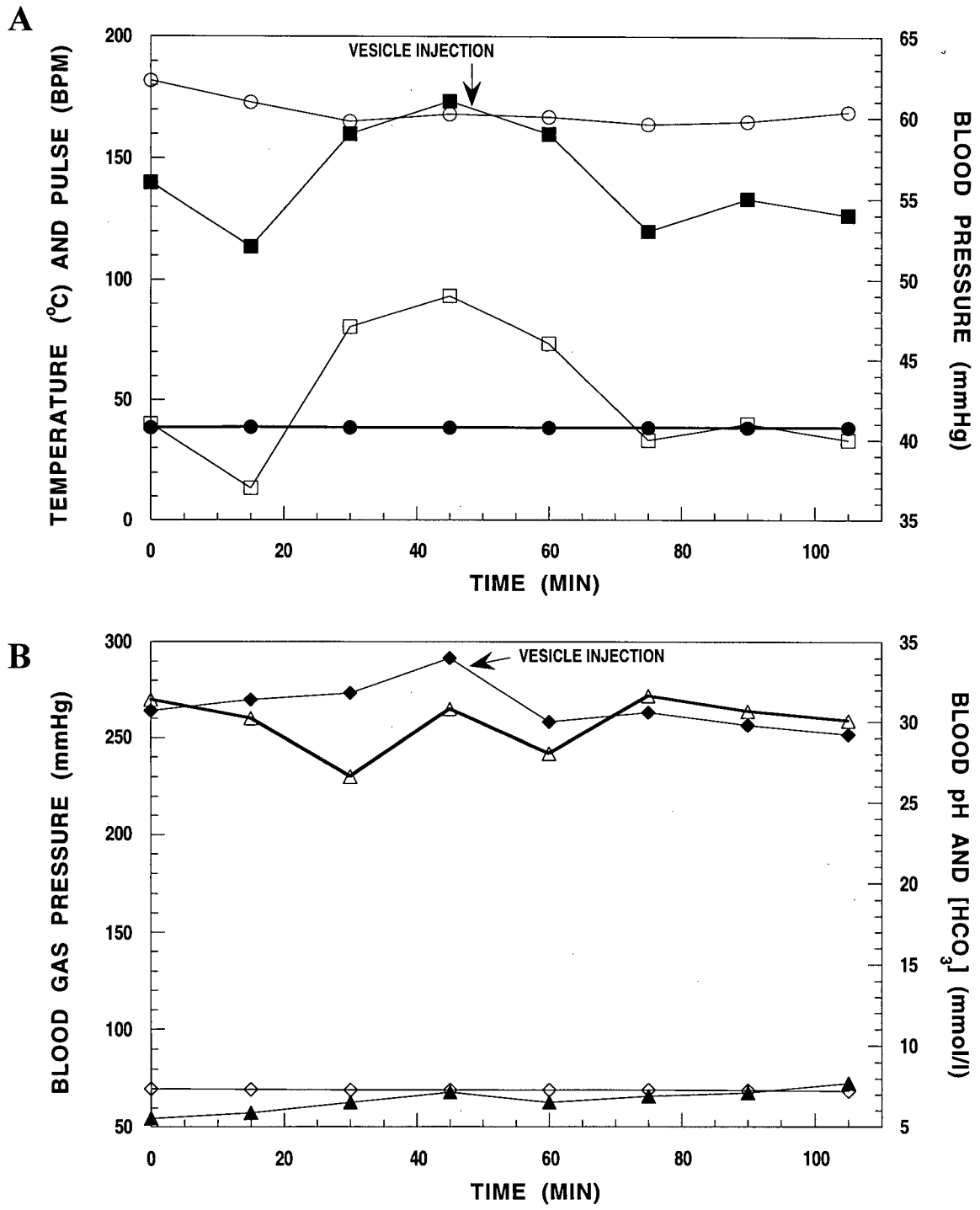

Figure 5.7. Hemodynamic data for experimental rabbit 6. Plot A displays variations in temperature (●), pulse (○), systolic (■) and diastolic (□) blood pressure. Plot B displays variations in pO_2 (Δ), pCO_2 (▲), blood pH (◊) and $[HCO_3]$ (◆). The rabbit was injected with 0.50 ml of saline at t = 0 and followed for 1 hour. After 1 hour the rabbit was injected with vesicles at a lipid dose of 1.5 μmol/kg and followed for another 1 hour.

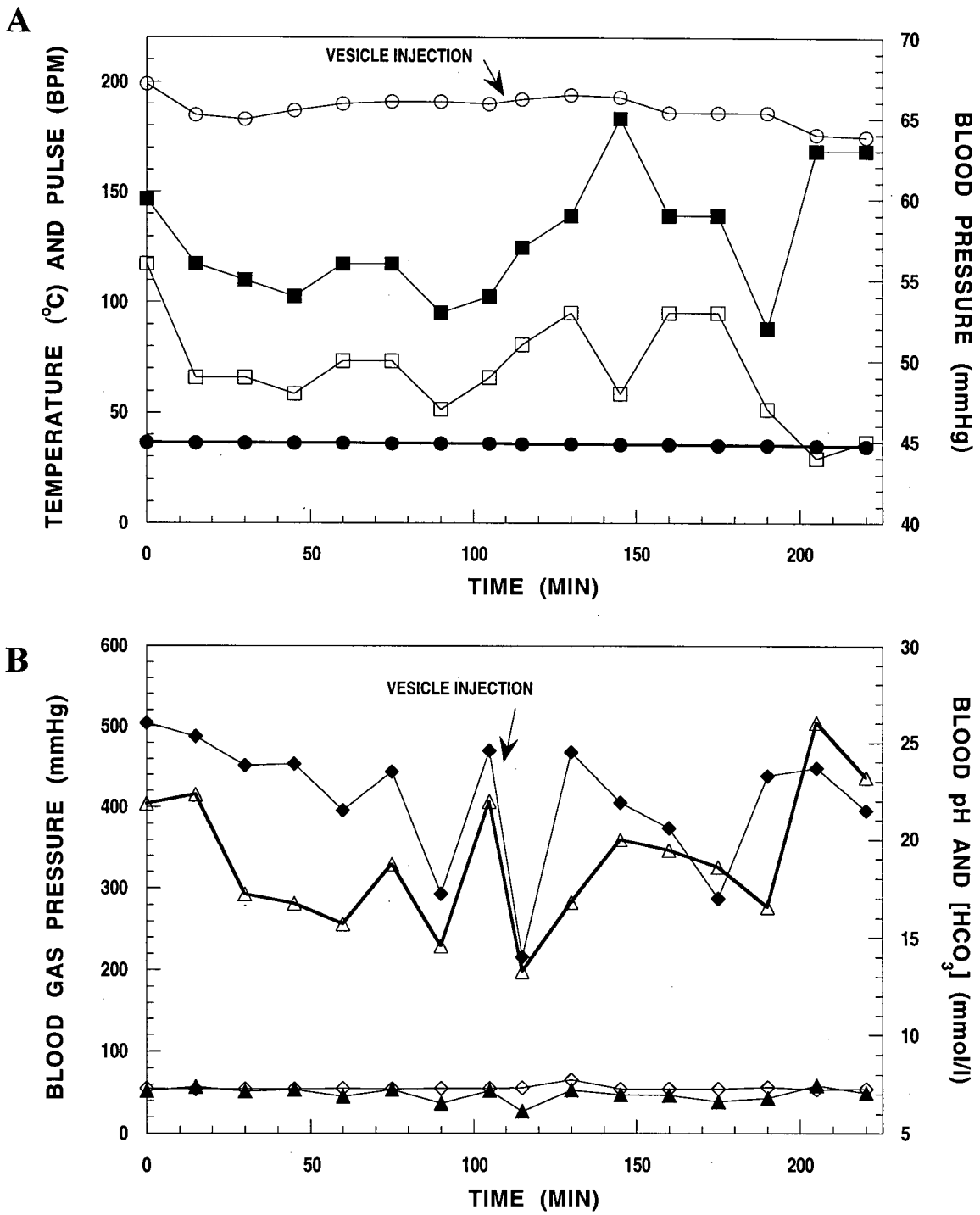

Figure 5.8. Hemodynamic data for experimental rabbit 7. Plot A displays variations in temperature (●), pulse (○), systolic (■) and diastolic (□) blood pressure. Plot B displays variations in pO_2 (Δ), pCO_2 (▲), blood pH (◊) and $[HCO_3]$ (◆). The rabbit was injected with 0.23 ml of saline at t = 0 and followed for ~2 hours. After 2 hours the rabbit was injected with vesicles at a lipid dose of 4.0 μmol/kg and followed for another 2 hour.

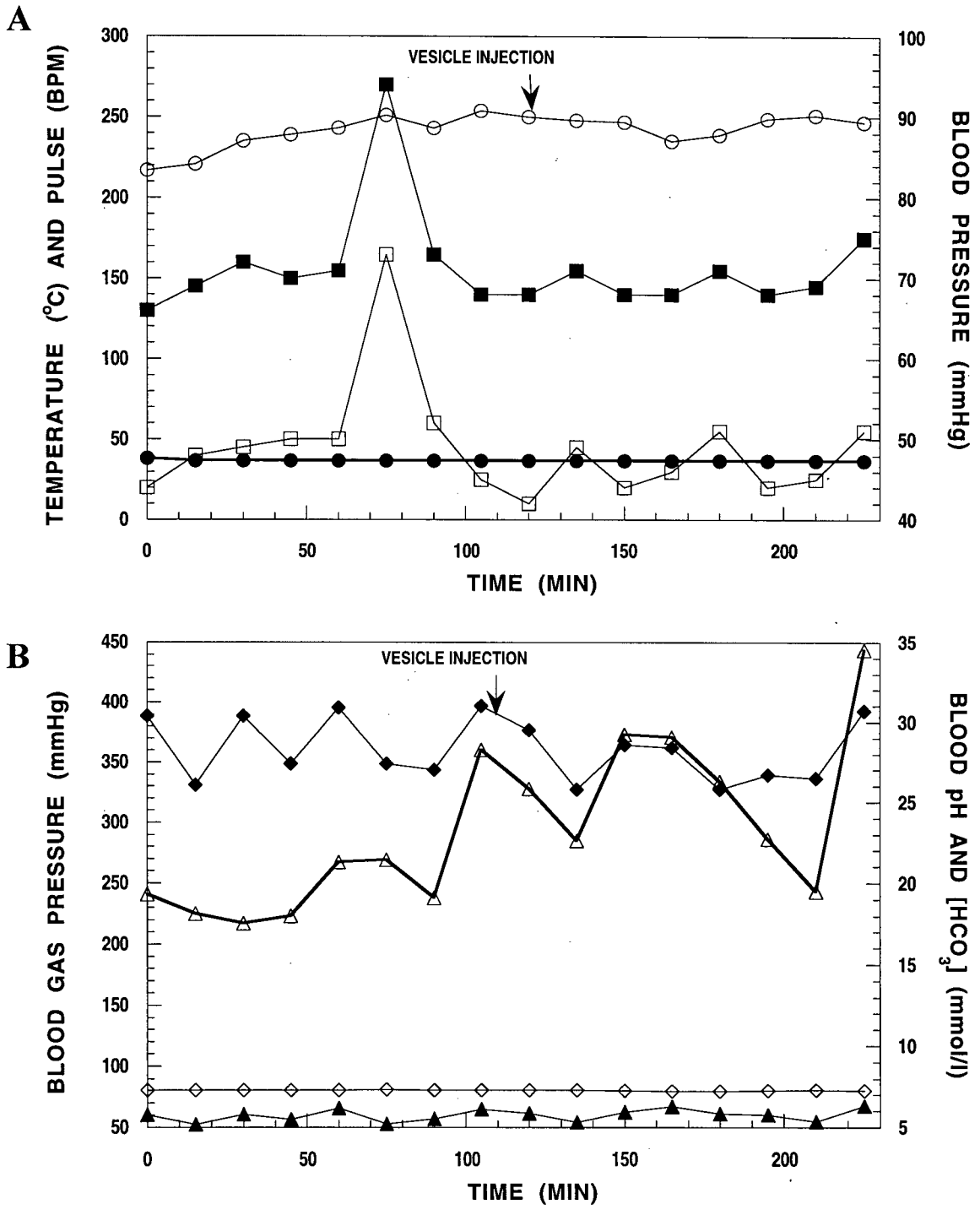

Figure 5.9. Hemodynamic data for experimental rabbit 8. Plot A displays variations in temperature (●), pulse (○), systolic (■) and diastolic (□) blood pressure. Plot B displays variations in pO_2 (Δ), pCO_2 (▲), blood pH (◊) and $[HCO_3]$ (◆). The rabbit was injected with 0.23 ml of saline at t = 0 and followed for ~2 hours. After 2 hours the rabbit was injected with vesicles at a lipid dose of 4.0 μmol/kg and followed for another 2 hour.

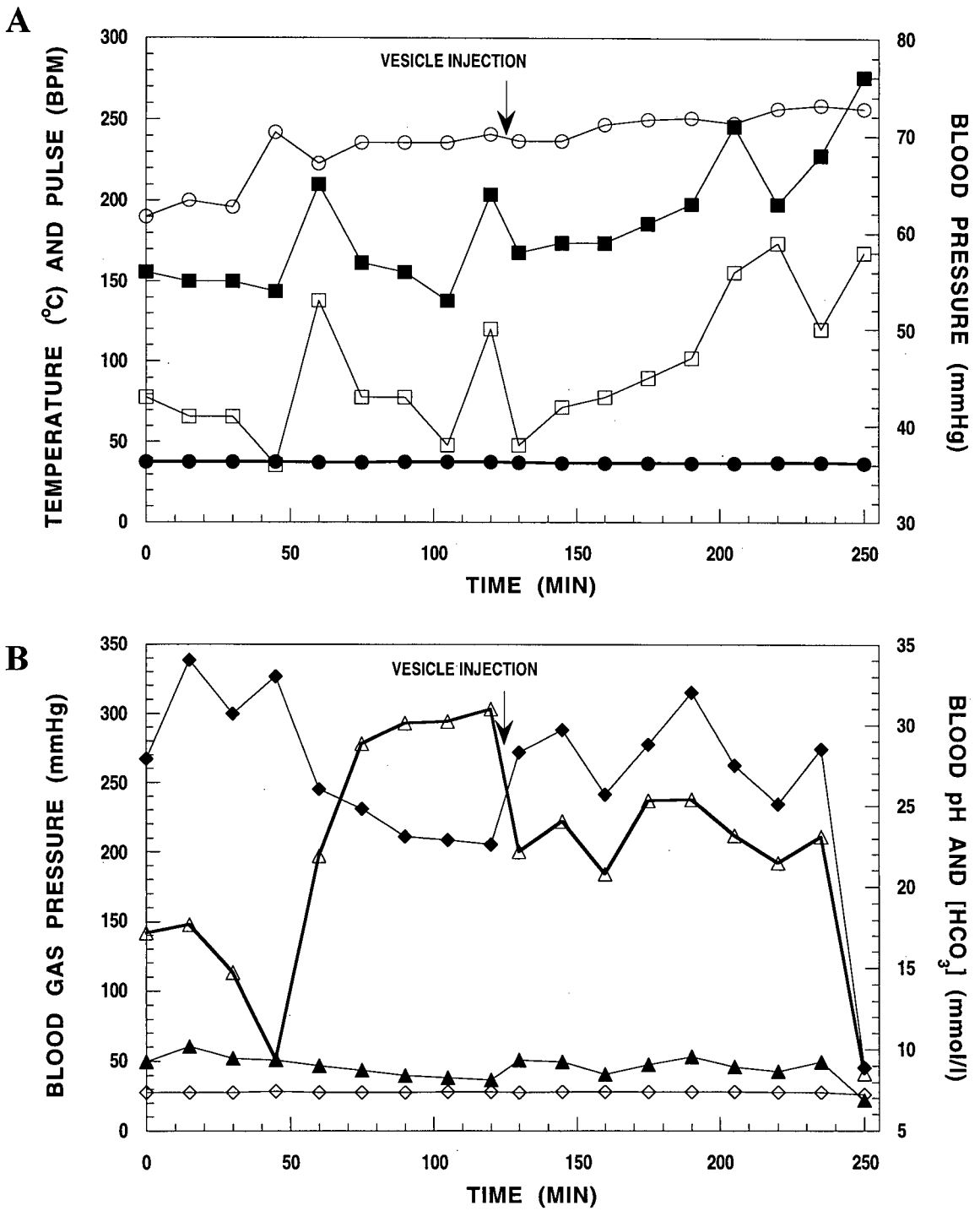

Figure 5.10. Hemodynamic data for experimental rabbit 9. Plot A displays variations in temperature (●), pulse (○), systolic (■) and diastolic (□) blood pressure. Plot B displays variations in pO_2 (Δ), pCO_2 (▲), blood pH (◊) and [HCO_3] (◆). The rabbit was injected with 0.23 ml of saline at t = 0 and followed for ~2 hours. After 2 hours the rabbit was injected with vesicles at a lipid dose of 4.0 μmol/kg and followed for another 2 hour.

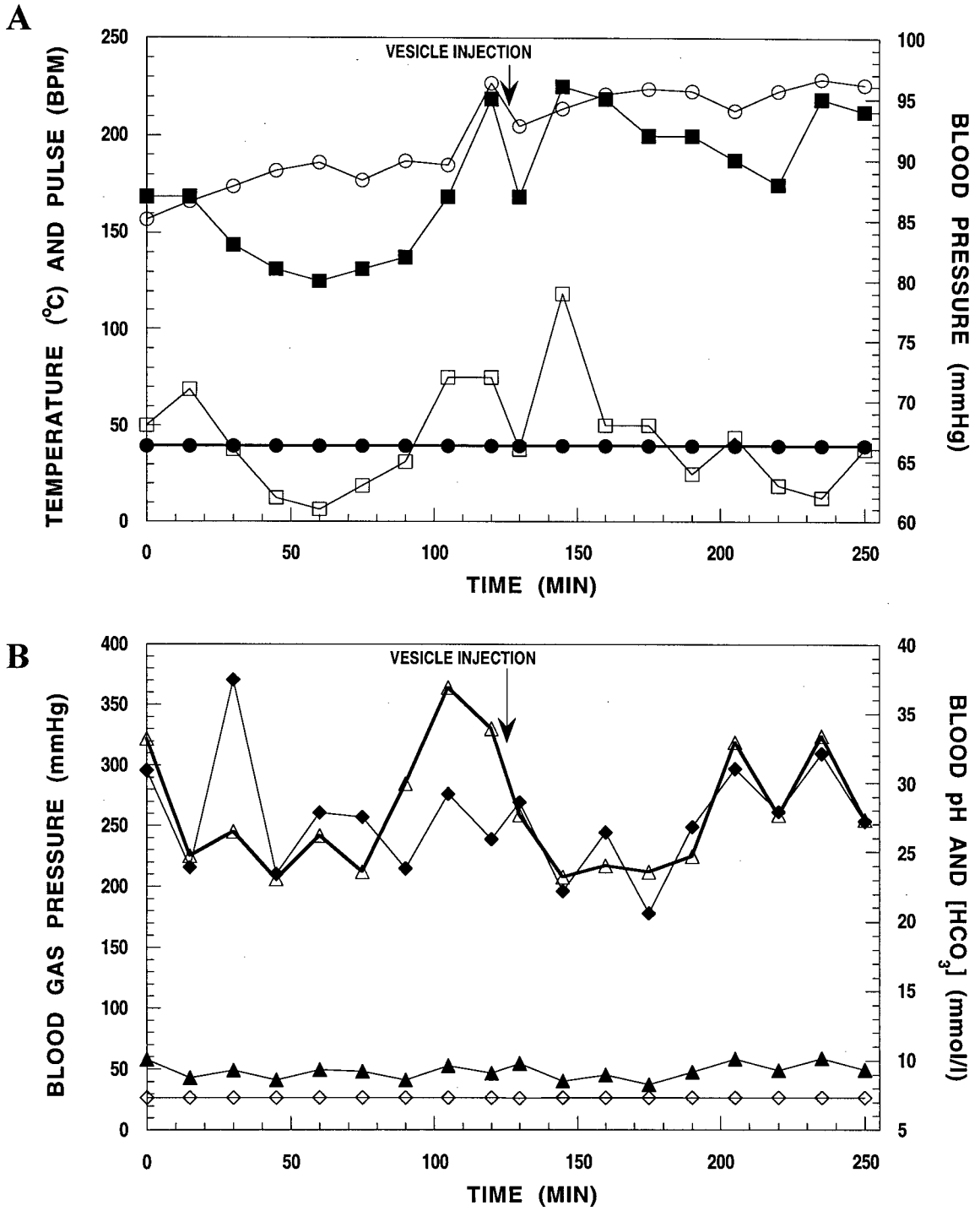

Figure 5.11. Hemodynamic data for experimental rabbit 10. Plot A displays variations in temperature (●), pulse (○), systolic (■) and diastolic (□) blood pressure. Plot B displays variations in pO_2 (Δ), pCO_2 (▲), blood pH (◊) and [HCO_3] (◆). The rabbit was injected with 0.23 ml of saline at t = 0 and followed for ~2 hours. After 2 hours the rabbit was injected with vesicles at a lipid dose of 4.0 μmol/kg and followed for another 2 hour.

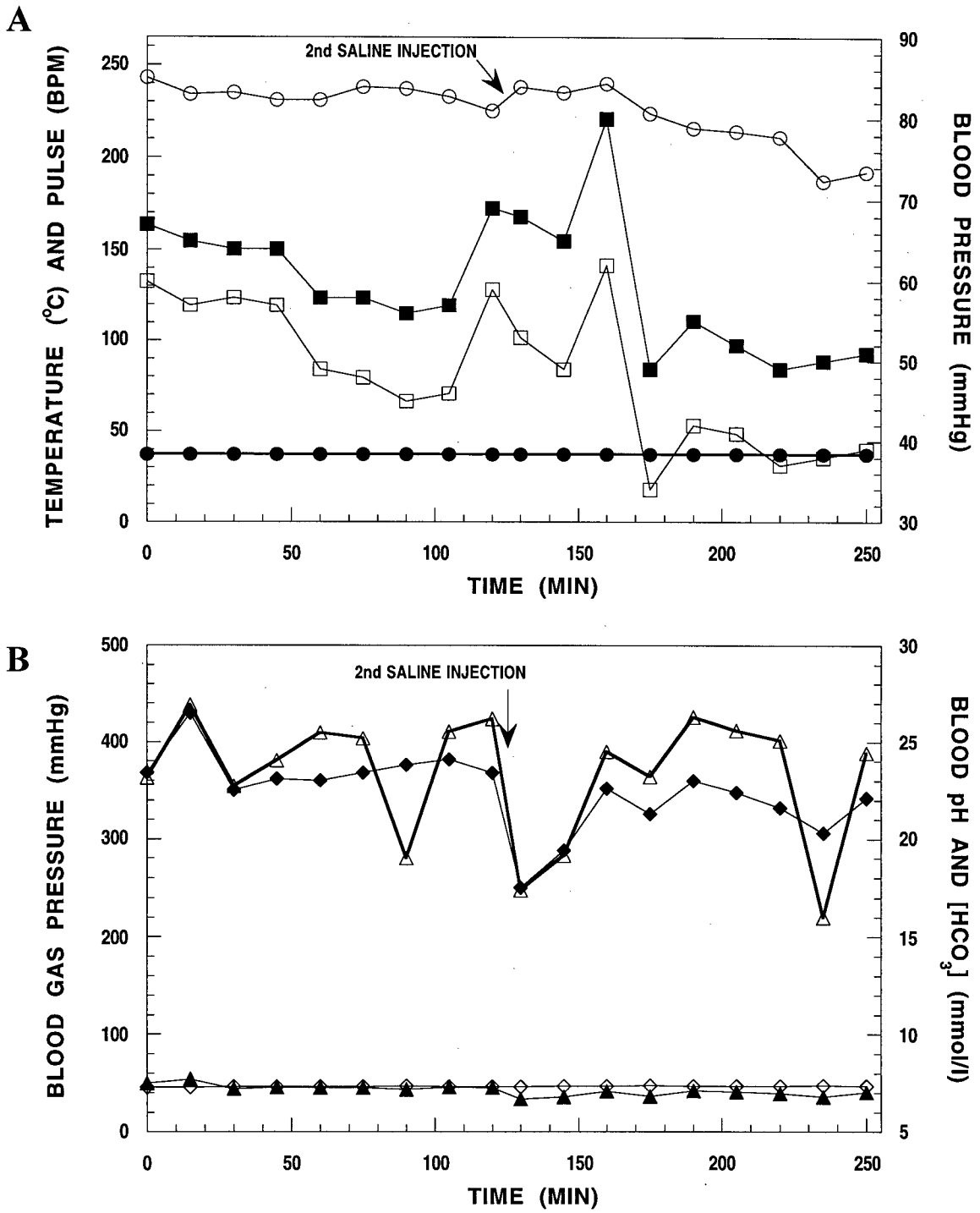

Figure 5.12. Hemodynamic data for control rabbit 1. Plot A displays variations in temperature (●), pulse (○), systolic (■) and diastolic (□) blood pressure. Plot B displays variations in pO_2 (Δ), pCO_2 (▲), blood pH (◊) and [HCO_3] (◆). The rabbit was injected with 0.23 ml of saline at t = 0 and followed for ~2 hours. After 2 hours the rabbit was injected with another 0.23 ml of saline and followed for another 2 hour.

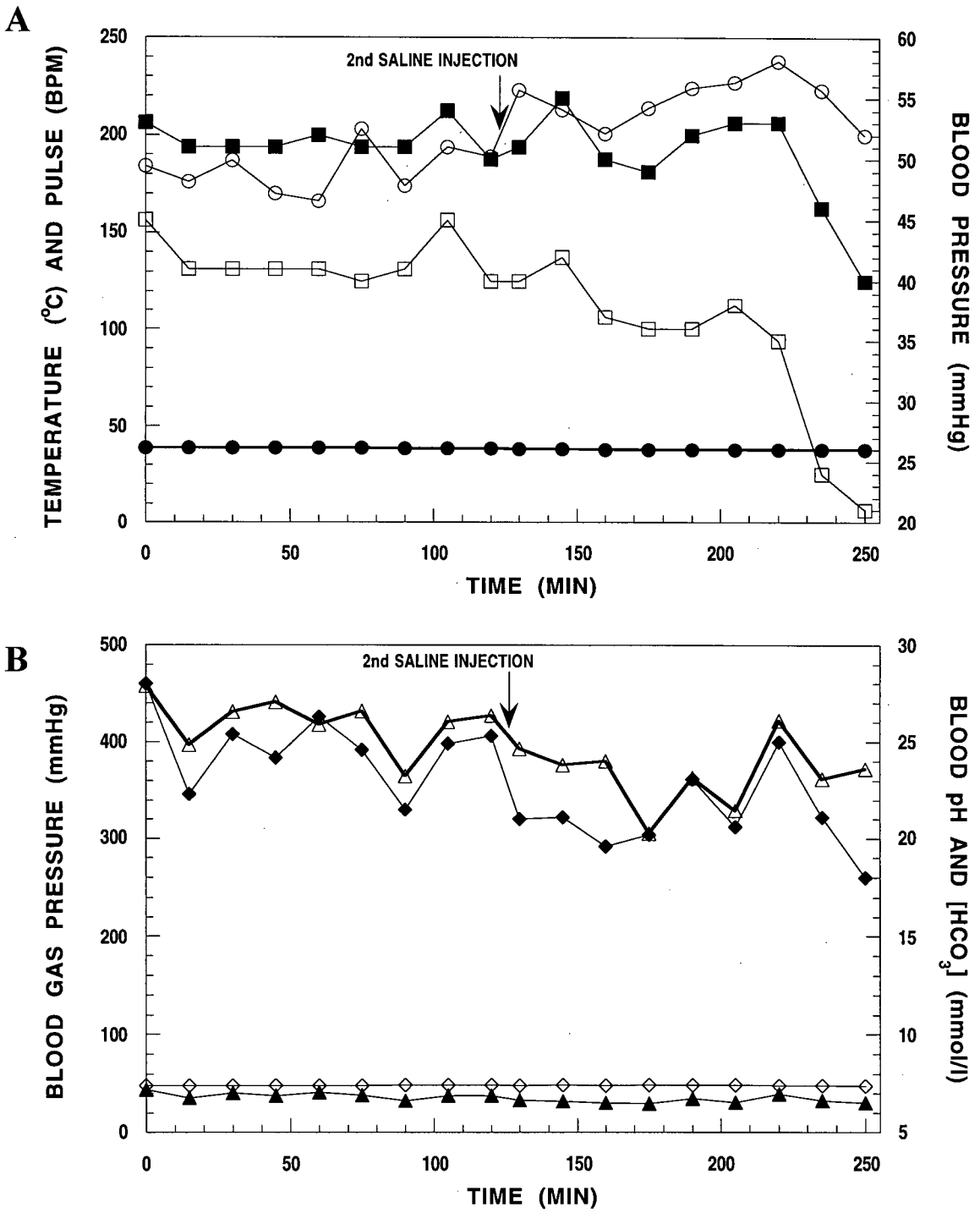

Figure 5.13. Hemodynamic data for control rabbit 2. Plot A displays variations in temperature (●), pulse (○), systolic (■) and diastolic (□) blood pressure. Plot B displays variations in pO_2 (Δ), pCO_2 (▲), blood pH (◊) and [HCO_3] (◆). The rabbit was injected with 0.23 ml of saline at t = 0 and followed for ~2 hours. After 2 hours the rabbit was injected with another 0.23 ml of saline and followed for another 2 hour.

Discussion

The results presented in this chapter address the issue of the safety and toxicity of PEG-coated vesicles before the administration in humans as a potential blood pool imaging agent. The pyrogenicity of the vesicle dispersion was determined to assess the sterility of the preparation procedure and the pyrogenicity of the vesicle components. There are essentially two recognized methods to assess the pyrogenicity of a substance: 1) Limulus Amebocyte Lysate (LAL) assay and 2) rabbit pyrogen testing.

The LAL assay is based on the observation that bacterial endotoxins, such as LPS, initiate the gelation of reagents made from freshly lysed blood cells from the American horseshoe crab [160]. This test is rapid, sensitive and cheaper than rabbit testing but is sensitive only to bacterial contamination. For rabbit pyrogen testing, US Pharmacopeia National Formulary (USPNS) protocol states that for a substance to be deemed as non-pyrogenic, none of three rabbits can show an individual temperature increase of 0.6°C or more and the sum of the individual temperature increases for all three rabbits can not exceed 1.4°C [161]. Any decrease in temperature is taken as a zero increase in temperature.

Discrepancies between the two pyrogen tests usually result in a positive LAL assay and a negative rabbit test due to the higher sensitivity of the LAL assay. However, studies have shown that certain substances (i.e. such as uridine, muramyl dipeptide (MDP) and Deodan) produce negative LAL assays and positive rabbit tests [164-166]. This indicates that these substances activate the pyrogen response not through bacterial contamination but through direct release of endogenous pyrogens, such as cytokines, to initiate the fever response. Guencheva et al. showed that the pyrogen response caused by Deodan can be modulated by administration of antibodies directed to interleukin-1 and -6 and tumor necrosis factor α [166]. These cytokines, as well as others, are thought to

modulate the pyrogen response [167-170]. Thus, the pyrogen testing of substances, especially experimental, in rabbits is important not only to determine bacterial contamination which may occur during production, but also to establish the substances' ability to directly activate the fever response.

For this reason, rabbit pyrogen testing was used to assay the pyrogenicity of PEG-coated vesicles before the administration to human subjects in preliminary trials. The administration of vesicles resulted in no individual temperature increase of greater than 0.2°C and the sum of the all the temperature increases was 0.3°C (Table 1). Thus, according to the USPNF guidelines, PEG-coated vesicles are deemed as being non-pyrogenic.

The interaction of vesicles with the complement system has been studied extensively [126,128,129,131]. Charge plays an important role in determining whether a lipid composition can activate the complement system. Vesicles, with either a positive or negative charge, activate the complement system at relatively low lipid concentrations (<1mM) while neutral vesicles do not activate the complement system over a wide range of lipid concentrations [143,146]. In general, the inclusion of negatively charged lipids activates the complement cascade via the classical pathway in a dose dependent fashion, and smaller diameter vesicles (<100 nm) activate the complement system to lesser degree than large diameter vesicles [128].

The importance of determining the degree of complement activation of PEG-coated vesicles is two fold - clearance and toxicity. Firstly, it has been shown that deposition of activated complement components on the surface of vesicles act as opsonins, tagging them for clearance by the RES [125]. Thus, the circulation half-life of a particular vesicle composition is inversely related to its ability to activate the complement cascade. Secondly, it was important to assess the safety of PEG-coated vesicles before

administration to human subjects. Activation of the complement system in healthy patients is generally asymptomatic but may result in mild transitory pulmonary dysfunction-related symptoms, like chest tightness and/or flushing [170]. For the preliminary testing of the PEG-coated vesicles as a blood pool imaging agent, the patient pool will consist of only healthy patients and possible activation of the complement system will not have serious adverse effects on this patient pool. However, in the case of using PEG-coated vesicles in determining the cardiac function in patients who have suffered a myocardial infarction or other cardiac dysfunction, complications which may arise from complement activation may have more serious effects.

Activation of the complement system has recently been implicated in what is known as reperfusion injury in patients during acute myocardial infarction [171-174]. The rapid re-establishment of coronary blood flow to affected myocardium via mechanical (i.e. angioplasty) or pharmacological means (i.e. streptokinase) greatly reduces infarct size and mortality [175-177]. However, a side effect of early reperfusion is that it may cause myocardial stunning, arrhythmias, or irreversible and sometimes lethal cell injury. Although the majority of tissue injury in the infarcted area is caused by ischemia, it has been well documented that the re-establishment of circulation in the infarcted area causes activation of the complement system which increases the extent of tissue damage [185,192]. Although the effect of further activation of the complement cascade by the administration of an imaging agent which may activate the complement system is unknown, presumably it would be desirable to have an agent which does not activate the complement system to prevent any further damage to the myocardium. Thus, PEG-coated vesicles were tested over a wide range of lipid doses for their ability to activate the complement system.

The results of the CH50 assay over the lipid concentration range of ~0.06-64 mM exhibited that there was no measurable activation of the complement system (Figure 5.1).

The preparation of the vesicles for injection, calls for the dilution of 0.5 ml of ~160 mM lipid dispersion with 0.5 ml of ^{99m}Tc/HM-PAO solution, resulting in final concentration of ~80 mM at the time of injection. Thus, the administration of PEG-coated vesicles in patients will result in transiently higher local lipid concentration at the site of injection. However, there is a rapid equilibration of vesicles within the volume of distribution within the body. Assuming that vesicles remain in the blood pool, a person six feet tall weighing 85 kgs will have an average blood volume of ~5.6 liters [179]. Thus, the approximate overall systemic lipid concentration is 0.014 mM, which is lower than the lowest lipid dose tested. Thus, activation of the complement system is not expected for both vesicle compositions consistent with observations.

The hemodynamic studies on the effect of vesicles administration on various parameters showed no significant changes after the administration of vesicles compared to the administration of saline. However, examination of the figures for each rabbit showed significant inter- and intra-rabbit variations in some parameters during the course of the experiment (Figures 5.2-5.13). The parameters which exhibited the greatest variations were pO_2, pCO_2, pulse and blood pressure. It should be noted that similar observation in variability were observed in the control rabbits which only received saline injections (Figures 5.12 and 5.13). Thus, it appears that under the experimental conditions these fluctuations are normal. A possible source of the variations may be due to the breathable anesthetic halothane used in all experiments. Studies have shown that halothane cause a decrease in blood pressure and an increase in heart rate which is dependent on the dose of inhaled anesthetic [180-182]. During the course of the experiment, the amount of halothane administered to the rabbits was adjusted in response to rabbit behavior (i.e. regaining of withdrawal reflex, waking up or holding breath) which may account for the observed variations. Another factor which could have contributed to the observed variations was that the rabbits were allowed to free breathe. Important parameters which were expected not to change were temperature and blood pH. Pyrogen testing showed

that the vesicles did not initiate a fever response in rabbits and significant changes in blood pH would have resulted in death during the course of the experiment which was not observed.

In summary, the toxicity of vesicles was assessed by testing the ability of vesicles to: 1) initiate a fever response by pyrogen testing, 2) activate the complement system via CH50 complement assay and 3) alter various hemodynamic parameters. The results of these studies demonstrate that PEG-coated vesicles are minimally toxic and safe for administration to humans in preliminary trials.

Chapter 6 :

Case Study :
Testing in a Normal Healthy Volunteer

Introduction

Assimilating the results from the previous chapters, a final pharmaceutical kit was developed. The timeline for the labeling of the vesicles is presented in figure 6.1. The kit components and labeling procedure is presented in Figure 6.2. The first step is the rehydration of an HM-PAO kit by the addition of 0.5 ml of saline, then 20-30 mCi of ^{99m}Tc followed by incubation at room temperature for 5 minutes. A second tube containing a pre-measured volume of vesicles and a syringe containing a pre-determined amount of NaOH will also be part of the kit. After the 5 minute incubation of the HM-PAO kit, the tagging efficiency will be determined. If greater than 90%, NaOH will be added to the vesicles and mixed thoroughly followed by the addition of the ^{99m}Tc/HM-PAO solution. The vesicles are incubated at room temperature for 5 minutes and are then ready for administration. Based on this kit design, PEG-coated vesicles were tested for LVEF determination in one normal healthy volunteer at a lipid dose of 1 μmol/kg.

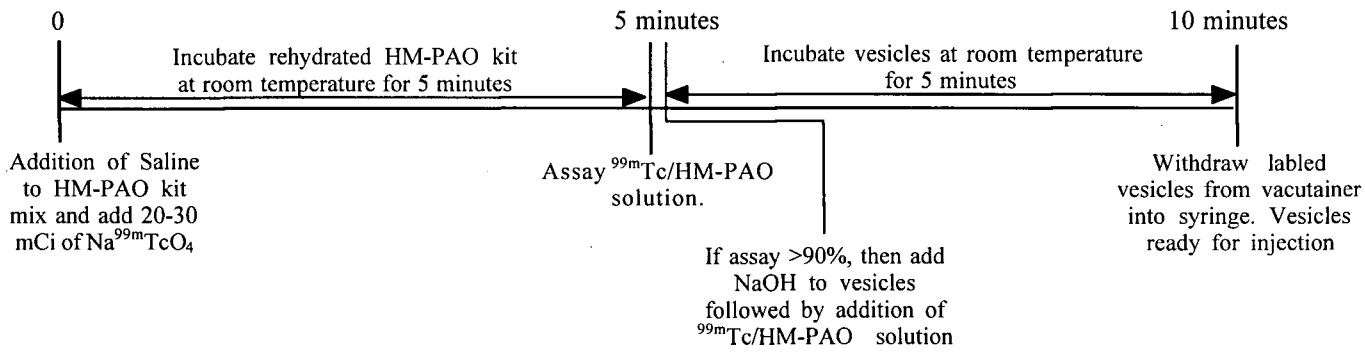

Figure 6.1. Timeline for labeling of vesicles.

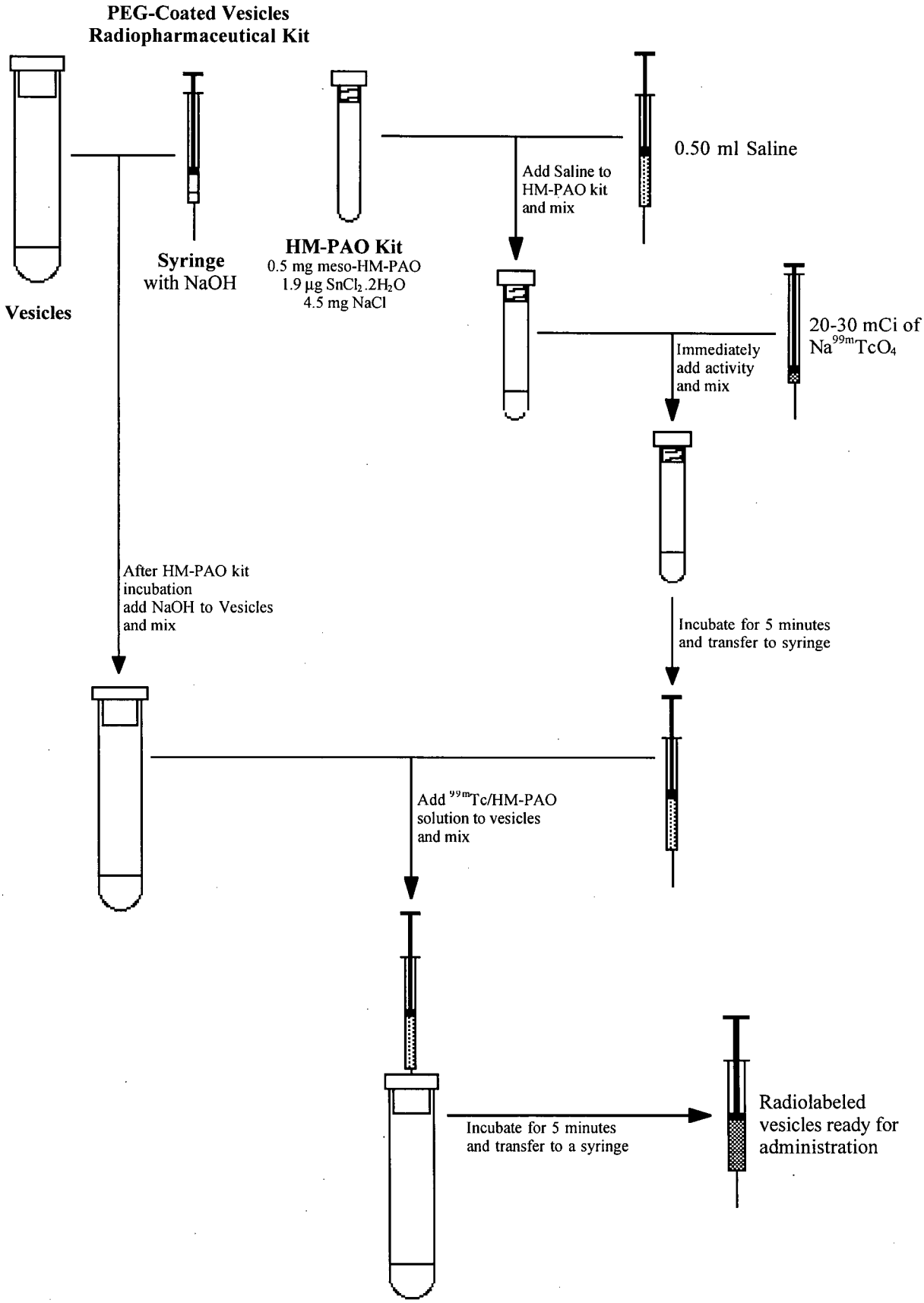

Figure 6.2. Diagram of proposed kit and labeling protocol.

Materials

As described in Chapter 2.

Methods

Preparation of vesicles

Lipids were combined from stock solution in chloroform in the final molar composition of DPPC:Chol:PE-PEG 5000 (47.75:47.75:4.5). Vesicle preparation as described in Chapter 2.

Preparation of Vesicles for Kit

The lipid concentration of the final lipid dispersion after extrusion was determined to be 141.86 mM and the weight of the volunteer was 80 kg. Thus, a sample of 0.56 ml of the vesicle dispersion was needed to achieve a lipid dose of ~1.0 μmol/kg. The vesicle sample was in filtered through 0.200 μm filter unit (Satorius Minisart NML, Toronto, ON) into a sterile vacutainer and stored at 4°C.

A syringe was filled with 76.5 μl of 250 mM NaOH which had been filtered through a 0.2 μm filter unit (Satorius Minisart NML, Toronto, ON). The volume of NaOH needed by calculating the number of moles of glutathione in 0.56 ml of vesicles and multiplying that value by 1.13 (0.56ml *30 mM*1.13).

Preparation of meso-HM-PAO kits

As described in Chapter 2.

Acquisition of Data

The procedure for the testing of vesicles in human subjects was approved by the Clinical Screening Committee for Research Involving Human Subjects at the University of British Columbia (certificate # C93-0602). The volunteer was positioned under the camera head (Siemens) in the supine position. A butterfly needle was placed in the left arm vein through which the activity was administered. Images were acquired during the injection of activity for first pass measurements. Serial images were then acquired of the biodistribution of activity through the body. After biodistribution measurements, the volunteer was then connect to a ECG and images acquired for determination of LVEF. Data was analyzed using commercially available software from Siemens on the ICON system.

Due to limitation of the size of the camera head, individual images of the head, chest, abdomen, upper thighs, lower legs and feet were acquired. Images were acquired for each region over a period of two minutes. Composites of the entire human body were prepared by aligning the images. Due to autocorrection of resolution, images of the legs appear darker than that associated with the chest. Thus, the individual images are not directly comparable and are provided only to give an overall picture of the biodistribution of activity.

Results

Labeled RBC Study

The volunteer was injected with stannous pyrophosphate followed by a 15 minute waiting period. After the waiting period, the volunteer was positioned under the camera and injected with pertechnetate. Images used to determine left ventricular ejection fraction (LVEF) are presented in Figure 6.3. The LVEF was calculated to be 69%.

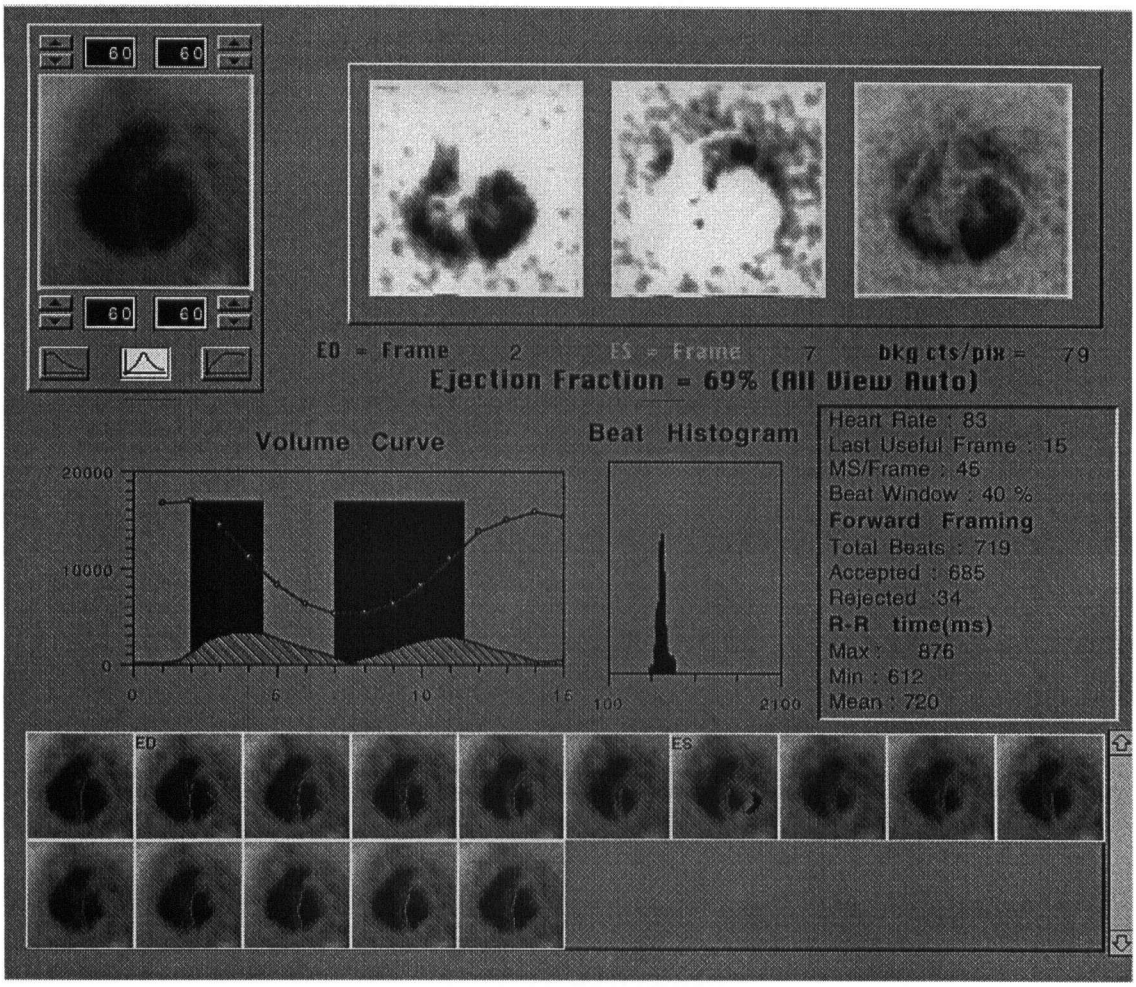

Figure 6.3. Calculation of left ventricular ejection fraction (LVEF) using labeled RBCs. Each heart beat was divided in a number of discrete divisions. The camera acquired data in each division and the individual images were combine to produce composite image of the heart during each division of the cardiac cycle. Images corresponding to end diastole (ED), were the ventricle has the greatest amount of blood, and end systole (ES), were the ventricle has the least amount of blood, were compared to give the percentage of blood ejection form the left ventricle during each contraction. The LVEF was determined to be 69%.

Labeled Vesicle Study

Approximately 4 months after the labeled RBC study, the volunteer was re-imaged using labeled PEG-coated vesicles. The HM-PAO kit was rehydrated with 0.5 ml of saline and mixed, immediately followed by the addition of 25 mCi of sodium pertechnetate. The tube was mixed and incubated at room temperature for 5 minutes. After incubation, the tagging efficiency was determined to be 92.6% by the partition assay described in Chapter 2. NaOH was added to the vesicles from the syringe and mixed. The ^{99m}Tc/HM-PAO solution was drawn into a syringe and added to the vesicles. The tube was mixed and incubated at room temperature for 5 minutes after which the labeled vesicles were injection into the volunteer. The labeling efficiency was determined to be 93.0% by chromatography on BioGel minicolumn (Chapter 4).

The biodistribution of activity at 1 and 4 hours after injection is presented in Figure 6.4. At the early time point, the majority of the activity is associated with the heart, liver and spleen. Also, the major structures of the vascular tree and the bladder are well defined. At 4 hours, there was a decrease in the activity associated with the heart, while the liver and spleen remained virtually constant. The major structures of the vascular tree were still well visualized.

Images used to calculated right ventricular ejection fraction (RVEF) from the first pass study are presented in Figure 6.5. Images used to determine left ventricular ejection fraction (LVEF) are presented in Figure 6.6. The RVEF and LVEF were calculated to be 58% and 73%, respectively.

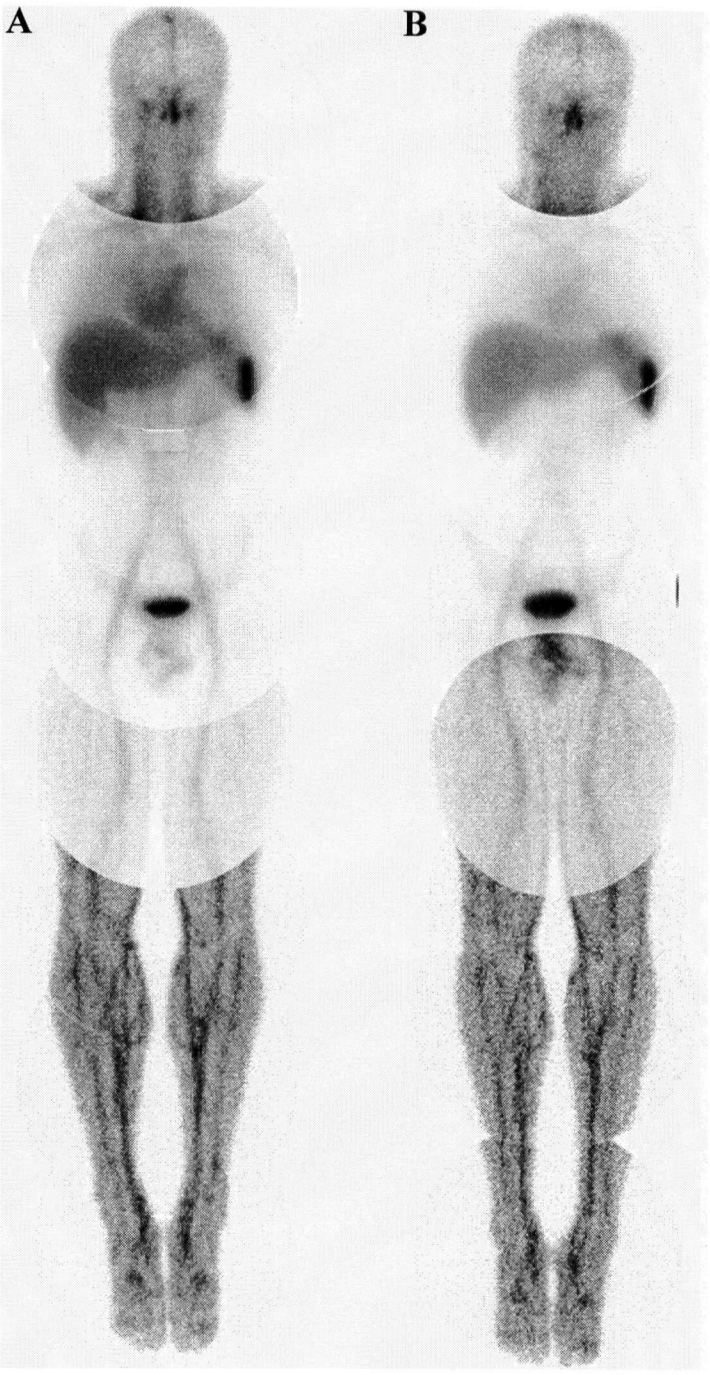

Figure 6.4 Biodistribution of activity in normal healthy volunteer using labeled vesicles at 1 (A) and 4 (B) hours. The composite images were assemble from the images acquire for each region. Acquisition of images in each region autocorrect for intensity of activity and resolution. This autocorrection accounts for the darker appearance of the leg images compared to chest, even though there is a greater amount of activity in the chest.

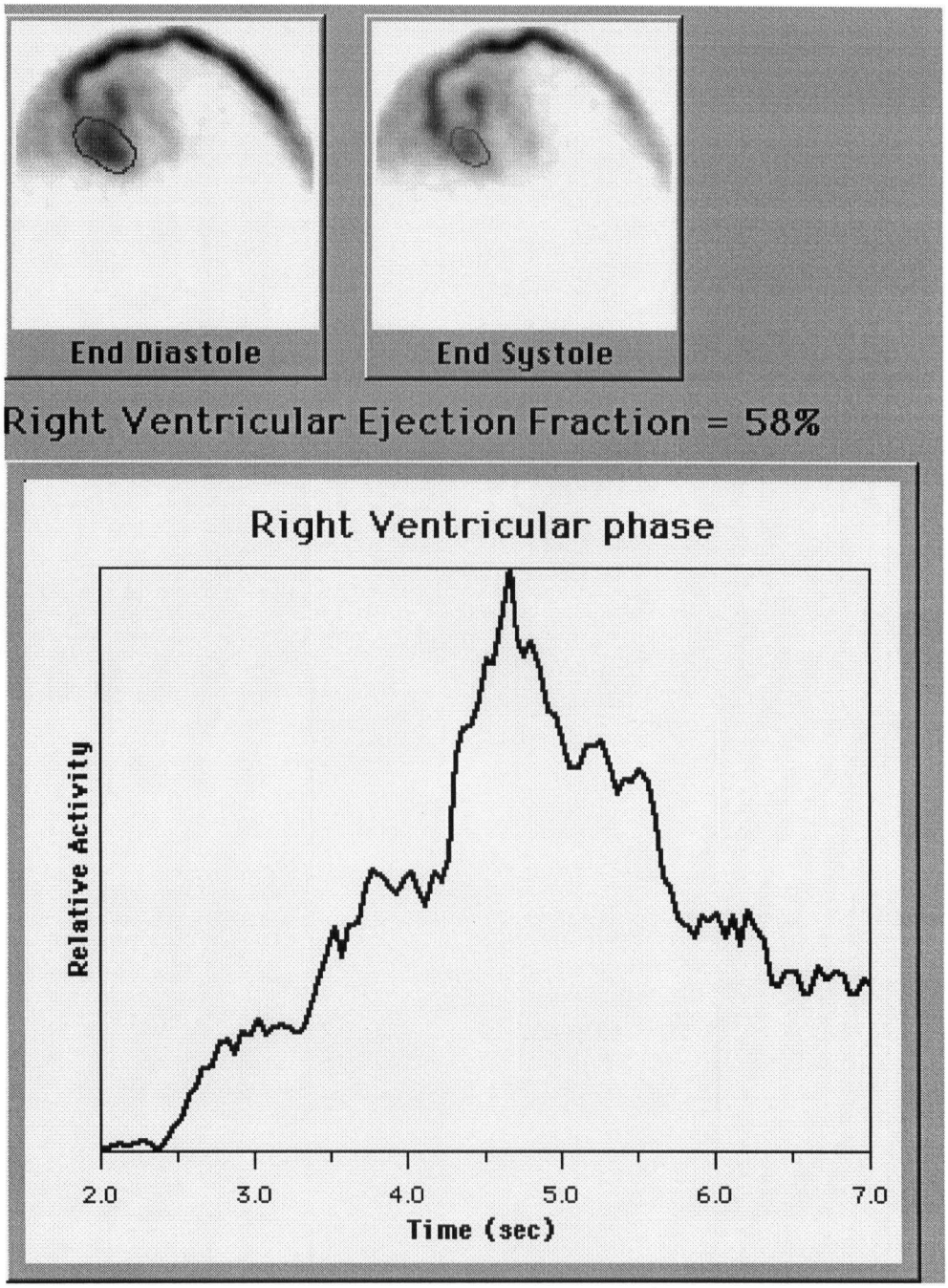

Figure 6.5. Calculation of right ventricular ejection fraction (RVEF) using labeled vesicles. Comparison of right ventricle images with maximal counts and minimal counts gives percentage of blood ejected from the right ventricle during contraction. The RVEF was calculated to be 58%.

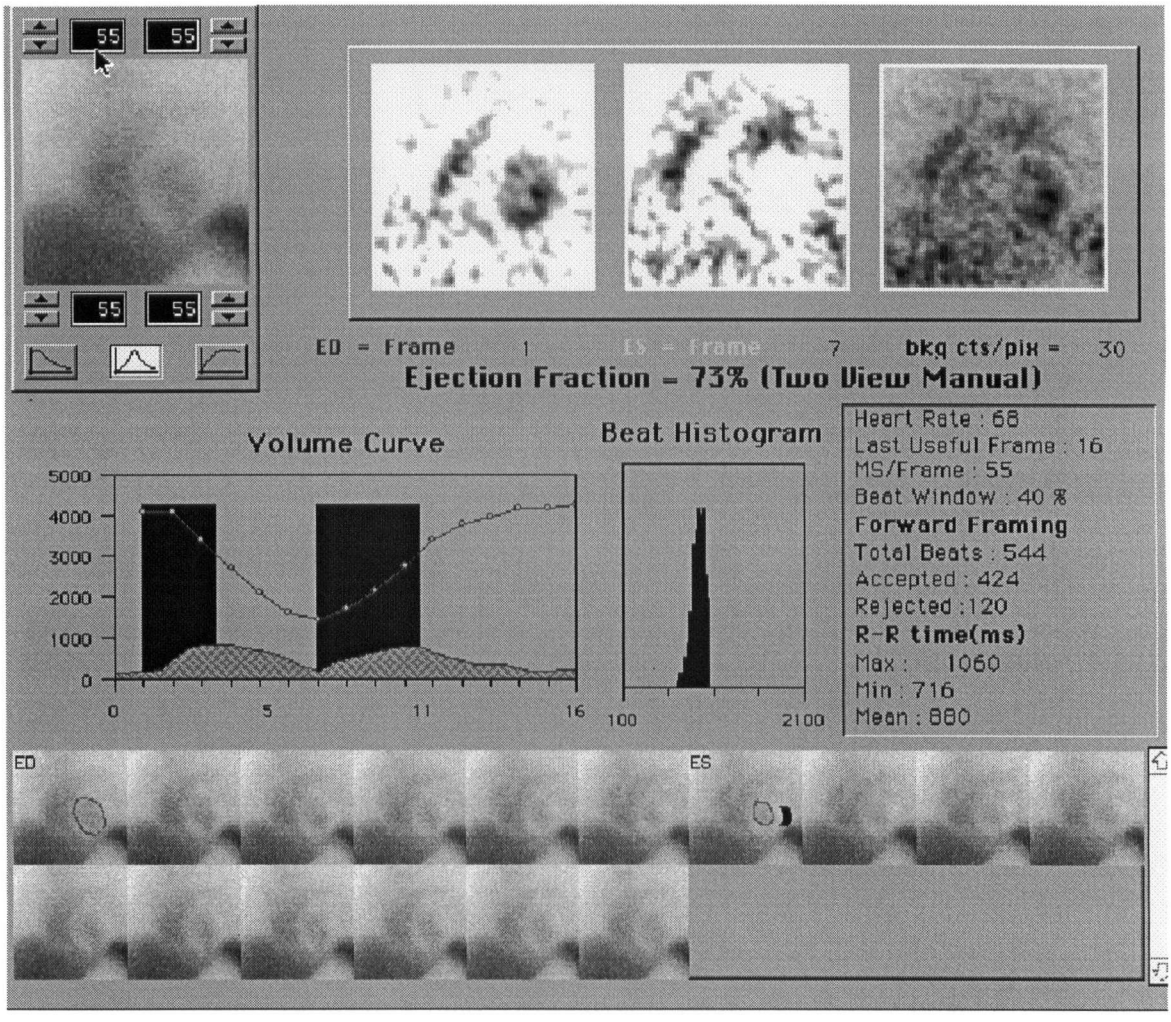

Figure 6.6. Calculation of left ventricular ejection fraction (LVEF) using labeled vesicles. Each heart beat was divided in a number of discrete divisions. The camera acquired data in each division and the individual images were combine to produce composite image of the heart during each division of the cardiac cycle. Images corresponding to end diastole (ED), were the ventricle has the greatest amount of blood, and end systole (ES), were the ventricle has the least amount of blood, were compared to give the percentage of blood ejection form the left ventricle during each contraction. The LVEF was determined to be 73%.

Discussion

The purpose of this study was to determine the utility and accuracy of radiolabeled PEG-coated vesicles as an alternative to radiolabeled RBCs for nuclear medicine imaging procedures. Left ventricular ejection fraction determination was chosen due to the fact that this procedure is conducted on a routine basis, has been extensively validated over the years and the relative ease of acquiring a volunteer pool. The value calculated for LVEF using radiolabeled vesicles was similar to value calculated for radiolabeled RBCs, 73% for vesicles compared to 69% for RBCs. Indicating that radiolabeled vesicles do hold great potential as cardiovascular imaging agents.

The images for LVEF determination were acquired ~1 hour after injection. At this time point the activity in the circulation was not as great as observed for radiolabeled RBCs but it must be emphasized that there was enough activity to determine LVEF. The biodistribution also showed that there was a high accumulation of activity in the liver and more significantly in the spleen indicating RES uptake of vesicles. Although there was active uptake, the renal excretion of activity was similar to that observed for radiolabeled RBCs, suggesting that activity is not released into the circulation after uptake by the RES. There was also little activity associated with the thyroid or the area of the GI tract, indicating little free activity.

The low circulation half-life was unexpected on the basis of the results from the animal biodistribution studies. From the animal studies a circulation half-life greater then ~15 hours was expected. Closer examination of the labeling and injection protocol revealed that the injection dose was less than ~1.0 μmol/kg. There was 0.56 ml of 141.86 mM vesicles dispersion in the vacutainer which corresponds to 80 μmol of lipid. After addition of ^{99m}Tc/HM-PAO solution to the vesicles, there was a total of 718.5 MBq in the vacutainer. The labeled vesicle solution was drawn into a syringe. The total counts in

the syringe was 641.9 MBq. Thus, assuming that 718.5 MBq represents 80 μmol of lipid, only 71.5 μmol of lipid was in the syringe (80 μmol/718.5MBq*641.9MBq). This decreased the injected lipid dose to 0.89 μmol/kg in the syringe. This does not account for any activity left in the syringe after injection which was not determined. Thus, the final lipid dose was less than 0.89 μmol/kg which may be part of the explanation of the observed low circulation half-life observed in these studies.

The low lipid dose could also explain the high activity associated with the liver and spleen compared to that of the heart. From the animal biodistribution studies at lower lipid doses, the activity associated with the liver and spleen was greater than associated with the heart (Chapter 3, Figure 3.4 and Table 3.1). In contrast, at higher lipid doses the activity associated with the heart was greater than associated with the liver and spleen even at the longest time point.

Further studies will have to be conducted to fine tune the required lipid dose and preparation procedure. The biodistribution and circulation kinetics of PEG-coated vesicles in humans is not exactly the same observed in rabbits. There appears to be a greater degree of activity which accumulates in the spleen and liver but this may be a result of the decreased lipid dose. Higher lipid dose will have to be tested in order to increase the circulation half-life of vesicles and also increase the heart-to-liver and heart-to-spleen ratios. The preparation procedure of the kits has to be modified to allow for the incomplete removal of labeled vesicles from the vacutainer while still providing a lipid dose adequate for imaging.

Chapter 7 :

Future Directions

During the course of this research, a number of interesting issues and questions arose which were not within the scope of this project, but may prove as interesting avenues for future investigation. For example, as discussed in the introduction to Chapter 1, vesicles can be labeled using a surface chelator. Although this labeling method is not as robust as internal labeling in terms of loss of label which results in a shorter circulation half-life, this variant may prove useful in imaging procedures which do not require long circulation half-lives, i.e. LVEF. The principle advantage of surface labeling is that it is technically simpler and cheaper than the HM-PAO based labeling method. Also of interest is the freeze drying of vesicles to provide a pharmaceutical with a longer shelf-life. Vesicles can maintain their size and structure during freeze drying and rehydration by the inclusion of various sugars into the vesicle dispersion, i.e. sucrose and trehalose. There were many other branches which could be investigated in greater detail. However, the next step in the development of the vesicle based radiopharmaceutical described in this thesis is the development of a fast and simple quality control assay to determine the labeling efficiency. Two other areas which I felt were not only a continuation of this work but were also interesting field of research were: 1) further human testing and 2) elucidating the mechanism of HM-PAO labeling.

Quality Control Assay of Labeled Vesicles

In nuclear medicine, all radiopharmaceuticals must be assayed for quality control before administration to the patient. During the production of labeled vesicles, one quality control assay is the determination of tagging efficiency for HM-PAO. This is simply done through the use of partition assay with saline and ethyl acetate. However, a second assay must be developed to assay the labeling percentage of vesicles. The labeling

percentage must be determined before injection to ensure that there is not an excessive amount of free activity present in the formulation. Although, the labeling percentage can be determined by chromatography on either Sephadex G50 column or BioGel minicolumn, these techniques are not practical in a clinical setting. These methods are time consuming and require special materials and apparatuses not normally available in nuclear medicine departments. Thus, a simple method must be developed to accurately determine the labeling percentage of vesicles before administration.

One possibility requiring further work is the use of a 2 phase (PEG/dextran) polymer partition system. It has been shown that in the absence of PEG on the surface, vesicles preferentially partition in the lower dextran-rich phase. However, in the presence of PEG, vesicles partition into the upper PEG-rich phase. Thus, this method may provide a relatively fast and simple method to determine labeling efficiency.

Further Human Testing

Further testing of radiolabeled PEG-coated vesicle in a larger population is required to better define the lipid doses which would be required for various nuclear medicine imaging studies. From the preliminary testing of labeled vesicles in one human, it appears that a lipid dose of ~1.0 μmol/kg would be adequate for RVEF and LVEF determinations. However, higher lipid doses should be tested not only to increase the accuracy of LVEF determinations but also to test the applicability of vesicles to localization of GI bleeding.

The first stage of testing will be to assess the biodistribution and circulation kinetics in normal healthy volunteers at various lipid doses starting at 1.0 μmol/kg. Using the same protocol outline in Chapter 6, volunteers will be imaged first with labeled RBCs using the *in vivo* labeling procedure. After 1-2 weeks, the same volunteer will be imaged

using labeled vesicles. Concurrent with the biodistribution studies, LVEF will also be determined in both studies for each volunteer. The values then compared to see if there is a significant difference in the values calculated for LVEF using vesicles compared to RBCs. RBCs will be used as the comparison because they are currently the standard and have been extensively validated. The null hypothesis will be that there is no significant difference in LVEF values of vesicles compared to RBCs.

After preliminary testing in normal healthy volunteers, to determine optimal lipid dose, labeled vesicles will be used to determine LVEF in patients with demonstrated cardiac insufficiencies. These studies will be undertaken to assess the applicability of labeled vesicles to accurately assess cardiac function in the patient pool that the agent was ultimately designed to be used. Another parameter that could be assessed by questionnaires to nuclear medicine technologists responsible for the preparation of labeled vesicles, would be the relative ease of use compared to labeled RBCs in terms of preparing the labeled vesicles, administration to patients and acquiring images.

What Happens To HM-PAO?

A basic mechanistic question which remains unanswered deals with the interaction between HM-PAO and the glutathione. As discussed in chapter 2, it is thought the ^{99m}Tc/HM-PAO complex exists in two forms, lipophilic and hydrophilic. It is also thought that glutathione plays an integral role in the conversion between the two forms. However, the secondary hydrophilic form has yet to be isolated. The work to date has been based on the assumption that HM-PAO undergoes some covalent modification by interaction with glutathione. However, this assumption may be incorrect.

An alternative hypothesis to the mechanism of interaction between glutathione and the ^{99m}Tc/HM-PAO lipophilic complex is simply an exchange process. By exchange

process I mean that ^{99m}Tc has a greater affinity for glutathione than HM-PAO, specifically the sulphydryl group of cysteine. Investigators have shown that other sulphydryl containing molecules are also effective at 'reducing' HM-PAO such as D,L-buthionine-sulfoximine (BSO), N-acetyl-L-cysteine (NAC), D,L dithiothreitol (DTT), 2-mercaptoethanol and also cysteine.

A similar process is used in the labeling of vesicles with gallium-67 (^{67}Ga) described by Woodle [95]. In this method two different chelators are used which have different lipophilicities and affinities for ^{67}Ga. The first chelator, desferoxamine mesylate (DF), is encapsulated within the vesicles. This chelator is hydrophilic and has a stronger affinity for ^{67}Ga than the second chelator, hydroxyquinoline (oxine). Oxine is lipophilic and can cross the lipid bilayer. Thus, ^{67}Ga is bound to oxine and added to vesicles with encapsulated DF. The ^{67}Ga/oxine complex crosses the lipid bilayer where it comes into contact with the DF. The stronger affinity of the DF for ^{67}Ga causes the transfer ^{67}Ga from the oxine to DF. The ^{67}Ga/DF complex can not cross the lipid bilayer thus trapping ^{67}Ga and labeling the vesicles. A similar mechanism can be drawn for HM-PAO with the substitution that HM-PAO and glutathione are the oxine and DF chelators, respectively and ^{99m}Tc is the radioisotope instead of ^{67}Ga. However, this hypothesis still requires testing and would be an interesting area for further research.

Chapter 8 :

Summary

The goal of this thesis was the development of an alternative pharmaceutical to radiolabeled RBCs for use in nuclear medicine as a cardiovascular imaging agent, specifically for the determination of LVEF. Chapter 2 dealt with issues concerning the preparation and formulation of the HM-PAO kits. It was found that HM-PAO labeling was not dependent on the lipid composition or fluid state of the bilayer. However, reducing the rehydration volume to 0.5 ml required that the amount of tin per kit be reduced to maintain high tagging efficiency, and consequently high labeling efficiency of the vesicles. Tagging efficiency also depended on the age of pertechnetate eluant used to reconstitute the kits and the order of rehydration - the eluant must not be older than 1 hour, and the kits must first be rehydrated with saline before the addition of activity.

Chapter 3 addressed the issue of the biodistribution and circulation kinetics of radiolabel associated with PEG-coated vesicles in rabbits. It was found that, contrary to published data, the rate of clearance of label from the circulation was dependent on the lipid dose. At lipid doses of 0.2, 0.5, 1.3 and 2.1 μmol of total lipid/kg of body weight, the circulation half-life of the label was 2.6, 4.3, 16.4 and 20.6 hours respectively. These data indicate that, depending of the imaging procedure to be performed, the lipid dose can be adjusted appropriately. For example, LVEF determination does not require that the label circulate for as long as procedure such as GI bleed detection, i.e. the lipid dose can be lower for LVEF measurements. There was no significant difference in the circulation half-life at lipid doses of 1.30 and 2.13 μmol/kg, indicating that the previously published lipid dose range in which the clearance PEG-coated vesicles is dose-independent, can be extended down to 1.30 μmol/kg. However, below 1.30 μmol/kg, the circulation half-life was dependent on lipid dose.

On the basis that 1.0 μmol/kg would probably be suitable for most cardiac imaging studies, and given the requirement to minimize the injection volume, an alternative vesicle preparation procedure was developed to increase the lipid concentration (Chapter 4). A human weighing ~80 kg, would require a total dose of 80 μmol of lipid. The chromatography procedure described in Chapter 2 for the removal of external glutathione resulted in dilution of the vesicle dispersion, resulting in volumes too large for first pass studies. Two alternative methods of vesicles preparation were developed. The first method was based on centrifugal filtration of chromatographed vesicles, that increased the lipid concentration by removal of excess external aqueous media. The second method used a pH gradient to inactivate the ability of external glutathione to convert HM-PAO from the lipophilic to the hydrophilic form. The second method proved superior to the first because it was simpler and required few manipulations.

Chapter 5 addressed the issue of the *in vivo* safety of radiolabeled PEG-coated vesicles. Vesicles were tested for their ability to activate the complement system and their effect on various hemodynamic parameters. The lipid composition and vesicle preparation procedure was also tested for pyrogenicity. It was found that PEG-coated vesicles did not activate the complement system, had no effect on various hemodynamic parameters and were non-pyrogenic.

Finally, based on these results a pharamaceutical kit was constructed and tested in one human subject [Chapter 6]. The kit was composed of a tube containing vesicles, an HM-PAO kit and a syringe with NaOH. The left ventricular ejection fraction (LVEF) was calculated using the vesicle kit and compared to the value determined by the current standard - radiolabeled RBCs. It was found that the calculated LVEF for RBCs was 69% and for vesicles was 73%.

In summary, all the major goals originally set out in the first section of the introduction have been achieved. An alternative pharmaceutical to radiolabeled RBCs based on PEG-coated vesicles, has been developed and characterized. PEG-coated vesicles would overcome all the disadvantages currently experienced with RBCs. Vesicles are labeled *in vitro* and can be prepared as a kit which is labeled before or just after the arrival of patients. This eliminates any concerns over drug interferences. The components of the proposed kit do not contain any blood products or derivatives eliminating the possibility of the transmission of blood borne diseases. Also, the administered lipid dose can be adjusted according to the procedure to be performed thereby minimizing the lipid dose. Finally, the administration requires only one venipuncture minimizing patient discomfort. Labeled PEG-coated vesicles were tested for LVEF measurements in a human and proof of principle demonstrated.

Chapter 9 :

References

1. Nuclear medicine-factors influencing the choice and use of radionuclide in diagnosis and therapy. National Council on Radiation Protection and Measurements (NCRP) Report No. 70. Bethesda, Maryland. 1982.

2. **Early, P.J. and Sodee, D.B**. (eds.) Principles and Practice of Nuclear Medicine, second edition. Mosby, St. Louis, Missouri. 1995.

3. **Nickel, R.A**. Radiopharmaceuticals. In *Principles and Practice of Nuclear Medicine* (Early, P.J. and Sodee, D.B. eds.) Mosby, New York. pp. 94-117, 1995.

4. **Walker, J.M. and Margoulett, D**. (eds.) A Clinical Manual of Nuclear Medicine. Appleton-Century-Crotts, Norwalk, Connecticut. 1984.

5. **Chilton, H.M., Callahan, R.J. and Thrall, J.H**. Radiopharmaceuticals for cardiac imaging: myocardial infarction, perfusion, metabolism, and ventricular function (blood pool). In *Pharmaceuticals in Medical Imaging* (Swanson, D.P., Chilton, H.M. and Thrall, J.H. eds.) MacMillan Publishing Co, Inc. New York, New York. pp. 419-461, 1990.

6. **Marshall, R.C., Berger, H.J., Costin, J.C., Freedman, G.S., Wolberg, J., Cohen, L.S., Gottschalk, A. and Zaret, B.L**. Assessment of cardiac performance with quantitative radionuclide angiocardiography: sequential left ventricular ejection fraction, normalized left ventricular ejection rate, and regional wall motion. *Circulation* (56(5): 820-829, 1977.

7. **Upton, M.T., Rerych, S.K., Newman, G.E., Bounous, E.P. and Jones, R.H**. The reproducibility of radionuclide angiographic measurements of left ventricular function in normal subjects at rest and during exercise. *Circulation* 62(1): 126-132, 1980.

8. **Rantis, P.C., Harford, F.J., Wagner, R.H. and Henkin, R.E**. Technetium-labeled red blood cell scintigraphy: is it useful in acute lower gastrointestinal bleeding? *International Journal of Colorecteral Disease* 10(4): 210-215, 1995.

9. **Sos, T.A., Lee, J.G., Wixson, D. and Sniderman, K.W**. Intermittent bleeding from minute to minute in acute massive gastrointestinal hemorrhage: arteriographic demonstration. *American Journal of Roentgenology* 131: 1015-1017, 1978.

10. **Wolf, G.L**. Safer, more expensive iodinated contrast agents: how do we decide? *Radiology* 159(2): 557-558, 1986.

11. **Katayama, H., Yamaguchi, K., Kozuka, T., Takashima, T., Seez, P. and Matsuura, K**. Adverse reactions to ionic and nonionic contrast media. *Radiology* 175(3): 621-628, 1990.

12. **Hirano, T., Nakamura, A., Iwata, S. and Sasaki, Y**. An active bleeding gastric ulcer demonstrated by Tc-99m RBC gastrointestinal bleeding study. *Clinical Nuclear Medicine* 18: 78-79, 1993.

13. **Morita, S., Ishibashi, M., Hirayama, T., Takahashi, K., Nomura, Y. and Ohtake, H**. Intermittent bleeding in a patient with multiple ulceration near the terminal ileum visualized on Tc-99m RBC gastrointestinal imaging. *Clinical Nuclear Medicine* 15: 923-924, 1990.

14. **Ben-Haim, S. and Rezai, K**. Intraperitoneal bleeding demonstrated by Tc-99m labeled red blood cells scintigraphy. *Clinical Nuclear Medicine* 17: 789-790, 1992.

15. **Czarnecki, D.J.** Intraperitoneal bleeding diagnosed by technetium-99m labeled RBC imaging. *Clinical Nuclear Medicine* 11: 617-618, 1986.

16. **Holloway, H., Johson, J. and Sandler, M**. Detection of an ileal cavernous hemangioma by technetium-99m red blood cell imaging. *Clinical Nuclear Medicine* 13: 32-34, 1988.

17. **Hansen, M.E. and Coleman, R.E**. Scintigraphic demonstration of gastrointestinal bleeding due to mesenteric varices. *Clinical Nuclear Medicine* 15: 488-490, 1990.

18. **Jacobson, A.F. and Cerqueira, M.D**. Prognostic significance of late imaging results in technetium-99m-labeled red blood cell gastrointestinal bleeding studies with early negative images. *Journal of Nuclear Medicine* 33(2): 202-7, 1992.

19. **Dewanjee, M.K., Rao, S.A. and Penniston, G.T**. Mechanism of red blood cell labeling with ^{99m}Tc-pertechnetate. The role of the cation pump at RBC membrane on the distribution and binding of Sn^{2+} and ^{99m}Tc with the membrane proteins and hemoglobin. *Journal of Labeled Compounds and Radiopharmaceuticals* 19: 1464-1465, 1982.

20. **Callahan, R.J. and Rabito, C.A**. Radiolabeling of erythrocytes with technetium-99m: role of band-3 protein in the transport of pertechnetate across the cell membrane. *Journal of Nuclear Medicine* 31(12): 2004-2010, 1990.

21. **Rehani, M.M. and Sharma, S.K**. Site of Tc-99m binding to the red blood cells: concise communication. *Journal of Nuclear Medicine* 27(7): 676-678, 1980.

22. **Dewanjee, M.K**. Binding of ^{99m}Tc ion to hemoglobin. *Journal of Nuclear Medicine* 15(8): 703-706, 1974.

23. **Chandler, W.M. and Shack, L.D**. Abnormal technetium-99m pertechnetate imaging following stannous pyrophosphate bone imaging. *Journal of Nuclear Medicine* 16: 518-519, 1975.

24. **Pavel, D.G., Zimmer, A.M. and Patterson, V.N**. *In vivo* labeling of red blood cells with 99mTc: a new approach to blood pool visualization. *Journal of Nuclear Medicine* 18: 305-308, 1977.

25. **Winzelberg, G.G., McKusick, K.A., Strauss, H.W., Waltman, A.C. and Greenfield, A.J**. Evaluation of gastrointestinal bleeding by red blood cells labeled *in vivo* with technetium-99m. *Journal of Nuclear Medicine* 20: 1080-1086, 1979.

26. **Callahan, R.J., Froelich, J.W., McKusick, K.A., Lippo, J. and Strauss, H.W**. A modified method for the *in vivo* labeling of red blood cells with Tc-99m: concise communication. *Journal of Nuclear Medicine* 23: 315-318, 1982.

27. **Smith, T.D. and Richards, P.A**. A simple kit for the preparation of 99mTc-labeled red blood cells. *Journal of Nuclear Medicine* 17: 126-132, 1976.

28. **Ness, P.M. and Stengle, J.M.** Historical introduction. In *The Red Blood Cell* (Surgenor, D.M. ed.) Academic Press Inc., New York, New York. pp. 1-50, 1974.

29. **Hladik, W.B., Nigg, K.K. and Rhodes, B.A**. Drug-induced changes in the biological distribution of radiopharmaceuticals. *Seminars in Nuclear Medicine* 12(2): 184-218, 1982.

30. **duCret, R.P., Boudreau, R.J., Larson, T., Levey, R.M. and Loken, M.K**. Suboptimal red blood cell labeling with 99mTc. *Seminars in Nuclear Medicine* 18(1): 74-75, 1988.

31. **Porter, W.C., Dees, S.M., Freitas, J.E. and Dworkin, H.J**. Acid-citrate-dextrose compared with heparin in the preparation of *in vivo/in vitro* technetium-99m red blood cells. *Journal of Nuclear Medicine* 24(5): 383-387, 1983.

32. **Adalet, I. and Cantez, S**. Poor-quality red blood cell labeling with technetium-99m: case report and review of the literature. *European Journal of Nuclear Medicine* 21(2): 173-175, 1994.

33. **Hambye, A.S., Vandermeiren, R., Vervaet, A. and Vandevivere, J**. Failure to label red blood cells adequately in daily practice using an *in vivo* method: methodological and clinical considerations. *European Journal of Nuclear Medicine* 22(1): 61-76, 1995.

34. **Lee, H.B., Wexler, J.P., Scharf, S.C. and Blaufox, M.D.** Pharmacologic alterations in Tc-99m binding by red blood cells: concise communication. *Journal of Nuclear Medicine* 24(5): 397-401, 1983.

35. **Leitl, G.P., Drew, H.M., Kelly, M.E. and Alderson, P.O.** Interferences with Tc-99m labeling of red blood cells (RBCs) by RBC antibodies. *Journal of Nuclear Medicine* 21(6): P44, 1980.

36. **Riordan, F. and Nelp, W.B.** Binding capacity of normal and sickle cell hemoglobin for technetium atoms. *Journal of Nuclear Medicine* 23(5): P91, 1982.

37. **Roy, S., Cottin, Y., Berriolo-Riedinger, A., Bonnotte, B., Wolf, J.E. and Brunotte, F.** Severe right ventricular contraction asynchronism revealing a large pericardial effusion. *Journal of Nuclear Medicine* 38(5): 777-779, 1997.

38. **Shapira, J., Gotfried, M., Lishner, M. and Ravid, M.** Reduced cardiotoxicity by a 6-hour infusion regimen. A prospective randomized evaluation. *Cancer* 65(4): 870-873, 1990.

39. **Bae, J.H., Schwaiger, M., Mandelkern, M., Lin, A. and Schelbert, H.R.** Doxorubicin cardiotoxicity: response of left ventricular ejection fraction to exercise and incidence of regional wall motion abnormalities. *International Journal of Cardiac Imaging* 3(4): 193-201, 1989.

40. **Ballinger, J.R., Gerson, B., Gulenchyn, K.Y., Ruddy, T.D. and Davies, R.A.** Technetium-99m red blood cell labeling in patients treated with doxorubicin. *Clinical Nuclear Medicine* 13: 169-170, 1988.

41. **Caride, V.J.** Technical and biological considerations on the use of radiolabeled liposomes for diagnostic imaging. *Nuclear Medicine and Biology* 17(1): 35-39, 1990.

42. **Hnatowich, D.J. and Clancy, B.** Investigations of a new, highly negative liposome with improved biodistribution for imaging. *Journal of Nuclear Medicine* 21: 662-669, 1980.

43. **Richardson, V.J., Jeyasingh, K., Jewkes, R.F., Ryman, B.E. and Tattersall, M.H.N.** Possible tumor localization of Tc-99m-labeled liposomes: effects of lipid composition, charge and liposome size. *Journal of Nuclear Medicine* 19: 1049-1054, 1978.

44. **Senior, J.H.** Fate and behavior of liposomes *in vivo*: a review of controlling factors. *CRC Critical Reviews in Therapeutic Drug Carrier Systems* 3: 123-193, 1987.

45. **Huang, K.J.** Liposome pharmacokinetics. In *Liposomes: From Biophysics to Therapeutics* (Ostro, M.J. ed.) Marcel Dekker,Inc. New York. pp. 109-156, 1987.

46. **Allen, T.M. and Chonn, A.** Large unilamellar liposomes with low uptake into the reticuloendothelial system. *FEBS Letters* 223(1): 42-46, 1987.

47. **Allen, T.M., Hansen, C. and Rutledge, J.** Liposomes with prolonged circulation times: factors affecting uptakes by reticuloendothelial and other tissues. *Biochimica et Biophysica Acta* 981: 27-35, 1989.

48. **Abuchowski, A., McCoy, J.R., Palczuk, N.C., van Es, T. and Davis, F.F.** Effect of covalent attachment of polyethylene glycol on immunogenicty and circulating life of bovine liver catalase. *Journal of Biological Chemistry* 252(11): 3582-3586, 1977.

49. **Abuchowski, A., van Es, T., Palczuk, N.C. and Davis, F.F.** Alteration of immunological properties of bovine serum albumin by covalent attachment of polyethylene glycol. *Journal of Biological Chemistry* 252(11): 3578-3581, 1977.

50. **Savoca, K.V., Abuchowski, A., van Es, T., Davis, F.F. and Palczuk, N.C.** Preparation of a non-immunogenic arginase by the covalent attachment of polyethylene glycol. *Biochimica et Biophysica Acta* 578(1): 47-53, 1979.

51. **Pyatak, P.S., Abuchowski, A. and Davis, F.F.** Preparation of a polyethylene glycol:superoxide dimutase adduct, and an examination of its blood circulation life and anti-inflammatory activity. *Research Communications in Chemical Pathology and Pharmacology* 29(1): 113-127, 1980.

52. **Davis, S., Abuchowski, A, Park, Y.K. and Davis, F.F.** Alteration of the circulating life and antigenic properties of bovine adenosine deaminase in mice by attachment of polyethylene glycol. *Clinical and Experimental Immunology* 46(3): 649-652, 1981.

53. **Chen, R.H., Abuchowski, A., van Es, T., Palczuk, N.C. and Davis, F.F.** Properties of two urate oxidases modified by covalent attachment of poly(ethylene glycol). *Biochimica et Biophysica Acta* 660(2): 293-298, 1981.

54. **Illum, L. and Davis, S.** The organ uptake of intravenously administered colloidal particles can be altered using non-ionic surfactant (Poloxamer 338). *FEBS Letters* 167(1): 79-82, 1984.

55. **Klibanov, A.L. Maruyama, K., Torchilin, V.P. and Huang, L.** Amphipathic polyethyleneglycols effectively prolong the circulation time of liposomes. *FEBS Letters* 268(1): 235-237, 1990.

56. **Allen, T.M., Hansen, C., Martin, F., Redemann, C. and Yau-Young, A.** Liposomes containing synthetic lipid derivatives of poly(ethylene glycol) show prolonged circulation half-lives *in vivo*. *Biochimica et Biophysica Acta* 1066: 29-36, 1991.

57. **Torchilin, V.P., Trubetskoy, V.S., Whiteman, K.R., Caliceti, P., Ferruti, P. and Veronese, F.M.** New synthetic amphipathic polymers for steric protection of liposomes *in vivo*. *Journal of Pharmaceutical Sciences* 84(9): 1049-1053, 1995.

58. **Zalipsky, S., Hansen, C.B., Oaks, J.M. and Allen, T.M.** Evaluation of blood clearance rates and biodistribution of poly(2-oxazoline)-grafted liposomes. *Journal of Pharmaceutical Sciences* 85(2): 133-137, 1996.

59. **Litzinger, D.C. and Huang, L.** Amphipathic poly(ethylene glycol) 5000-stabilized dioleoylphosphatidylethanolamine liposomes accumulate in the spleen *Biochimica et Biophysica Acta* 112: 249-254, 1992.

60. **Allen, T.M. and Papahadjopoulos, D.** (1992) Sterically stabilized ("stealth") liposomes: Pharmacokinetics and therapeutic advantages. In *Liposome Technology* (Gregoriadis G. ed.) Volume III, 2nd edition. CRC Press, Boca Raton. pp. 59-72, 1992.

61. **Allen, T.M. and Hansen, C.** Pharmacokinetics of stealth versus conventional liposomes: effect of dose. *Biochimica et Biophysica Acta* 1068: 133-141, 1991.

62. **Papahadjopoulos, D., Allen, T.M., Gabizon, A., Mayhew, E., Matthay, K., Huang, S.K., Lee, K.D., Woodle, M.C., Lasic, D.D., Redemann, C. and Martin, F.J.** Sterically stabilized liposomes: improvements in pharmacokinetics and antitumor therapeutic efficacy. *Proceedings of the National Academy of Science USA* 88: 11460-11464, 1991.

63. **Woodle, M.C. and Lasic, D.D.** Sterically-stabilized liposomes. *Biochimica et Biophysica Acta* 1148: 77-84, 1993.

64. **Woodle, M.C., Matthay, K.K., Newman, M.S., Hidayat, J.E., Collins, L.R., Redemann, C., Martin, F.J. and Papahadjopoulos, D.** Versatility in lipid compositions showing prolonged circulation with sterically stabilized liposomes. *Biochimica et Biophysica Acta* 1105: 193-200, 1992.

65. **Liu, D., Hu, Q. and Song, Y.K.** Liposome clearance from blood: different animal species have different mechanisms. *Biochimica et Biophysica Acta* 1240: 277-284, 1995.

66. **Atkins, H.L., Klopper, J.F. and Ansari, A.N**. A comparison of Tc-99m-labeled human serum albumin and *in vivo* labeled red blood cells for blood pool studies. *Clinical Nuclear Medicine* 5: 166-169, 1980.

67. **Vanbilloen, H.P. Verbeke, K.A., De Roo, M.J. and Verbruggen A.M.** Technetium-99m labeled human serum albumin for ventriculography: a comparative elavuation of six labeling kits. *European Journal of Nuclear Medicine* 20(6): 465-472, 1993.

68. **Baidoo, K.E. Scheffel, U. and Lever, S.Z.** ^{99m}Tc-labeling of proteins: initial evaluation of a novel diaminedithiol bifunctional chelating agent. *Cancer Research* 50: S799-S803, 1990.

69. **Verbeke, K., Hjelstuen, O., Debrock, E., Cleynhens, B. De Roo, M. and Verbruggen, A**. Comparative evaluation of 99mTc-Hynic-HSA and 99mTc-MAG3-HSA as possible blood pool agents. *Nuclear Medicine Communications* 16(11): 942-957, 1995.

70. **Verbeke, K.A. Vanhecke, W.B., Mortelmans, L.A. and Verbruggen, A.M**. First evaluation of technetium-99m dimercaptopropionyl albumin as a possible tracer agent for ventriculography in a volunteer. *European Journal of Nucelar Medicine* 21: 906-912, 1994.

71. **McDougall, I.R., Dunnick, J.K., Goris, M.L. and Kriss, J.P.** *In vivo* distribution of vesicles loaded with radiopharmaceuticals: a study of different routes of administration. *Journal of Nuclear Medicine* 16(6): 488-491, 1975.

72. **McDougall, I.R., Dunnick, J.K., McNamee, M.G. and Kriss, J.P**. Distribution and fate of synthetic lipid vesicles in the mouse: a combined radionuclide and spin label study. *Proceedings of the National Academy of Science USA* 71(9): 3481-3491, 1974.

73. **Espinola, L.G., Beaucaire, J., Gottschalk, A. and Caride, V.J**. Radiolabeled liposomes as metabolic and scanning tracers in mice. II. In-111 oxine compared with Tc-99m-DTPA entrapped in multilamellar lipid vesicles. *Journal of Nuclear Medicine* 20: 434-440, 1979.

74. **Caride, V.J., Taylor, W., Cramer, J.A. and Gottschalk, A**. Evaluation of liposome-entrapped radioactive tracers as scanning agents. Part 1: organ distribution of liposome [^{99m}Tc-DTPA] in mice. *Journal of Nuclear Medicine* 17: 1067-1072, 1976.

75. **Mayer, L.D., Bally, M.B., Hope. M.J. and Cullis, P.R**. Techniques for encapsulating bioactive agents in liposomes. *Chemistry and Physics of Lipids* 40: 333-345, 1986.

76. **Caride, V.J.** Technical and biological considerations on the use of radiolabeled liposomes for diagnostic imaging. *Nuclear Medicine and Biology* 17(1): 35-39, 1990.

77. **Richardson, V.J., Jeyasingh, K., Jewkes, R.F., Ryman, B.E. and Tattersall, M.H.N.** Possible tumor localization of Tc-99m-labeled liposomes: effects of lipid composition, charge, and liposome size. *Journal of Nuclear Medicine* 19(9): 1049-1054, 1978.

78. **Love, W.G., Amos, N., Williams, B.D. and Kellaway, I.W.** Effect of liposome surface charge on the stability of technetium (^{99m}Tc) radiolabeled liposomes. *Journal of Microencapsulation* 6(1) 105-113, 1989.

79. **Osborne, M.P., Richardson, V.J., Jeyasingh, K. and Ryman, B.E.** Radionuclide-labeled liposomes - a new lymph node imaging agent. *International Journal of Nuclear Medicine and Biology* 6: 75-83, 1979.

80. **Perez-Soller, R., Lopez-Berestein, G., Kasi, L., Cabanillas, F., Jahns, M., Glenn, H., Hersh, E.M. and Haynie, T.** Distribution of technetium-99m-labeled multilamellar liposomes in patients with Hodgkin's disease. *Journal of Nuclear Medicine* 26(7): 743-749, 1985.

81. **Patel, H.M., Boodle, K.M. and Vaughan-Jones, R.** Assessment of the potential uses of liposomes for lymphoscintigraphy and lymphatic drug delivery. Failure of 99m-technetium maker to represent intact liposomes in lymph nodes. *Biochimica et Biophysica Acta* 801: 76-86, 1984.

82. **Fresta, M. and Puglisi, G.** Application of liposomes as potential cutaneous drug delivery systems. *In vitro* and *in vivo* investigation with radioactively labeled vesicles. *Journal of Drug Targeting* 4(2): 95-101, 1996.

83. **Allen, T.M., Murray, L., Alving, C.R. and Moe, J.** Effects on the murine mononuclear phagocyte system of chronic administration of liposomes containing cytotoxic drug or lipid A compared with empty liposomes. *Canadian Journal of Physiology and Pharmacology* 65(2): 185-190, 1987.

84. **Roerdink, F., Regts, J., Van Leeuwen, B. and Scherphof, G.** Intrahepatic uptake and processing of intravenously injected small unilamellar phospholipids vesicles in rats. *Biochimica et Biophysica Acta* 770(2): 195-202, 1984.

85. **Stevenson, R.W., Patel, H.M., Parsons, J.A. and Rymen, B.E.** Prolonged hypoglycemic effects in diabetic dogs due to subcutaneous administration of insulin in liposomes. *Diabetes* 31: 506-511, 1982.

86. **Grant, C.W., Karlik, S. and Florio, E**. A liposomal MRI contrast agent: phosphatidylethanolamine-DTPA. *Magnetic Resonance in Medicine* 11: 236-243, 1989.

87. **Tilcock, C., Ahkong, Q.F. and Fisher, D**. Polymer-derivatized technetium ^{99m}Tc- labeled liposomal blood pool agents for nuclear medicine applications. *Biochimica et Biophysica Acta* 1148: 77-84, 1993.

88. **Ahkong, Q.F. and Tilcock, C**. Attachment of ^{99m}Tc to lipid vesicles containing the lipophilic chelate dipalmitoylphosphatidylethanolamine-DTTA. *Nuclear Medicine and Biology* 19(8): 831-840, 1992.

89. **Tilcock, C., Ahkong, Q.F. and Fisher, D**. ^{99m}Tc-labeling of lipid vesicles containing the lipophilic chelator PE-DTTA: effect of tin-to-chelate ratio, chelate content and surface polymer on labeling efficiency and biodistribution behavior. *Nuclear Medicine and Biology* 21(1): 89-96, 1994.

90. **Vemuri, S. and Rhodes, C.T**. Development and characterization of a liposome preparation by a pH-gradient method. *Journal of Pharmacy and Pharmacology* 46(10): 778-783, 1994.

91. **Haran, G., Cohen, R., Bar, L.K. and Barenholz, Y**. Transmembrane ammonium sulphate gradients in liposomes produce efficient and stable entrapment of amphipathic weak bases. *Biochimica et Biophysica Acta* 1151(2): 201-215, 1993.

92. **Madden, T.D., Harrigan, P.R., Tai, L.C., Bally, M.B., Mayer, L.D., Redelmeier, T.E., Loughrey, H.C., Tilcock, C.P., Reinish, L.W. and Cullis, P.R**. The accumulation of drugs within large unilamellar vesicles exhibiting a proton gradient: a survey. *Chemistry and Physics of Lipids* 53(1): 37-46, 1990.

93. **Mayer, L.D., Bally, M.B. and Cullis, P.R**. Uptake of adriamycin into large unilamellar vesicles in response to a pH gradient. *Biochimica et Biophysica Acta* 857(1): 123-126, 1986.

94. **Utkhede, D., Yeh, V., Szucs, M. and Tilcock, C**. Uptake of yttrium-90 in lipid vesicles. *Journal of Liposome Research* 4: 1049-1061, 1994.

95. **Woodle, M.C**. 67Gallium-labeled liposomes with prolonged circulation: preparation and potential as nuclear imaging agents. *Nuclear Medicine and Biology* 20(2): 149-155, 1993.

96. **Reichmann, K., Biersack, H.J., Basso, L., Hartmann, A., Matthews, I.T., Neirinckx, R.D., Pickett, R.D. and Winkler, C**. A comparative study of the brain uptake and early kinetics of 99mTc-dl HM-PAO and other PnAO derivatives in baboons. *Nuklearmedizin* 25(4): 134-137, 1986.

97. **Nowotnik, D.P., Canning, L.R., Cumming, S.A., Harrison, R.C., Higley, B., Nechvatal, G., Pickett, R.D., Piper, R.D., Bayne, V.J. and Forster, A.M.** Development of a 99mTc-labeled radiopharmaceutical for cerebral blood flow imaging. *Nuclear Medicine Communications* 6(9): 499-506, 1985.

98. **Neirinckx, R.D., Canning, L.R., Piper, I.M., Nowotnik, D.P., Pickett, R.D., Holmes, R.A., Volkert, W.A., Forster, W.A., Weisner, P.S., Marriott, J.A. and Chaplin, S.B.** Technetium-99m d,l-HM-PAO: a new radiopharmaceutical for SPECT imaging of regional cerebral blood perfusion. *Journal of Nuclear Medicine* 28(2): 191-202, 1987.

99. **Andersen, A.R., Friberg, H., Knudsen, K.B., Barry, D.I., Paulson, O.B., Schmidt, J.F., Lassen, N.A. and Neirinckx, R.D.** Extraction of [99mTc]-d,l-HM-PAO across the blood brain barrier. *Journal of Cerebral Blood Flow and Metabolism* 8(6): S44-S51, 1988.

100. **Sharp, P.F., Smith, F.W., Gemmell, H.G., Lyall, D., Evans, N.T., Gvozdanovic, D., Davidson, J., Tyrrell, D.A., Pickett, R.D. and Neirinckx, R.D.** Technetium-99m HM-PAO stereoisomers as potential agents for imaging regional cerebral blood flow: human volunteers. *Journal of Nuclear Medicine* 27(2): 171-177, 1986.

101. **Jurisson, S., Schlemper, E.O., Troutner, D.E., Canning, L.R., Nowotnik, D.P. and Neirinckx, R.D.** Synthesis, characterization, and x-ray structural determinations of technetium(V)-oxo-tetradentate amine oxime complexes. *Inorganic Chemistry* 25(4): 543-549, 1986.

102. **Neirinckx, R.D., Burke, J.F., Harrison, R.C., Forster, A.M., Anderson, A.R. and Lassen, N.A.** The retention mechanism of technetium-99m-HM-PAO: Intracellular reaction with glutathione. *Journal of Cerebral Blood Flow and Metabolism* 8: S4-S12, 1988.

103. **Ballinger, J.R., Reid, R.H. and Gulenchyn, K.Y.** Technetium-99m HM-PAO stereoisomers: differences in interaction with glutathione. *Journal of Nuclear Medicine* 29(12): 1998-2000, 1988.

104. **Phillips, W.T., Rudolph, A.S., Goins, B., Timmons, J.H., Klipper, R. and Blumhardt, R.** A simple method for producing a technetium-99m-labeled liposome which is stable *in vivo*. *Nuclear Medicine and Biology* 19(5): 539-547, 1992.

105. **Phillips, W.T., Rudolph, A.S., Goins, B. and Klipper, R.** Biodistribution studies of liposome encapsulated hemoglobin (LEH) studied with a newly developed 99m-technetium liposome label. *Biomaterials, Artificial Cells and Immobilization Biotechnology* 20: 757-760, 1992.

106. **Jacquier-Sarlin, M.R., Polla, B.S. and Slosman, D.O.** Oxido-Reductive state: The major determinant for cellular retention of technetium-99m-HM-PAO. *Journal of Nuclear Medicine* 37(8): 1413-1416, 1996.

107. Ceretec^{TM} package insert, Amersham Canada limited (Oakville, ON).

108. **Hung, J.C., Volkert, W.A. and Holmes, R.A.** Stabilization of technetium-99m-d,l-hexamethylpropylene amine oxime (^{99m}Tc-HM-PAO) using gentisic acid. *Nuclear Medicine and Biology* 16: 675-680, 1989.

109. **Amir, R., Hupez, P., Binnon, J.P, Van Nerom, C., Verbruggen, A. and Delcourt, E.** Potential usefulness of stabilization methods for ^{99m}Tc-HM-PAO in cerebral blood flow imaging. *European Journal of Nuclear Medicine* 20: 848, 1993.

110. **Byne, V.J., Forster, A.M. and Tyrrell, D.A.** Use of sodium iodide to overcome the eluate age restriction for Ceretec reconstitution. *Nuclear Medicine Communication* 10: 29-33, 1989.

111. **Mang'era, K.O., Vanbilloen, H.P., Schiepers, C.W. and Verbruggen, A.M.** Stabilization of high-activity 99mTc-d,l-HMPAO preparations with cobalt chloride and their biological behavior. *European Journal of Nuclear Medicine* 22: 1163-1172, 1995.

112. **Canning, L.R., Nowotnik, D.P., Neirinckx, R.D. and Piper, I.M.** Complexes of technetium-99m with propylene amine oximes. Canadian Patent 1 243 329.

113. **Ballinger, J.R., Reid, R.H. and Gulenchyn, K.Y.** Radiochemical purity of [^{99m}Tc]HM-PAO. *Journal of Nuclear Medicine* 29: 572-573, 1988.

114. **Feinstein-Jaffe, I., Boazi, M. and Tor, Y.** Assessment of the purity of d,l HM-PAO from diastereomeric mixtures using NMR techniques. *Journal of Nuclear Medicine* 30: 106-109, 1989.

115. **Semon, W.L. and Damerell, V.R.** Dimethylglyoxime. In *Organic Syntheses*, Volume 10 (Clarke, H.T. ed.). John Wiley and sons Inc. New York, New York. pp. 204-207, 1930.

116. **Cotton, F.A. and Wilkinson, G.** The group IVA(14) elements: Si, Ge, Sn, Pb. In *Advanced Inorganic Chemistry*, Fifth Edition (Cotton, F.A. and Wilkinson, G eds.) John Wiley & Sons, New York. pp. 265-304, 1988.

117. **Liang, F.H., Virzi, F. and Hnatowich, D.J**. Serum stability and non specific binding of technetium-99m labeled diaminodithiol for protein labeling. *Nuclear Medicine and Biology* 14(6): 555-561, 1987.

118. **Kirstein, M., Fridrich, R. and Seiler, H**. Some chemical aspects of labeling human fibrinogen with 99m-technetium. *Thrombosis Research* 28(3): 351-360, 1982.

119. **Tofe, A.J. and Francis, M.D**. Optimization of the ratio of stannous tin:ethane-1-hydroxy-1,1-diphosphonate for bone scanning with 99mTc-pertechnetate. *Journal of Nuclear Medicine* 15(2): 69-74, 1974.

120. **Goins, B., Phillips, W.T. and Klipper, R**. Blood-pool imaging using technetium-99m-labeled liposomes. *Journal of Nuclear Medicine* 37(8): 1374-1379, 1996.

121. **Torchilin, V.P., Omelyanenko, V.G., Papisov, M.I., Bogdanov, A.A., Trubetskoy, V.S., Herron, J.N. and Gentry, C.A**. Poly(ethylene glycol) on the liposome surface: on the mechanism of polymer coated longevity. *Biochimica et Biophysica Acta* 1195: 11-20, 1994.

122. **Needham, D., McIntosh, T.J. and Lasic, D.D**. Repulsive interactions and mechanical stability of polymer-grafted lipid membranes. *Biochimica et Biophysica Acta* 1108: 40-48, 1992.

123. **Blume, G. and Cevc, G**. Molecular mechanism of the lipid vesicle longevity *in vivo*. *Biochimica et Biophysica Acta* 1146: 157-168, 1993.

124. **Liu, D., Song, Y.K. and Liu, F**. Antibody dependent, complement mediated liver uptake of liposomes containing GM1. *Journal of Pharmaceutical Research* 12: 1775-1780, 1995.

125. **Harashima, H., Sakata, K., Funato, K. and Kiwada, H**. Enhanced hepatic uptake of liposomes through complement activation depending on the size of liposomes. *Journal of Pharmaceutical Research* 11: 402-406, 1994.

126. **Liu, D., Liu, F. and Song, Y.K**. Recognition and clearance of liposomes containing phosphatidylserine are mediated by serum opsonins. *Biochimica et Biophysica Acta* 1235: 140-146, 1995.

127. **Liu, F. and Liu, D**. Serum independent liposome uptake by mouse liver. *Biochimica et Biophysica Acta* 1278: 5-11, 1996.

128. **Marjan, J., Xie, Z. and Devine, D**. Liposome-induced activation of the classical complement pathway does not require immunoglobins. *Biochimica et Biophysica Acta* 1192: 35-44, 1994.

129. **Oja, C.D., Semple, S.C., Chonn, A. and Cullis, P.R.** Influence of dose on liposome clearance: critical role of blood proteins. *Biochimica et Biophysica Acta* 1281: 31-37, 1996.

130. **Harashima, H., Sakata, K. and Kiwada, H.** Distinction between the depletion of opsonins and the saturation of uptake in the dose-dependent hepatic uptake of liposomes. *Journal of Pharmaceutical Research* 10: 606-610, 1993.

131. **Devine, D.V., Wong, K., Serrano, K., Chonn, A. and Cullis, P.** Liposome-complement interactions in rat serum: implications for liposome survival studies. *Biochimica et Biophysica Acta* 1191: 43-51, 1994.

132. **Krowczynska, A.M., Donaghue, K. and Hughes, L.** Recovery of DNA, RNA and proteins from gels with microconcentrators. *Biotechniques* 18(4): 698-703, 1995.

133. **Kinekawa, Y. and Kitabatake, N.** Purification of beta-lactoglobin from whey protein concentrate by pepsin treatment. *Journal of Dairy Science* 79(3): 350-356, 1996.

134. **Donovan, J.M. and Jackson, A.A.** Rapid determination by centrifugal ultrafiltration of inter-mixed micellar/vesicular (non-lecithin-associated) bile salt concentrations in model bile: influence of Donnan equilibrium effects. *Journal of Lipid Research* 34: 1121-1129, 1993.

135. **Tardi, P.G., Boman, N.L. and Cullis, P.R.** Liposomal Doxorubicin. *Journal of Drug Targeting* 4(3): 129-140, 1996.

136. **Mowat, J.J., Mok, M.J., MacLeod, B.A. and Madden, T.D.** Liposomal bupivacaine: extended duration nerve blockade using large unilamellar vesicles that exhibit a proton gradient. *Anesthesiology* 85(3): 635-643, 1996.

137. **Madden, T.D., Harrigan, P.R., Lai, L., Bally, M.B., Mayer, L.D., Redelmeier, T., Tilcock, C. and Cullis, P.R.** The accumulation of drugs within large unilamellar vesicles exhibiting a proton gradient. *Chemistry and Physics of Lipids* 53: 37-46, 1990.

138. **Hosoda, J., Unezaki, S., Maruyama, K., Tsuchiya, S. and Iwatsuru, M.** Antitumor activity of doxorubicin encapsulated in poly(ethylene glycol)-coated liposomes. *Biological and Pharmaceutical Bulletin* 18(9): 1234-1237, 1995.

139. **Hung, J.C., Corlija, M., Volkert, W.A. and Holmes, R.A.** Kinetic analysis of technetium-99m d,l-HM-PAO decomposition is aqueous media. *Journal of Nuclear Medicine* 29(9): 1568-1576, 1988.

140. Merck Index, Eleventh edition (Budavari, S. ed.). Merck & Co., Inc. Rahway, New Jersey. pp. 4374, 1989.

141. **Campbell, P.I.** Toxicity of some charged lipids used in liposome preparations. *Cytobios* 37: 21-26, 1983.

142. **Nasso, F., Sala, F., Biondi, O., Casati, A., Cestro, B. and deCarli, L.** Liposomes induce chromosome aberrations in human cultured cells. *Experimental Cell Research* 157:397-408, 1985.

143. **Mayhew, E., Ito, M. and Lazo, R.** Toxicity of non-drug containing liposomes for cultured human cells. *Experimental Cell Research* 171: 195-202, 1987.

144. **Dunnick, J.K., Kallman, R.F. and Kriss, J.P.** Lipid vesicle interactions with EMT-6 tumor cells and effect on subsequent cell growth. *Biochemical and Biophysics Research Communications* 73(3): 619-624, 1976.

145. **Yoshihara, E. and Nakae, T.** Cytolytic activity of liposomes containing stearylamine. *Biochimica et Biophysica Acta* 854: 93-101, 1986.

146. **Storm, G., Oussoren, C., Peeters, P.A.M. and Barenholz, Y.** Tolerability of liposomes *in vivo*. In *Liposome Technology*, Volume III (Gregoriadis, G. ed.) CRC Press, Inc, Boca Raton, Fl. pp. 345-383, 1993.

147. **Allen, T.M. and Smuckler, E.A.** Liver pathology accompanying chronic liposome administration in mouse. *Research Communications in Chemical Pathology and Pharmacology* 50(2): 281-290, 1985.

148. **Allen, T.M., Murry, L., Alving, C.R. and Moe, J.** Effects on the murine mononuclear phagocyte system of chronic administration of liposomes containing cytotoxic drug or lipid A compared with empty liposomes. *Canadian Journal of Physiology and Pharmacology* 65: 185-190, 1987.

149. **Allen, T.M., Murray, L., MacKeigan, S. and Shah, M.** Chronic liposome administration in mice: effect on reticuloendothelial function and tissue distribution. *The Journal of Pharmacology and Experimental Therapeutics* 229(1): 267-275, 1984.

150. **Harrison, M., Tomlison, D. and Stewart, S.** Liposomal-entrapped doxorubicin: an active agent in AIDS-related Kaposi's sarcoma. *Journal of Clinical Oncology* 13(4): 914-920, 1995

151. **Gabizon, A., Catane, R., Uziely, B., Kaufman, B., Safra, T., Cohen, R., Martin, F., Huang, A. and Barenholz, Y.** Prolonged circulation time and enhanced accumulation in malignant exudates of doxorubicin encapsulated in polyethylene-glycol coated liposomes. *Cancer Research* 54: 987-992, 1994.

152. **James, N.D., Coker, R.J., Tomlinson, D., Harris, J.R., Gompels, M., Pinching, A.J. and Stewart, J.S.** Liposomal doxorubicin (Doxil): an effective new treatment for Kaposi's sarcoma in AIDS. *Journal Clinical Oncology* 6(5): 294-6, 1994.

153. **Coker, R.J., Viviani, M., Gazzard, B.G., Du Pont, B., Pohle, H.D., Murphy, S.M., Atouguia, J., Champalimaud, J.L. and Harris, J.R.** Treatment of cryptococcosis with liposomal amphotericin B (AmBisome) in 23 patients with AIDS. *AIDS* 7(6): 829-835, 1993.

154. **Goebel, F.D., Goldstein, D., Goos, M., Jablonowski, H. and Stewart, J.S.** Efficacy and safety of Stealth liposomal doxorubicin in AIDS-related Kaposi's sarcoma. The International SL-DOX Study Group. *British Journal of Cancer* 73(8): 989-94, 1996.

155. **Sturzl, M., Zietz, C., Eisenburg, B., Goebel, F.D., Gillitzer, R., Hofschneider, P.H. and Bogner, J.R.** Liposomal doxorubicin in the treatment of AIDS-associated Kaposi's sarcoma: clinical, histological and cell biological evaluation. *Research in Virology* 145(3-4): 261-9, 1994.

156. **Bogner, J.R., Kronawitter, U., Rolinski, B., Truebenbach, K. and Goebel, F.D.** Liposomal doxorubicin in the treatment of advanced AIDS-related Kaposi sarcoma. *Journal of Acquired Immune Deficiency Syndrome* 7(5): 463-8, 1994.

157. **Uziely, B., Jeffers, S., Isacson, R., Kutsch, K., Wei-Tsao, D., Yehoshua, Z., Libson, E., Muggia, F.M. and Gabizon, A.** Liposomal doxorubicin: antitumor activity and unique toxicities during two complementary phase I studies. *Journal of Clinical Oncology* 13(7): 1777-85, 1995.

158. **Gabizon, A., Isacson, R., Libson, E., Kaufman, B., Uziely, B., Catane, R., Ben-Dor, C.G., Rabello, E., Cass, Y., Peretz, T.** Clinical studies of liposome-encapsulated doxorubicin. *Acta Oncologica* 33(7): 779-86, 1994.

159. **Muggia, F.M., Hainsworth, J.D., Jeffers, S., Miller, P., Groshen, S., Tan, M., Roman, L., Uziely, B., Muderspach, L., Garcia, A., Burnett, A. and Greco, F.A.** Phase II study of liposomal doxorubicin in refractory ovarian cancer: antitumor activity and toxicity modification by liposomal encapsulation. *Journal of Clinical Oncology* 15(3): 987-93, 1997.

160. **Weary, M**. Pyrogen testing of parental products-status report. *Journal of Parental Science and Technology* 38(1): 20-23, 1984.

161. Pyrogen Testing. In US Pharmacopeia National Formulary (USPNF), 22nd Edition, 1515-1515, 1990.

162. **Lehninger, A.L**. The biosynthesis of amino acids and some derivatives; metabolism of organic nitrogen. In *Biochemistry* (Lehninger, A.L ed.) Worth Publishing, Inc., New York, New York. pp. 693-727, 1975.

163. **Rabinovici, R., Rudolph, A.S., Vernick, J. and Feuerstein, G**. Lyophilized liposome encapsulated hemoglobin: evaluation of hemodynamic, biochemical, and hematologic responses. *Critical Care Medicine* 22(3): 480-485, 1994.

164. **Cradock, J.C., Vishnuvajjala, B.R., Chin, T.F., Hochstein, H.D. and Ackerman, S.K**. Uridine-induced hyperthermia in the rabbit. *Journal of Pharmacy and Pharmacology* 38: 226-229, 1986.

165. **Dinarello, C.A., Elin, J., Chedid, L. and Wolff, S.M.** The pyrogenicity of the synthetic adjuvant muramyl dipeptide and two structural analogues. *Journal of Infectious Disease* 138(6): 760-767, 1978.

166. **Guencheva, G., Popova, P., Daivkova, G., Mincheva, V., Mihailova, S., Bogdanov, A., Pacelli, E. and Auteri, A**. Determination of cytokine release after *in vivo* and *in vitro* administration of Deodan (a preparation from Lactobacillus bulgarius "LB51") by the rabbit pyrogen test. *Immunopharmacology* 14(8): 1429-1436, 1992.

167. **Minano, F.J., Fernandez-Alonso, A., Benamar, K., Myers, R.D., Sancibrian, M., Ruiz, R.M. and Armengol, J.A**. Macrophage inflammatory protein-1b (MIP-1 b) produced endogenously in brain during E.coli fever in rats. *European Journal of Neuroscience* 8: 424-428, 1996.

168. **Arras, M., Hoche, A., Bohle, R., Eckert, P., Riedel, W. and Schaper, J**. Tumor necrosis factor-α in macrophages of heart, liver, and in the pituitary gland. *Cell and Tissue Research* 285: 39-49, 1996.

169. **Davidson, J., Milton, A.S. and Rotondo, D**. A study of the pyrogenic actions of interleukin-1a and interleukin-1b: interactions with a steroidal and a non-steroidal anti-inflammatory agent. *British Journal of Pharmacology* 100: 542-546, 1990.

170. **Szebeni, J., Wassef, N.M., Rudolph, A.S. and Alving, C.R**. Complement activation by liposome-encapsulated hemoglobin *in vitro*: the role of endotoxin contamination. *Artificial Cell, Blood Substitutes, and Immobilization Biotechnology* 23(3): 355-363, 1995.